Russian Chemical Reviews **83** (5) 391 – 438 (2014) © 2014 Russian Academy of Sciences and Turpion Ltd

DOI 10.1070/RC2014v083n05ABEH004299

Radical anion salts and charge transfer complexes based on tetracyanoquinodimethane and other strong π-electron acceptors

V A Starodub, T N Starodub

Institute of Chemistry, Jan Kochanowski University
15G Świętokrzyska Str., 25-406 Kielce, Poland

The unique properties of radical anion salts and charge transfer complexes formed by tetracyanoquinodimethane and other strong π-electron acceptors are analyzed. Their ability to form fusible conductive materials and magnetically ordered structures, including ferromagnetic ones with high Curie temperatures, spin ladders and quasi-two-dimensional organic conductors and superconductors is considered. Particular attention is given to the possible areas of application of these radical anion salts in electronic industry as nanomaterials, materials for the fabrication of field effect transistors, photodiodes and ion selective electrodes.
The bibliography includes 421 references.

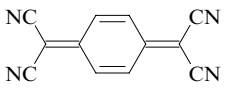
Contents

I. Introduction 391
II. Charge transfer complexes based on TCNQ and other strong π-electron acceptors 392
III. Radical anion salts based on TCNQ and other strong acceptors 417
IV. Magnetic exchange interactions in the TCNQ radical anion salts 422
V. Practical application of the radical anion salts of TCNQ 428

I. Introduction

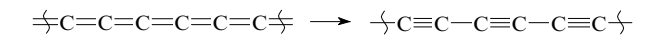
Radical anion salts (RAS) formed by 7,7,8,8-tetracyanoquinodimethane (**1**, TCNQ) attracted researchers' attention back in the mid-1960s. Early reviews[1,2] described the unusual properties of TCNQ as one of the most potent π-electron acceptors. Owing to high electron affinity (A = 2.8 or 3.0 eV[3,4]), TCNQ can form charge transfer complexes (CTC) and radical anion salts of both simple and complex composition. The salts of simple composition contain the $TCNQ^{-\bullet}$ radical anion, for example, LiTCNQ, $Fe(TCNQ)_2$ and $Al(TCNQ)_3$. The salts of complex composition contain TCNQ species with the charge (q) of $0 < q < -1$, *i.e.*, the crystals of these RAS formally contain both TCNQ molecules and $TCNQ^{-\bullet}$ radical anions. These include, for example, the radical anion salts $Cs_2(TCNQ)_3$ and $QnH(TCNQ)_2$ (QnH^+ is the quinolinium cation) in which the oxidation state of TCNQ is $-2/3$ and $-1/2$, respectively. An unusual feature of the RAS of complex composition is high electrical conductivity. Therefore, it is not surprising that the interest in these RAS markedly increased after the publication of US physicist Little[5] devoted to the problem of high-temperature superconductors. This study presented a new, in principle, type of superconductors in which the Cooper electron pairs are formed due to the exciton – electron interaction rather than the electron – phonon interaction as in usual superconductors.[5–7] A specific feature of the Little model is that the exciton superconductor should be a one-dimensional organic system.

Structure 1



1 (TCNQ)

Immediately after the appearance, the Little model provoked some fundamental objections (for example, according to the Peierls theorem, a one-dimensional metal is in principle impossible, as it is unstable with respect to transition to the more stable dielectric state[8]). It follows from the Peierls theorem, for example, that 'one-dimensional carbon' — carbyne — should have acetylene rather than cumulene structure:



V A Starodub Doctor of Chemical Sciences, Professor at the chair of chemical engineering, Institute of Chemistry, Jan Kochanowski University. Telephone: (041) 349 70 58,
e-mail: Wladimir.starodub@ujk.edu.pl
T N Starodub Candidate of Chemical Sciences, assistant at the same institute.
Current research interests of the authors: synthetic metals and semiconductors, molecular magnets, coordination compounds, radical ion salts.

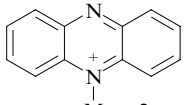
Received 27 November 2012
Uspekhi Khimii **83** (5) 391 – 438 (2014); translated by Z P Svitanko

Nevertheless, in the early 1970s, systematic research aimed at the preparation of quasi-one-dimensional metals and superconductors was started. The prefix 'quasi' implies high anisotropy of the physical properties of organic conducting crystals, for example $\rho_a \approx \rho_b \gg \rho_c$ (here ρ_i is the resistivity along some crystallographic direction). Particularly these properties are inherent in the radical anion salts formed by TCNQ: in the crystals of these salts, the TCNQ particles are stacked and the overlap of their π-orbitals gives rise to a one-dimensional band, which is partly occupied in the case of fractional oxidation state, and this may give rise to metallic properties.

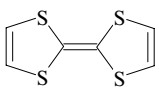
The first studies devoted to organic metals were started in the USSR at the Branch of the Institute of Chemical Physics (Chernogolovka). They were preceded by the appearance of two reviews,[6,7] which summarized virtually all known information on low-dimensional conducting substances — Krogmann salts,[9] iridium carbonyl halides [10] and TCNQ radical ion salts. As a result, back in the 1960s the first organic metals — the radical anion salts $QnH(TCNQ)_2$ and NMP(TCNQ) (NMP^+ is the *N*-methylphenazinium cation, **2**) — were obtained.

In the crystals of NMP(TCNQ), the metallic state is retained up to ~200 K, and then transition to the dielectric phase, the Mott transition,[11] takes place (one more type of instability of the metallic state caused by competition of the tendency for delocalization of conduction band electrons and the Coulomb interaction of electrons, which is minimized upon electron localization; see, for example, Refs 6 and 12). In 1973, a sensational publication appeared [13] describing the charge transfer complex TTF(TCNQ) (TTF is tetrathiafulvalene, **3**).

Structures 2, 3



2



3 (TTF)

This complex is an organic metal; its conductivity increases upon cooling. At $T = 58$ K, a giant increase in the conductivity was noted,[13] which was attributed to the onset of the superconducting transition. Further cooling induces the Peierls transition at $T = 54$ K.

The physical properties of low-dimensional materials depend substantially on the impurities and on the quality of crystals. Charge transfer complexes can be prepared by the exchange reaction between a radical cation salt (RCS) and a RAS, which allows better control over the crystal growth:

$$TTF^{+\bullet}Y^- + Li^+TCNQ^{-\bullet} \longrightarrow TTF(TCNQ)\downarrow + LiY$$

In a study of the crystals of the complex TTF(TCNQ), it was found that the $TTF^{+\bullet}Cl^-$ radical cation salt has a high conductivity: $\sigma_{rt} = 1\ \Omega^{-1}\,cm^{-1}$ measured on compressed pellets (rt is room temperature).[14] Soon RCS became the key subject of investigations, which resulted in the synthesis of organic metals that retain their metallic state down to helium temperatures [15,16] and then the first organic superconductors.[17] Therefore, little attention was paid to RAS formed by TCNQ and other strong electron acceptors.

A sort of revival of the chemistry of these RAS dates to the mid-1980s when the first fusible conducting organic materials were obtained.[18,19] Later, it was found that TCNQ salts are able to form magnetically ordered structures, in particular, ferromagnetic structures and spin ladders, at room temperature.[20–22] This opens up the way of broad use of these RAS as materials for microelectronics, spintronics or nonlinear optics.[23] Due to the absence of up-to-date reviews devoted to RAS and CTC based on TCNQ and other potent electron acceptors capable of forming CTC with a high degree ($q > 0.5$) of charge transfer or RAS of simple and complex compositions in the world literature (except for the publication [24] of 2009 dealing with the classification of these RAS and determination of the charge states of TCNQ), there is a need to summarize and analyze the achievements of the last two decades.

II. Charge transfer complexes based on TCNQ and other strong π-electron acceptors

Currently, various polycyanide organic compounds and benzoquinone derivatives are used as strong π-electron acceptors in molecular electronics (Fig. 1). All of them are able to form RAS.

Several principles of the CTC classification exist. For example, it was proposed to classify them according to the degree of charge transfer (CT).[25] The complexes $(D^{\delta+})_m(A^{\delta'-})_n$ are classified into three groups: fully ionic CTC (δ, $\delta' = 1$); mixed-valence CTC ($\delta < 1$, $\delta' > \delta_c$; $\delta < \delta_c$, $\delta' \geqslant \delta_c$ where $\delta_c = 0.5$ is usually taken as the critical value) and neutral CTC ($\delta < \delta_c$, $\delta' \geqslant 0$). In our review, the following terms are used: a compound formed as a complex of a donor with an acceptor is called CTC even if the CT is great, for example, in the complex TTF(TCNQ), the CT is 0.59. If the compound is a salt, that is, it contains a radical anion of a strong acceptor and a closed-shell cation (onium or inorganic), or a transition metal cation, or an inorganic complex cation, this compound will be called a radical anion salt. This approach eliminates many problems: indeed, the degree of CT is not always exactly known; it is

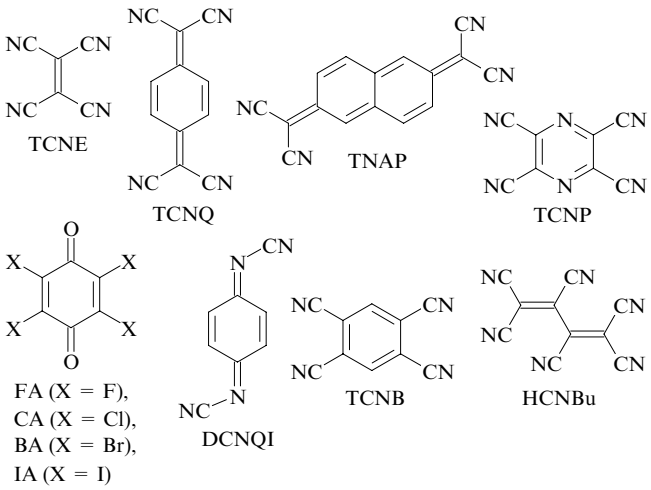


Figure 1. Key π-electron acceptors: tetracyanoethylene (TCNE); 7,7,8,8-tetracyanoquinodimethane (TCNQ); 11,11,12,12-tetracyanonaphtho-2,6-quinodimethane (TNAP); tetracyanopyrazine (TCNP); halogenanils: fluoranil (FA), chloranil (CA), bromanil (BA), iodanil (IA); *N*,*N*′-dicyanoquinodiimine (DCNQI); 1,2,4,5-tetracyanobenzene (TCNB); hexacyanobutadiene (HCNBu).

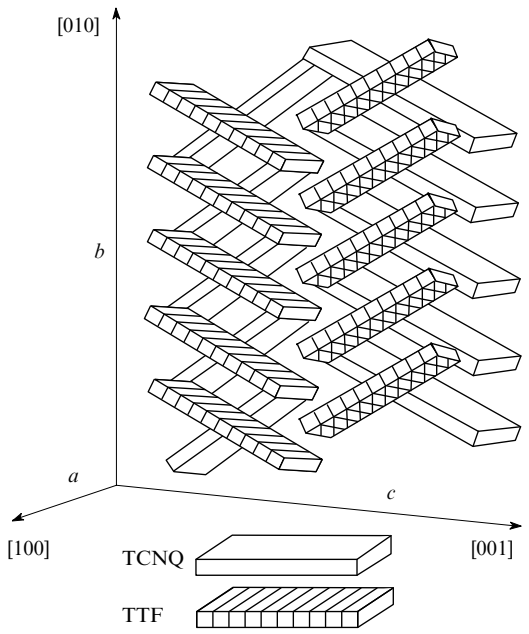


Figure 2. Schematic view of the structure of the complex TTF(TCNQ). The molecular planes are not perpendicular to the *b* axis of stacks but are rotated around the *a* axis. Two oppositely rotated molecules per unit structure repeating along the *c* axis are present. The TTF and TCNQ stacks alternate along the *a* axis.

not equal to unity even for RAS such as LiTCNQ or NMP(TCNQ); in addition, the CT value, as shown below, depends on the external conditions. Since both CTC and RAS can contain TCNQ with a fractional or indefinite charge, we will use the term 'species' when it is impossible to clearly distinguish between the TCNQ molecule and the $TCNQ^{-\bullet}$ radical anion.

In terms of structural type, all CTC can be subdivided into CTC with mixed-type stacks (the acceptor and donor molecules alternate in the stacks as ...D – A – D – A... or ...D – D – A – D – D – A...) and CTC with segregated stacks, TTF(TCNQ) being a classical example of the latter (Fig. 2). Note that CTC containing isolated acceptor molecules or their dimers also exist.

Relying on the statistical analysis of data from the Cambridge Crystallographic Data Centre, Huang *et al.*[26] proposed subdividing RAS structures based on TCNQ into three types. In the first type, the TCNQ species are arranged parallel to one another with a $\sim$1 Å shift in the perpendicular direction; in the second type, the species are displaced by $\sim$2 Å along the principal axes, while no shift is present in the perpendicular direction; in the third structural type, the neighbouring TCNQ species are linked into σ-dimers with a relatively long C – C bond (1.6 – 1.7 Å).

1. Charge transfer complexes in which L → H transition takes place

The CTC with alternating stacking structure (mixed stacks) can undergo phase transitions from a low CT state to a high CT state. This transition was first detected in 1981 in the crystals of the CTC TTF(CA) (CA is chloranil).[27] Following the authors of this publication, this transition was called neutral-to-ionic phase transition. Actually this is the transition from a low CT state to a high CT state (we will designate it by L → H transition). As shown in our earlier paper based on IR and X-ray photoelectron spectra,[28] the degree of CT in TTF(CA) is $\sim$0.27. In other words, the CT is 0.27 in the so-called neutral phase, while in the so-called ionic phase, it increases to 0.73.

The CT value can be determined using virtually any physical method — spectroscopy, the dipole moment method and X-ray diffraction (see, for example, Refs 29 – 31). Note that the obtained results are rough. However, the use of several independent methods increases the reliability of estimates. Thus, we determined the CT value in the complex TTF(CA) by IR spectroscopy from the known dependence of the chloranil ν(C=O) frequency on the charge of the CA^{q-} species (here q is 0 for chloranil, 1 for simple chloranil salts and 0.5 for complex chloranil salts). In the X-ray photoelectron spectroscopy technique, one can use the linear dependence of the ES2p binding energy on the charge of the TTF species. Similar CT values were obtained in later studies (0.25 – 0.3,[32,33] 0.3 [34]) and confirmed by density functional theory calculations.[35,36]

The L → H transition was observed [27] upon pressure increase to $\sim$15 kbar. Since the temperature decrease is accompanied by lattice contraction, it is quite expected that the L → H transition would occur also on cooling. Indeed, in the same year of 1981, this transition was observed [37] in the CTC TTF(CA) crystals at 84 K. According to this publication, the L → H transition is, most likely, a second-order phase transition. Theoretical analysis [38] indicates that this should be a first-order phase transition but the Coulomb interactions between neighbouring stacks stabilize the intermediate state in which both phases, L and H, coexist.

The L → H transition in the TTF(CA) crystals is related not only to a change in the CT but also to a change in the crystal lattice symmetry; therefore, the transition can be studied by optical methods. Initially, the research was focused on the intramolecular vibrations of the components of this CTC.[39,40] In the centrosymmetric L phase, the mutual exclusion principle holds:[41] only vibrations that are odd upon inversion are IR-active and only vibrations that are even upon inversion are Raman-active. Due to conjugation in the chloranil molecule, the carbonyl groups are involved in compound modes antisymmetric stretching $\nu(b_{2u})$ and symmetric $\nu(a_{2g})$ modes. In the IR spectrum of the L phase, the $\nu(b_{2u})$ mode occurs at 1690 cm^{-1}, while in the H phase, this mode is at 1532 cm^{-1} (see Ref. 39). This corresponds to a decrease in the C – O bond order upon the formation of the radical anion.

It is convenient to study the L → H transition using lattice vibrations, which can be classified in terms of the irreducible representations of space groups. The high-temperature phase of TTF(CA) corresponds to centrosymmetric space group $P2_1/n$.[42] The symmetry of the H phase is fairly difficult to establish due to the above-mentioned coexistence of the L and H phases below the transition temperature. Nevertheless, neutron diffraction [43] and ^{35}Cl NQR studies [44] showed that the space group of the H phase is P_n (non-centrosymmetric). For TTF(CA), lattice vibrations can be classified according to the symmetry types as follows:[45]

$$\Gamma(\mathrm{L}) = 6\,A_g \oplus 6\,B_g \oplus 5\,A_u \oplus 4\,B_u$$

$$\Gamma(\mathrm{H}) = 10\,A' \oplus 11\,A''$$

Thus, the low-frequency IR spectrum of the L phase will exhibit 9 lines and the Raman spectrum will contain 12 lines. The corresponding spectra of the H phase will show 21 lines in each of the IR and Raman spectra. Therefore, both IR and Raman spectroscopy can serve to investigate the L → H transition.[45,46] An important result of these studies is the discovery of possible coexistence of the L and H phases. It was shown[47] that one-dimensional fluctuating nanodomains of the H phase can occur in the initial L phase above the L → H transition temperature and *vice versa*. These nanodomains can form upon irradiation of H phase crystals below the L → H transition temperature (81 K).[48,49] The photoinduced transformation of the H phase to the L phase at 4 K produces nanodomains of the L phase with a lifetime of 300 ps. The photoexcitation at 77 K, close to the L → H transition temperature, results in the macroscopic H–L conversion with an excited phase lifetime of 20 ps.[48]

The theory of photoinduced L → H phase transitions was developed by Yonemitsu.[50] The coexistence of L and H phases under normal pressure is also observed in the TTF(CA) crystals in which some of chloranil has been replaced by trichloro-*p*-benzoquinone.[32]

The disappearance of the inversion centres in the TTF(CA) crystals upon the L → H transition may result in ferroelectric ordering. This ordering was detected[32] based on anomalous dielectric response at $T = 81$ K. A study[51] is devoted to the theory of spontaneous polarization of the TTF(CA) crystals. The theory predicts a polarization of 0.10–0.12 C m^{-2}, which is much greater than the experimental value of 0.004 C m^{-2}. This discrepancy is attributable to the antiparallel contributions of the electron and lattice polarization of the TTF(CA) crystals.[52]

An EPR study of the L → H transition in the crystals of TTF(CA)[53] indicates that there exist mobile soliton-like paramagnetic defects (*i.e.*, defects able to move in the crystal like 'solitary structurally stable waves' — solitons). This may account for the increase in the electrical conductivity of the crystals at temperatures below 84 K.

In the H phase, not only spontaneous polarization is possible but also spin ordering in mixed stacks composed of radical cations and radical anions. In this case, ferroelectric and antiferromagnetic nature (multiferroicity) of the H phase can be considered. In some studies,[54,55] the multiferroicity of the H phase of TTF(CA) was confirmed both experimentally and theoretically. In particular, it was demonstrated[35] that the H phase of TTF(CA) can be described as alternating Heisenberg antiferromagnetic chain with the exchange integral $J = 1124$ cm^{-1} and the alternation parameter $\delta = 0.46$. Spontaneous polarization was attributed[54] to the Peierls transition of the H phase. The subsequent antiferromagnetic ordering results in a sharp increase in the electronic contribution to polarization.

Nishizawa *et al.*[56] showed the possibility of the solid-state synthesis of TTF(CA). Stirring a mixture of TTF and CA for 20 min yields a black phase of the CTC TTF(CA), whereas the L phase known before is green. Later, this phase was identified as a new modification of TTF(CA) with a segregated stacking mode.[57] Unfortunately, the publication does not give an estimate for the degree of CT or electrical conductivity measurements.

An attempt to prepare the CTC of TTF with *o*-chloranil affords a cycloaddition product — compound **4**.[58] However, at low temperatures (below −65 °C), it is possible to obtain black crystals of the complex with an alternating stacking structure and a much greater CT value compared to that in the CTC with chloranil (0.6).[58]

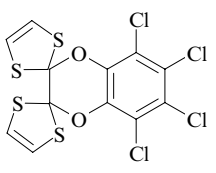
The L → H type transitions also occur in other CTC with alternating stacking. Thus in the crystals of the complex TMB(TCNQ) (TMB is 3,3′,5,5′ -tetramethylbenzidine), this transition occurs at $T \approx 205$ K, the change in the degree of ionicity in this CTC being much lower than in TTF(CA).[59] In this case, the transition was characterized as a first-order phase transition. In the crystals of the complex DMTTF(CA) (DMTTF is 2,6-dimethyltetrathiafulvalene), the L → H transition occurs at $T \approx 65$ K.[60] In this case, coexistence of both phases at $T < T_c$ was also noted. The unit cell parameters *a*, *b* and *c* regularly decrease with lowering of the temperature. The parameter *c* decreases most appreciably: by more than 2.5% as the temperature decreases from room to helium temperature.[61] The molecular structure also changes. The length of the central C–C bond in DMTTF increases from 1.349 Å at room temperature (which is equal to the length of this bond in neutral TTF) to 1.372 Å at 29 K (in the $TTF^{+\bullet}$ radical cation, this length is equal to 1.393 Å).

The L → H transition in the crystals of the CTC DMTTF(CA) occurs also upon pressure build-up and $p_c \approx 1.2$ GPa.[62] As the pressure grows, the *v*(CO) stretching frequency of chloranil decreases: at 0.7 GPa, lines are observed for both neutral CA and the CA radical anion, while at 1.4 GPa, only the *v*(CO) line of the radical anion is observed.[62]

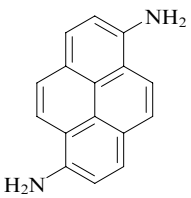
The complex DAP(CA) (DAP is 1,6-diaminopyrene, **5**) also has an alternating stacking structure. At room temperature, it is a high-resistance conductor ($\rho_{rt} = 10^8$ Ω cm). On gentle heating or mechanical grinding, the irreversible transition to high-conducting phase takes place — the resistance decreases 10^6–10^8-fold.[63] The cause for this sharp change in the electrophysical properties is unknown: according to the results of optical and structural studies and NMR data, the high-conducting phase contains almost neutral DAP and CA molecules.[63]

The L → H transition occurs in the crystals of the CTC TTF(DMDCNQI) at $p > p_c = 0.9$ GPa (DMDCNQI is 2,5-dimethyl-*N*,*N*′-dicyanoquinodiimine).[64] According to estimates based on IR spectroscopy data, the degree of CT increases from 0.1 in the L phase to 0.9 in the H phase. Basaki and Matsuzaki[64] estimate the CT values in the L and H phases of TTF(CA) as 0.2 and 0.8, respectively, which is close to our results.[28] Thus, in the TTF(DMDCNQI) crystals, the degree of ionicity changes upon the L → H transition most appreciably, by 80%. In addition, the authors cited[64] noted gradual dimerization of stacks in the crystals of the complex TTF(DMDCNQI), as was noted earlier[65] for the crystals of TTF(IA).

Structures 4, 5



4



5 (DAP)

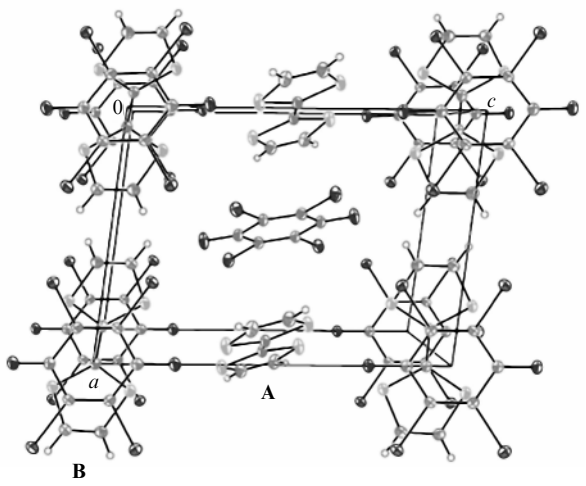


Figure 3. Packing of molecules in the complex TTF(BA) at room temperature.[66]

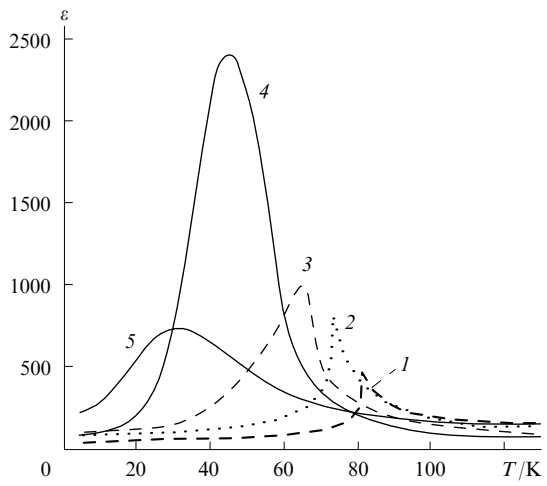


Figure 4. Temperature dependences of the dielectric constant (ε) for a series of CTC $TTF(CA)_{1-y}(QCl_3)_y$ (at 100 kHz).[69] y = 0 (*1*), 0.08 (*2*), 0.10 (*3*), 0.12 (*4*), 0.25 (*5*).

The structure of the CTC TTF(BA) differs markedly from the structure of the above-mentioned complexes.[66] The molecules of the donor and the acceptor form mixed donor–acceptor (D–A) stacks of two types along the crystallographic axes *a* and *b* (Fig. 3). They are designated as stacks **A** and **B**.

The planes of stacks **A** alternate with the planes of stacks **B** along the *c* axis (see Fig. 3). The structural transition is related to dimerization of stacks of both types. The CT value was estimated [66] as 1.0 for both phases, *i.e.*, the degree of CT does not change upon structural transition. Thus, the CTC TTF(BA) remains highly ionic over a broad temperature range. Upon the structural phase transition, the inversion centre disappears (the space group of the high-temperature phase is $P\bar{1}$ and that of the low-temperature phase is $P1$). The disappearance of the inversion centre is also manifested in the IR spectra: the low-temperature phase gives rise to absorption lines that are forbidden for centrosymmetric systems by the exclusion rules.[66] The $P\bar{1} \rightarrow P\,1$ transition is related to dimerization of both types of stacks and distortion of TTF molecules. This corresponds to two different interplanar spacings in the stacks: d_{intra} (the distance within the dimer) and d_{inter} (the distance between the dimers). In stacks **A**, d_{intra} = 4.075 Å, d_{inter} = 4.235 Å; in stacks **B**, d_{intra} = 4.244 Å, d_{inter} = 4.425 Å.

The 2 : 1 CTC of halogenanils with TTF were prepared. The crystals of the CTC $(TTF)_2IA$ consist of mixed stacks of donors and acceptors, which form symmetric trimers D–A–D.[67] The L → H transition in the crystals of this CTC occurs at $p > p_c$ = 3.1 GPa. In the H phase, the symmetric trimers are converted to asymmetric ones; the authors proposed the following model:

$$TTF^0-IA^0-TTF^0 \longleftrightarrow TTF^0-IA^--TTF^+$$

The cause of this asymmetry remains obscure. Structural studies of the CTC $(TTF)_2BA$ carried out at temperatures of 300, 100 and 25 K show the absence of the L → H transition in this CTC.[68] The authors attributed this to the presence of appreciable intermolecular interactions owing to shortened S···S contacts.

The reversible L → H type phase transitions are of interest not only from the theoretical standpoint but also for practical applications. As noted above, transitions with the change in the degree of CT may be related to ferro- or antiferroelectric ordering of the crystal lattice. This ordering gives a considerable dielectric response near the critical point (T_c or p_c). These properties of CTC with L → H transitions can find use in electronics or quantum optics. Figure 4 shows the temperature dependence of the dielectric constant for a series of CTC of the composition $TTF(CA)_{1-y}(QCl_3)_y$ (QCl_3 is trichlorobenzoquinone) in which this response takes place.

Table 1 summarizes the data on CTC that were found to undergo L → H transitions.

Table 1. Charge transfer complexes in which the L → H transition takes place.

CTC	T_c/K	p_c/GPa	Ref.
TTF(CA)	81	1.1	37
(TTF-d_4)(CA)	84	–	70
$TTF(QBrCl_3)$	68	1.1	71, 72
(TTF-d_4)($QBrCl_3$)	73	–	70
DMTTF(CA)	65	0.95	60, 62
$DMTTF(QBrCl_3)$	54	–	73
$DMTTF(2,5\text{-}QBr_2Cl_2)$	49	–	73
$DMTTF(2,6\text{-}QBr_2Cl_2)$	~0	–	73
DMTTF(BA)	–	1.25	73
TMB(TCNQ)	205	0.5	59, 74, 75
ClMePD(DMDCNQI) [a]	~225	~0.5	76–78
ClMePD(Et_2TCNQ) [b]	115	–	76–78
Cl_2PD(ClMeTCNQ) [c]	~220	–	76–78
(TTC_1TTF)(FMeTCNQ) [d]	14	0.85	76–78
TTF(DMDCNQI)	–	0.9	64, 79
ET(ClMeTCNQ) [e]	–	1.0	80, 81

[a] ClMePD is 2-chloro-5-methyl-*p*-phenylenediamine, [b] Et_2TCNQ is 2,5-diethyltetracyanoquinodimethane, [c] Cl_2PD is 2,5-dichloro-*p*-phenylenediamine, [d] TTC_1TTF is tetra(methylthio)tetrathiafulvalene, [e] ET is bis(ethylenedithiolo)tetrathiafulvalene.

It is known that ferroelectric phase transitions can refer to two types: order–disorder transitions and transitions associated with displacement of structural units. A classical example of first type transitions is sodium nitrite containing a polar nitrite ion; ferroelectrics of the second type are exemplified by barium titanate ($BaTiO_3$).[82] The CTC such as TTF(CA) consist of symmetric molecules (having an inversion centre) and, therefore, ferroelectric transitions can occur in them only as a result of displacement of components in mixed stacks. This gives rise to a dipole moment of the unit cell. Indeed, the space group of the CTC TTF(CA) in the high-temperature phase is $P2_1/n$, both molecules, TTF and CA, being located at the inversion centres. The space group of the low-temperature phase is P_n, *i.e.*, it is non-centrosymmetric.[83] The ferroelectric transition in the alternatively stacked crystals of the CTC D(A) is also associated with displacement resulting in stack dimerization, as is depicted in Fig. 5.

Thus, ferro- or antiferroelectric crystals based on CTC do not necessarily require asymmetric components. The nature of the crystals, either ferro- or antiferroelectric, is determined by three-dimensional ordering of polar stacks.[82] The materials subject to spontaneous electric polarization can be used in photonics for the development of sensors and memory elements. Organic ferroelectrics are of particular interest, as they are light, cheap and technology intensive. A drawback of the existing organic ferroelectrics is a low transition temperature of the paraelectric to ferroelectric phase. For example, the CTC TTF(CA) and TTF(BA) and the TTF complex with bromotrichloro-*p*-benzoquinone [TTF($QBrCl_3$)] have cryogenic transition temperatures (below 81 K).[55,84] However, the first CTC-based organic ferroelectrics in which the ferroelectric phase exists at room temperature have already been synthesized.[85]

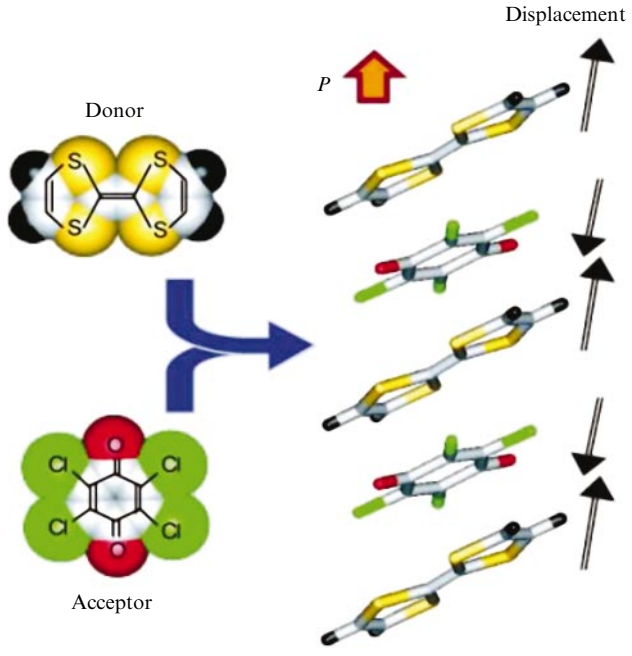


Figure 5. Schematic of the ferroelectric transition accomplished by displacement of the donor and acceptor molecules in the CTC with alternating stacking.[82]
P is polarization.

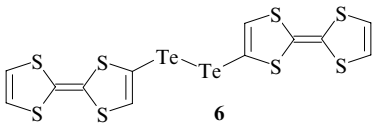
2. Methods for design of materials for electronics based on strong π-acceptors

Being a strong acceptor, TCNQ forms CTC characterized by high degrees of CT with most of strong organic donors. In the case of segregated stacking structure, these CTC are either organic metals or narrow band-gap semiconductors. The search for new effective donors for the design of organic metals and superconductors and materials for electronics is still topical. Note that the metallic state in highly anisotropic quasi-one-dimensional materials is unstable with respect to structural distortion (Peierls instability) and with respect to transition from the state with delocalized electrons to a state with localized electrons (Mott transition).[12,86] An effective method for suppression of the Peierls instability is a decrease in the anisotropy, which is attained through contacts between the stacks that are shortened compared to the sum of van der Waals radii. These contacts are possible upon introduction of heteroatoms with high polarizability: for example, upon replacement of sulfur by selenium or tellurium and chlorine by bromine or iodine. In addition, high polarizability of CTC components prevents the Mott transition.

The CTC (TETeTTF)TCNQ [TETeTTF is 2,3,6,7-tetrakis(ethyltelluro)tetrathiafulvalene] reported by Aharon-Shalom *et al.*[87] contains mixed-type stacks. The CT value for this CTC was estimated as 0.6. Despite the mixed type of stacks, CTC has a relatively high conductivity: $\sigma_{rt} = 10^{-2}\ \Omega^{-1}\ cm^{-1}$. This high electrical conductivity in the CTC with mixed stacks may be caused by shortened contacts between the chalcogen atoms of different stacks. Indeed, Aharon-Shalom *et al.*[87] found such contacts between sulfur and tellurium atoms (S···Te). In principle, the L → H type transition can also occur in the CTC (TETeTTF)TCNQ. The change in the CT value would be minor in this case (~0.2). The authors[87] noted that a transition of this type may occur upon grinding of the compound in a mortar. This is confirmed only by a change in the ν(C≡N) vibration frequency. Note also that the structure of this CTC does not correspond to the so-called anticomplementarity principle:[88] the complex contains mixed-type stacks despite the anticomplementarity of the TETeTTF and TCNQ structures.

One more tellurium-containing ligand, $(TTFTe)_2$ (**6**), forms two CTC with TCNQ: $(TTFTe)_2TCNQ$ and $(TTFTe)_2TCNQ_2$.[89] The structure of the former is shown in Fig. 6.

Structure 6



6

As can be seen from Fig. 6, a structure with a segregated stacking mode is formed: planar TCNQ species form stacks along the crystallographic axis *c*. The donor molecules form stacks extended in the same direction as the stacks formed by the acceptor. Therefore, despite the non-planar structure of $(TTFTe)_2$, the planes of the TTF moieties in this CTC also form stacks, although irregular. The crystal packing shown in Fig. 6 is stabilized by shortened intermolecular contacts: one nitrile nitrogen atom forms two contacts with the tellurium atom of the donor. The complex has the conductivity $\sigma_{rt} = 0.3\ \Omega^{-1}\,cm^{-1}$. The temperature depend-

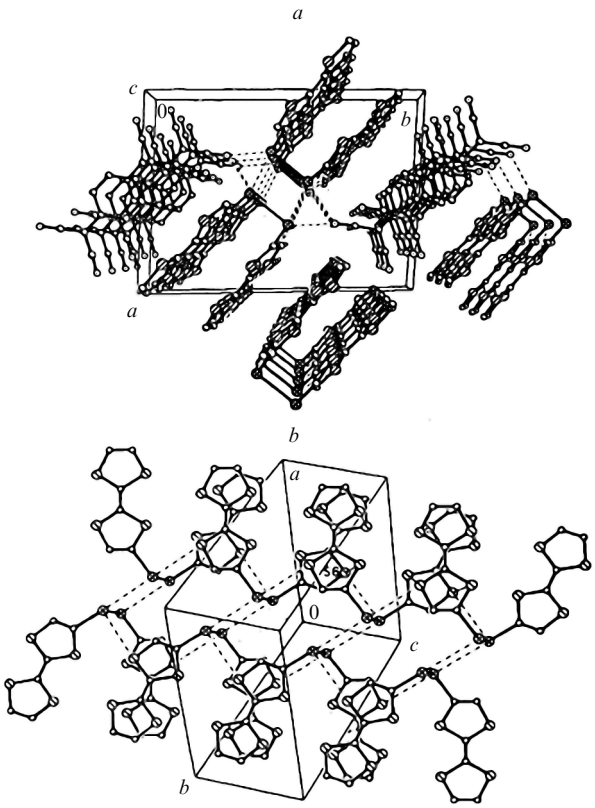


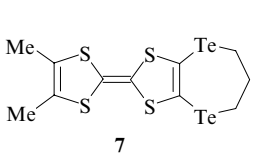
Figure 6. Structure of the complex $(TTFTe)_2(TCNQ)$: projection onto the *ab* plane (*a*) and structural motif of the donor molecules in the CTC structure (*b*).[89]
The dashed lines show the intermolecular contacts shortened with respect to the sum of the van der Waals radii.

ence of the resistance is described by the simple activation model with a very narrow band gap: $\Delta = 62$ meV. The complex $(TTFTe)_2(TCNQ)_2$ was obtained as very fine crystals; however, electrical resistance measurements for pressed pellet samples gave the value $\sigma_{rt} = 8.2\ \Omega^{-1}\,cm^{-1}$. In view of the high anisotropy of properties of CTC of this type, one can expect a much higher conductivity for single crystals. The complex $(TTFTe)_n(DCNQI)_m$, which is a dielectric, $\sigma_{rt} = 10^{-9}\ \Omega^{-1}\,cm^{-1}$, was also reported.[89]

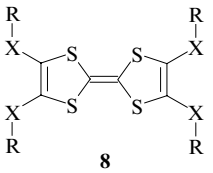
4,5-Dimethyl-4′,5′-propyleneditellurotetrathiafulvalene (**7**) forms a mixed-stacked CTC with TCNQ.[90] The CT value estimated from the IR spectra is 0.74. Despite the alternating stacked packing, the conductivity of the single crystals is rather high: $\sigma_{rt} = 10^{-3}\ \Omega^{-1}\,cm^{-1}$, which is also attributable to the presence of strong intermolecular S···Te contacts.

Imaeda *et al.*[91] described a series of CTC with the composition $(TXC_n\text{-}TTF)(TCNQ)$ (TXC_n-TTF = **8**; X = S, Se, Te; $n = 2, 3$). All of the CTC are isostructural and have an alternating stacked packing; correspondingly these CTC are high-resistance semiconductors ($\sigma_{rt} \approx 10^{-6}$–$10^{-7}\ \Omega^{-1}\,cm^{-1}$). In the case of tellurium-based ligands, the conductivity of the CTC is much higher — σ is up to $0.2\ \Omega^{-1}\,cm^{-1}$. The band gap of tellurium-based CTC is also much smaller, being 0.3–0.35 eV for CTC with sulfur- and selenium-based donors and about 0.06–0.11 eV for tellurium-based donors.[91] These CTC also differ in the CT values, which are $\leqslant$0.13, 0.5 and 0.71 for S, Se and Te donors, respectively.

Structures 7, 8



7

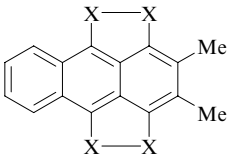


8

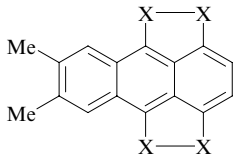
R = Et, Pr^n

All three members of the series of tetrachalcogentetracenes — tetrathio- (TTT), tetraseleno- (TST) and tetratellurotetracenes (TTeT) — are known.[92] However, their low solubility in most organic solvents restricts the possibility of comparative analysis of the CTC based on them. Therefore, attention is drawn to the publication [93] describing a series of CTC with donors based on substituted tetrachalcogenoanthracenes, which have sufficiently high solubility for the preparation of single-crystalline CTC with such acceptors as TCNQ, 2,3,5,6-tetrafluoro- (F_4TCNQ), 2,5-dimethyl- (DMTCNQ), 2,5-dimethoxytetracyanoquinodimethane (DMOTCNQ), 3,3′-dichloro-5,5′-bis(dicyanomethyleno)-$\Delta^{2,2'}$-di(3-thiolene) (DCBT) and 3,3′-dibromo-5,5′-bis(dicyanomethyleno)-$\Delta^{2,2'}$-di(3-selenolene) (DBBS) (Fig. 7).

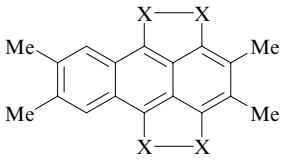
This complexes mainly have 1 : 1 stoichiometry; however, TCNQ and its derivatives also form CTC of different compositions, for example, $(2,3\text{-DMTTA})_2(TCNQ)_3$, $(2,3\text{-DMTSA})(TCNQ)_2$, $(TMTTA)(TCNQ)_2$, $(TMTSA)(TCNQ)_2$, but (TMTTeA)(TCNQ).[93] The electrical conductivity of the CTC varies over a broad range, from $8\ \Omega^{-1}\,cm^{-1}$ [for (2,3-DMTSA)(DBBS)] to $1.9 \times 10^{-9}\ \Omega^{-1}\,cm^{-1}$ [for $(6,7\text{-DMTSA})_2$(DMOTCNQ)]. This is apparently related to differences in the structures and CT values. For example, the strong donor TMTTeA and the very strong acceptor F_4TCNQ form an CTC with $\sigma_{rt} = 4.4 \times 10^{-6}\ \Omega^{-1}\,cm^{-1}$, whereas a weaker acceptor, DMTCNQ, forms a much more conducting CTC: $\sigma_{rt} = 4.6 \times 10^{-2}\ \Omega^{-1}\,cm^{-1}$. Since not all of the CTC were isolated as single crystals by the researchers cited,[93] their



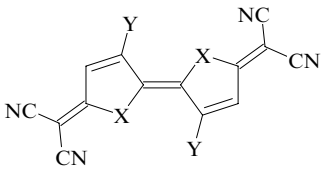
2,3-DMTTA (X = S),
2,3-DMTSA (X = Se),
2,3-DMTTeA (X = Te)



6,7-DMTTA (X = S),
6,7-DMTSA (X = Se)



TMTTA (X = S),
TMTSA (X = Se),
TMTTeA (X = Te)



DCBT (X = S, Y = Cl),
DBBS (X = Se, Y = Br)

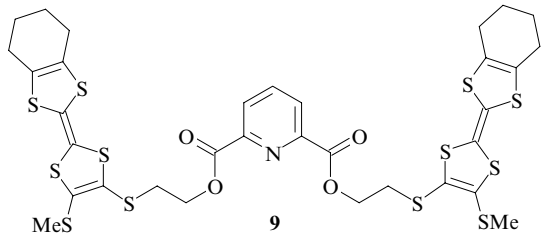
Figure 7. Structural formulae of the donors and acceptors used in Ref. 93.

structures can be considered based on the IR spectra: some CTC have an electron continuum in the IR region characteristic of high-conductivity CTC with segregated stacks. On the other hand, DMTCNQ forms mainly 2 : 1 complexes with alternating stacking: ···D···D···A···. The conductivity of these CTC is unusually high for an CTC with mixed-type stacks, reaching 0.95 Ω^{-1} cm^{-1}. This can be attributed to strong intra- and interstack interactions through the system of shortened contacts (shorter than the sum of the van der Waals radii). The complex (2,3-DMTSA)$_2$(DMTCNQ) has the highest CT (almost 100%) and high electrical conductivity: $\sigma_{rt} = 0.53\ \Omega^{-1}$ cm^{-1}.

The studies of CTC formed by TCNQ and other strong acceptors can currently be classified into two groups. On the one hand, this is the molecular design of new high-performance functional materials: self-ordering nanostructures, Langmuir–Blodgett films, nonlinear optical (NLO) materials, field-effect transistors, *etc*., on the other hand, this is the design of new narrow band-gap organic semiconductors, metals and superconductors. The latter trend includes search for structures and electronic properties of donors that ensure the production of highly conducting materials.

These problems are the subjects of reviews[94–96] published in 2004. Kaboub *et al*.[97] described the TCNQ-based CTC with the composition (**9**)$_2$(TCNQ)(CH$_2$Cl$_2$)$_2$ where donor **9** represents two TTF molecules separated by a pyridinodiester bridge.

Structure 9

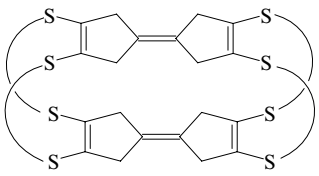


9

These donors are of interest as regards an increase in the dimensionality of the electron subsystem (quasi-2D or quasi-3D structures). In addition, the presence of the pyridine ring implies the possibility to obtain complexes with paramagnetic metal ions, which may serve to design magnetic conducting materials. The CTC reported by Kaboub *et al*.[97] contains mixed-type stacks; the CT value estimated from crystallographic data is close to zero, which is consistent with electrophysical measurements: $\sigma_{rt} = 2 \times 10^{-6}\ \Omega^{-1}$ cm^{-1}.

Experiments with solutions of a new belt-shaped donor **10** with TCNQ in deuterochloroform were reported.[98]

Structure 10



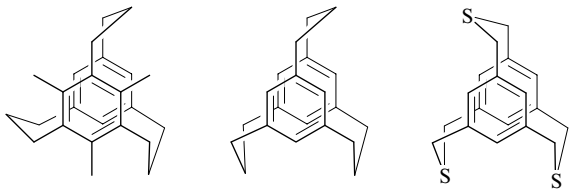
10

According to X-ray diffraction data, this donor crystallizes with two chloroform molecules inside the cavity. Upon the addition of a solution of this donor to a solution of TCNQ, the proton signals of the latter disappear from the ^{1}H NMR spectrum, while the signals of the donor are broadened, suggesting the formation of clathrates with TCNQ.

The properties of [3$_6$](1,2,3,4,5,6)cyclophane (**11**) have been studied.[99] Two equivalent conformers with C_{6h} symmetry are separated by an energy barrier of 10.9 kcal mol^{-1}; the interconversion of the conformers (flipping) affords effective D_{6h} structure. Cyclophane forms the CTC with TCNQ and 2,3,5,6-tetrafluorotetracyanoquinodimethane (F_4TCNQ). Both CTC are composed of mixed-type stacks but the crystals of (**11**)(TCNQ)(C$_6$H$_6$) contain D_{6h}-symmetric cyclophane molecules even at a temperature of 93 K, whereas in the crystals of (**11**)(F_4TCNQ), the symmetry of these molecules is C_{6h} (Scheme 1).

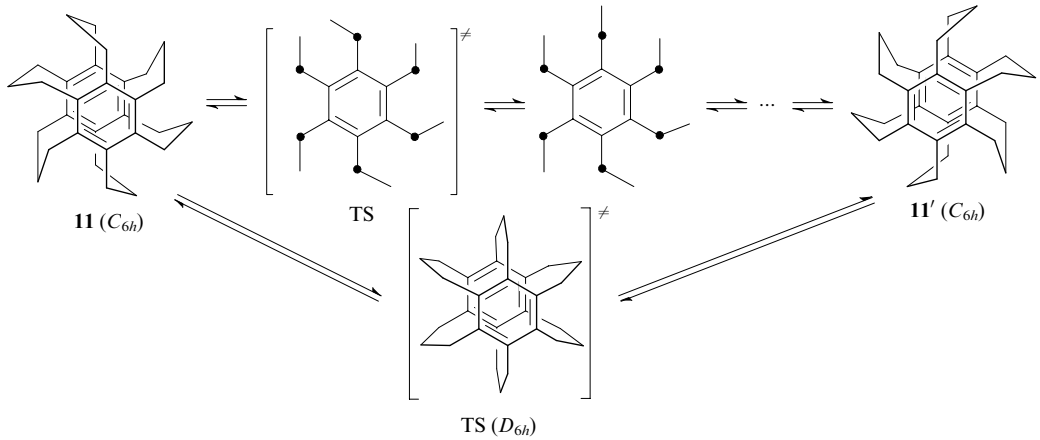
A minor structural modification of molecules **11** affects substantially the D : A overlap and the crystal packing of CTC. Yasutake *et al*.[100] studied the TCNQ CTC with the Me$_3$[3$_3$]CP (**12a**), [3$_3$]CP (**12b**) and S$_3$[3$_3$]CP (**13**) donors.

Structures 12, 13



12a **12b** **13**

Scheme 1



11 (C_{6h}) TS **11′** (C_{6h})

TS (D_{6h})

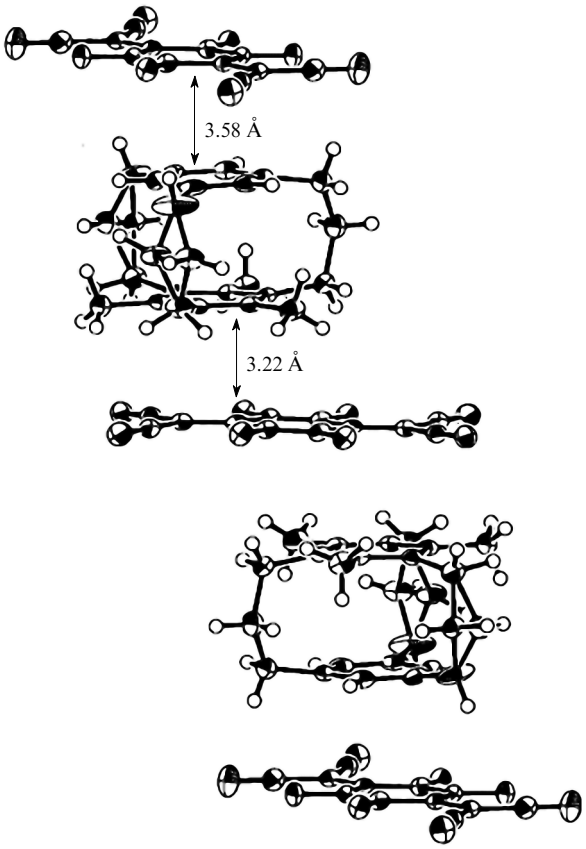


Figure 8. Mixed stacks ···D–A–D–A··· in the CTC ($Me_3[3_3]CP$)(F_4TCNQ).[100]

The molecule of $Me_3[3_3]CP$ (**12a**) has C_3 symmetry both in solution at 183 K and in the crystalline state (103 K), whereas the $[3_3]CP$ (**12b**) molecule has C_s symmetry. In the mixed-stacked CTC ($Me_3[3_3]CP$)(F_4TCNQ), the methyl-substituted benzene ring interacts with the acceptor more strongly than the unsubstituted ring. This is manifested as a considerable difference in the interplanar spacings (Fig. 8).

A shorter distance means stronger interaction. The $S_3[3_3]CP$ (**13**) molecules have C_s symmetry both in the free state and in the complex ($S_3[3_3$]CP)(F_4TCNQ). The structures of complexes with the donors $[3_3]CP$ and S_3 $[3_3]CP$ are similar; however, shorter interplanar spacing in the CTC ($[3_3]CP$)(F_4TCNQ) (2.93 Å) compared to 3.10 Å in ($S_3[3_3]CP$)(F_4TCNQ) implies, contrary to expectations, weakening of the donor properties upon the introduction of sulfur atoms. In the same way, no expected enhancement of intermolecular interaction is observed due to the possible shortened S···S contacts.[100]

An CTC formed by TCNQ with a macrocyclic pyrrolo TTF derivative **14** was described.[101] The authors suggested the possibility of clathrate formation with the acceptor in the macrocyclic cavity of the donor. However, according to X-ray diffraction data, the donor in the TCNQ-based CTC has a flattened configuration and cannot accommodate the acceptor molecules. Nevertheless, a clathrate CTC was prepared by using bis(tetrathiafulvalene)calix[2]pyrrole[2]-thiophene (**15**) (Fig. 9).[102]

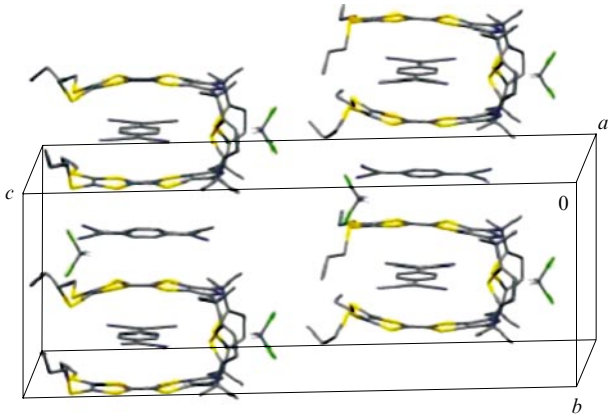
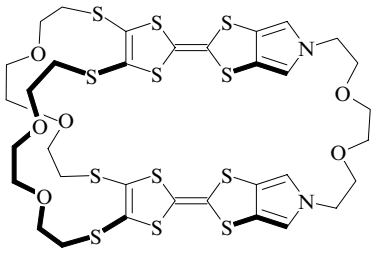


Figure 9. Packing of the molecules in the CTC (**15**)$(TCNQ)_2 \cdot CH_2Cl_2$.
The hydrogen atoms are omitted (except for those in the dichloromethane molecule).[102]

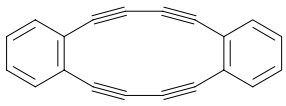
As can be seen in Fig. 9, one TCNQ molecule is located inside the receptor cavity and oriented in such a way that its longer axis is perpendicular to the longer axes of the TTF fragments. The other TCNQ molecule is located between the two neighbouring receptor molecules, its longer axis being parallel to the longer axes of the neighbouring TTF fragments.[102]

The TCNQ complex with an *o*-diethynylbenzene cyclic dimer (**16**) crystallizes in the host–guest fashion. In the CTC (**16**)(TCNQ), the TCNQ molecules are inserted in the host lattice so that the quinoid nucleus of TCNQ is positioned exactly at the centre of the dehydroannulene moiety.[103]

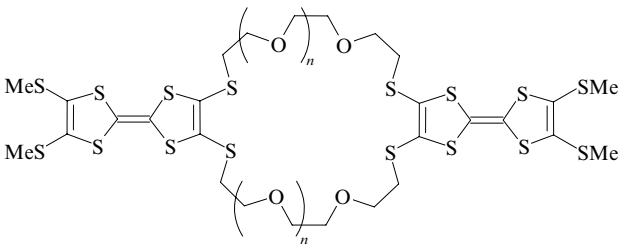
Structures 14, 16, 17



14



16



17a,b

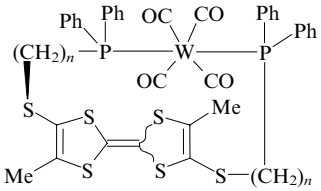
$n = 1$ (**a**), 2 (**b**)

One more interesting type of donors that are, in principle, able to form supramolecular structures are dimeric fulvalenes linked by crown-like macrocycles.

Akutagawa *et al.*[104] described donor molecules **17a**,**b** and the CTC (**17b**)$(F_4TCNQ)_2(DCE)_{1.5}$ (DCE is 1,2-dichloroethane). According to optical measurements,[104] this CTC is a radical ion salt containing dication $(\mathbf{17b})^{2+}$ and the radical anion $(F_4TCNQ)^{-\bullet}$. Despite the large cavity in the 30-membered macrocycle, radical anion pairs are located between the bulky macrocyclic cations.

A similar mixed type of packing was found in the TCNQ CTC with macrocyclic donors **18a**,**b**,[105] $(\mathbf{18a})_2(TCNQ)(MeCN)_3$ and $(\mathbf{18b})_2(TCNQ)(MeCN)_2$, in which the CT value is close to zero. The complexes have a sandwich structure of the type ···DAD···, the acceptor molecules being located between the TTF moieties of the metal macrocycles.[105]

Structures 18



18a,**b**

n = 3 (**a**), 4 (**b**)

An interesting example of self-assembly is the CTC formed by *trans*-1-ferrocenyl-2-pyrenylethene (**19**) with TCNQ (Fig. 10).[106]

Donor **19** is of interest for the fact that its height equal to 3.3 Å is optimal for effective π–π interaction between the donor and the acceptor, which may be responsible for the formation of the herringbone structure. This CTC shows an unusual temperature dependence of the electrical conductivity: below 176 K the conductivity varies according to the activation law and decreases from $2.8 \times 10^{-4}\ \Omega^{-1}\ cm^{-1}$, while at $T > 176$ K it also decreases, which is typical of metals. Nevertheless, a metal–dielectric transition at $T = 176$ K cannot be considered, as the absolute magnitude of σ is very low. In the authors' opinion,[106] some structural phase transition can take place at this temperature.

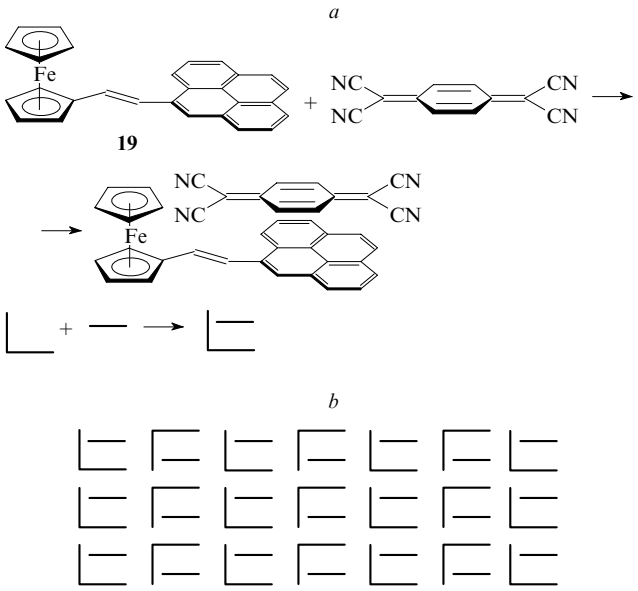
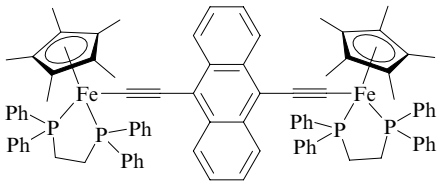
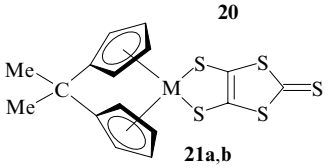


Figure 10. Formation of the CTC (**19**)(TCNQ) (*a*) and schematic view of a self-ordering stacked structure of the L-shaped donor molecules and planar acceptor molecules (*b*).[106]

Structures 20–23

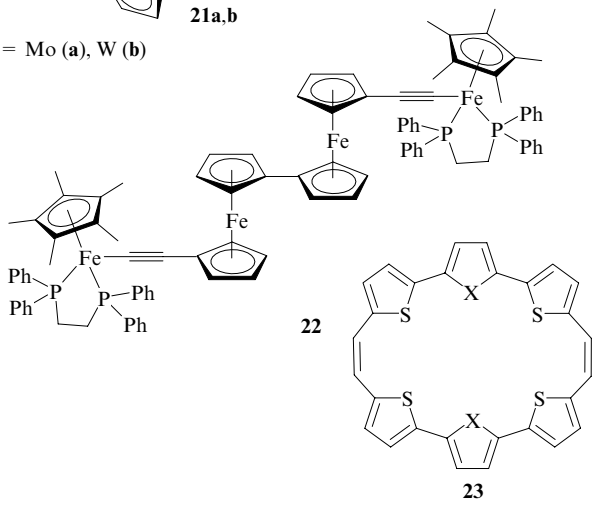


20



21a,**b**

M = Mo (**a**), W (**b**)



22

23

X = S, NMe

A number of papers[107–109] report the F_4TCNQ-based CTC with other ferrocene derivatives **20**–**22**, in particular, comprising a coordinated isotrithionedithiolate ion (dmit) (**21a**,**b**). The structure of one of these complexes is shown in Fig. 11.

The CTC formed by F_4TCNQ with 22-membered annulenes **23** were reported.[110] Relying on the IR spectroscopy data, the authors draw conclusion about a 100% CT in these complexes. Both CTC are narrow band-gap semiconductors. These data were obtained by the two-probe method the drawbacks of which as applied to organic semiconductors are well-known.

The mixed-stacked crystals are formed in the CTC of dimethylquaterthiophene (DMQtT) with F_4TCNQ (Fig. 12).[111] As can be seen from the Fig. 12, the donor and acceptor molecules alternate in neighbouring stacks forming layers. The CT value in this CTC is $q = 0.46 \pm 0.05$, *i.e.*, a L → H type transition cannot be ruled out. The charge transfer complex of α-sesquitiophene with F_4TCNQ can be obtained directly on the Au(111) surface.[112] This is accompanied by a considerable rearrangement of the donor and acceptor MO systems and new hybrid MO are formed; the HOMO is mainly located on the acceptor and the LUMO is

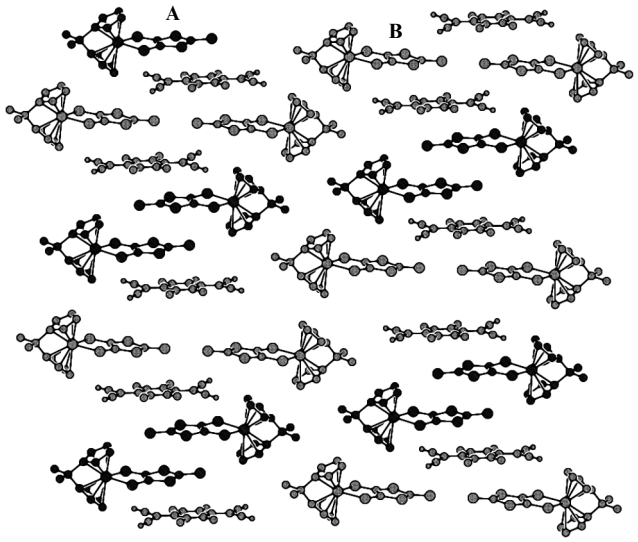


Figure 11. Packing of the molecules in the CTC (**21b**)$_2$(F_4TCNQ).[108]
A and **B** are two crystallographically non-equivalent molecules **21b**.

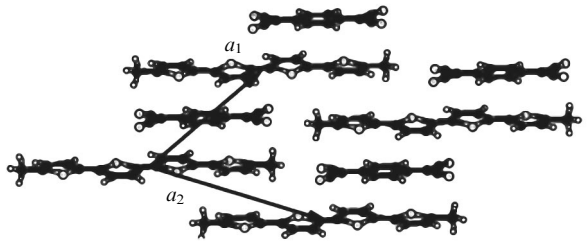


Figure 12. Projection of the crystal structure (space group *P*) of the CTC (DMQtT)(F_4TCNQ).[111]
a_1 = 10.185 Å, a_2 = 13.070 Å, a_3 = 6.842 Å; α = 118.56°, β = 98.92°, γ = 58.65°.

mainly located on the donor. In the electrophoretic measurements, jumpwise reversible switching of the semiconductor from the high-resistivity to low-resistivity state induced by electric field exceeding the threshold value was noted; this effect may find use in molecular electronic devices of a new type.[112]

3. Langmuir–Blodgett films based on charge transfer complexes

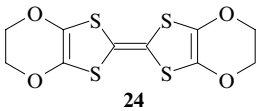
From the standpoint of practical application of CTC, of interest are the reported conducting Langmuir–Blodgett films.[113,114] These are complexes of octadecyltetracyanoquinodimethane with *p*-phenylenediamine and tetramethyl-*p*-phenylenediamine[113] and the CTC of 2-decyltetracyanoquinodimethane ($C_{10}H_{21}$-TCNQ) with bis(ethylenedioxy)tetrathiafulvalene (**24**).[114]

A sharp and irreversible increase in the electrical conductivity was noted in the films of (**24**)($C_{10}H_{21}$-TCNQ), $\sigma = 2\ \Omega^{-1}\ cm^{-1}$ being attained at 10 kbar. The researchers[114] attributed this to self-ordering of particles in the films.

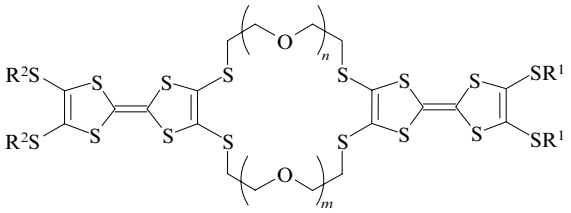
Amphiphilic macrocycles **25a–d** with two TTF moieties containing four alkyl chains form conducting Langmuir–Blodgett films with F_4TCNQ.[115]

The films can be formed on a mica surface. The complex (**25a**)(F_4TCNQ)$_2$ forms oriented nanofibres with typical dimensions $2 \times 50 \times 1000$ nm on a mica surface. The morphology of films based on the CTC Y(F_4TCNQ)$_2$ (Y = **25b–d**) considerably differs from the morphology of (**25a**)(F_4TCNQ)$_2$ films. More hydrophobic nature of the CTC (**25b**)(F_4TCNQ)$_2$ is manifested as the trend towards formation of two-dimensional layers from small spherical domains and no nanofibres are formed. The structure of the CTC (**25c**)(F_4TCNQ)$_2$ films is similar but in this case, the domains are polygonal rather that spherical. Leaf-shaped domains are formed in the films of the CTC (**25d**)(F_4TCNQ)$_2$. The typical size of these leaves is 1 μm^2. On keeping in air, the CT value gradually decreases from $(D^{2+})(F_4TCNQ^{-})_2$ to $(D^{2\delta+})(F_4TCNQ^{\delta-})_2$ ($\delta < 1$). Despite the similarity of the electronic structures of these CTC, their conductivities are noticeably different: (**25b**)(F_4TCNQ)$_2$ has σ_{rt} of $5 \times 10^{-4}\ \Omega^{-1}\ cm^{-1}$, while this value of CTC with donor **25c**,**d** is three orders of magnitude lower.[115] Charge transfer complexes of this type can find use for the design of nanoelectronic devices.

Structures 24, 25



24



25a–d

$n = m = 2$, R^2 = n-$C_{10}H_{21}$: R^1 = Me (**a**), n-$C_{10}H_{21}$ (**b**);
$R^1 = R^2$ = n-$C_{10}H_{21}$: $n = 2$, $m = 1$ (**c**); $n = m = 1$ (**d**)

4. Nanostructures formed by strong acceptors with graphene and other materials

A new carbon allotrope, graphene, is exceptionally promising for molecular electronics and nanotechnologies.[116] The extraordinary electronic properties of graphene are related to high quality of the 2D crystal lattice, resulting in exceptionally high carrier mobility of up to 200 000 $cm^2\ V^{-1}\ s^{-1}$.[117] However, the method used for graphene manufacture has a substantial influence on its properties. Thus the manufacture of graphene by top-down exfoliation of graphite gives a product with metallic impurities, which may change qualitatively the graphene properties.[118]

Of particular interest is the possibility to obtain graphene samples in solution; this requires the use of stabilizers. The same stabilizers that are used for functionalization of nanotubes are applicable here, *e.g.*, sodium 4-(pyren-1-yl)butyrate or poly(*m*-phenylenevinylene-co-2,5-dioctyloxy-*p*-phenylenevinylene) (PmPV).[119] However, these stabilizers contain bulky groups, which

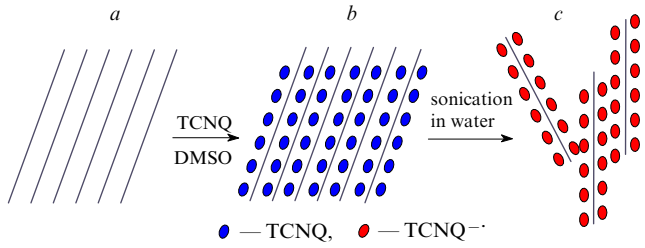


Figure 13. Chart of the preparation of an aqueous suspension of TCNQ-stabilized graphene.[120]
(*a*) Initial activated graphite obtained by annealing high-purity graphite at 1000 °C; (*b*) graphite intercalation with tetracyanoquinodimethane using DMSO; (*c*) long-term ultrasonic treatment gives an aqueous suspension of TCNQ-anion-stabilized graphene.

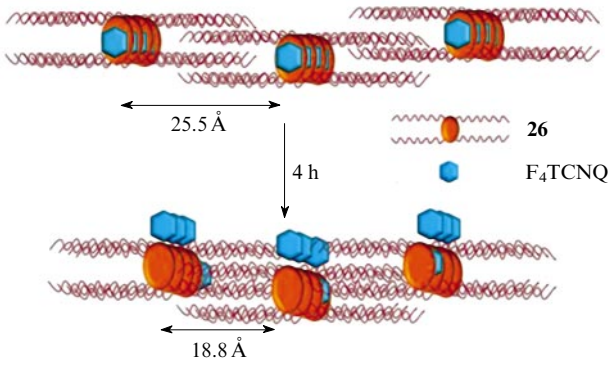


Figure 14. Time variation of the molecular structure of the CTC (**26**)(F_4TCNQ) in a 50% chloroform–methanol mixture (the CTC concentration is 10^{-4} mol litre^{-1}).[124]

markedly deteriorate the electrophysical properties of functionalized graphene.

In view of the dual behaviour of graphene (donor properties with respect to strong acceptors and acceptor properties with respect to strong donors), TCNQ can be used to functionalize graphene. Owing to the conjugation with the graphene lattice, it may promote the effective electron delocalization, thus increasing the electrical conductivity of graphene. This idea was successfully implemented in the manufacture of graphene from graphite in a solution containing TCNQ.[120] Figure 13 presents the chart for the preparation of an aqueous suspension of TCNQ-stabilized graphene.

Centrifuging of this suspension gives stabilized graphene as a powder suitable for the preparation of graphene suspensions in water or in polar organic solvents (DMF, DMSO).

From the physical standpoint, stabilization of graphene (electronic type of conduction) by acceptors can be considered as doping of graphene with holes. The electron affinity of TCNQ is 3.00 eV and that of F_4TCNQ is 5.2 eV.[3,4] According to theoretical calculations,[121] the degree of CT is 0.34 electrons per molecule for the graphene–TCNQ system and 0.4 electrons per molecule for the graphene–F_4TCNQ system. The TCNQ adsorption energy is 0.175 eV and that of F_4TCNQ is 0.198 eV. Thus, the adsorption is strong and the concept of CTC is quite applicable. The graphene properties change linearly with the concentration of the adsorbed acceptor, which opens up the way for controlled variation of the graphene properties.[121] It was shown by scanning tunelling microscopy that the adsorbed acceptor species are capable of self-assembling.[122] Attraction forces act between the TCNQ species, giving rise to a compact monomolecular layer; repulsion forces predominate between the adsorbed F_4TCNQ species; therefore, this coating is less dense and the adsorbed acceptor species retain the rotational degrees of freedom around the adsorption site.[122]

The ordered two-dimensional ionic layers consisting of the TCNQ$^{-\cdot}$ radical anions are fabricated on the Au(111) gold surface in the following way: alkali metal halides are sublimed and then deposited onto a gold substrate coated with adsorbed TCNQ molecules.[123] Chemisorbed TCNQ molecules react with the deposited lithium or sodium chloride to give a 2D ionic layer:

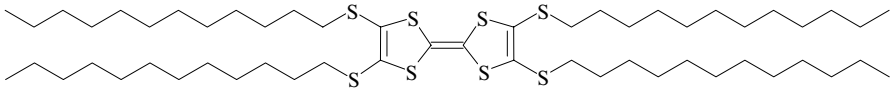
$$TCNQ + Cl^- \longrightarrow TCNQ^{-\cdot} + 1/2\,Cl_2$$

The size of these monolayers can reach several hundred nanometres.[123] The complexes of F_4TCNQ with hydrophobic (**26**) and amphiphilic (**27**) donors form ordered one-dimensional nanostructures[124] both in solution and on the substrate surface. A scanning electron microscopic examination demonstrated[124] that the CTC based on donor **27** retain the self-assembled fibrillar morphology, whereas the CTC based on donor **26** undergo spontaneous transition from the coaxial structure to a structure with segregated donor and acceptor species (Fig. 14).

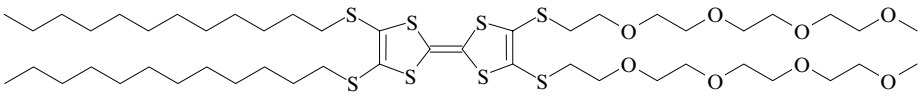
5. Design of new organic conductors

The design of polufunctional CTC-based materials implicates modification of the structure of the initial donor (TTF) and the search for new donors. Numerous organic metals and superconductors have been obtained along this route.[125–130] At the early stage of investigations of CTC-based organic metals, the opinion prevailed that components of conducting CTC should be highly symmetrical (at least D_{2h} symmetry) and the structures of donors and acceptors should be anti-complementary.[12,88] Further

Structures 26, 27

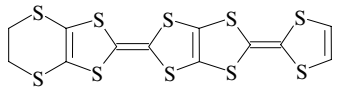


26

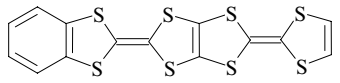


27

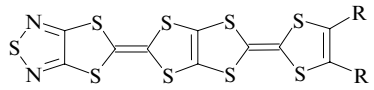
Structures 28–31



28

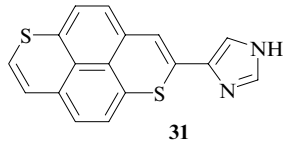


29



30a,**b**

R = Me (**a**), SMe (**b**)



31

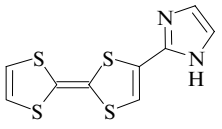
development of the theory and practice of organic metals demonstrated that this requirement is not obligatory. Indeed, unsymmetrical donor **28** forms TCNQ-based CTC, which is highly conducting (σ_{rt} = 77 Ω^{-1} cm^{-1}) and exhibits metallic properties down to helium temperatures.[131]

Complexes of TCNQ with structurally related donors **29** and **30a**,**b** are narrow band-gap semiconductors: the band gap width is 0.035–0.052 eV.[132]

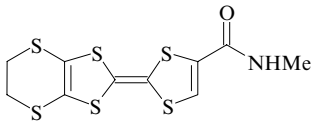
Symmetrical 1,6-diaminopyrene (**5**) forms TCNQ-based CTC with segregated stacks and very high degree of CT (0.9). Thus, the conduction band is occupied by 45%, which is expected to stabilize somewhat the metallic state. However, this CTC is a spin-Peierls semiconductor with a rather wide band gap: 0.8 eV below 40 K.[133] Unsymmetrical 2-(imidazol-4-yl)-1,6-dithiapyrene (**31**) capable of hydrogen bonding with the acceptor forms with TCNQ a charge transfer complex with segregated stacks in which the degree of CT is 0.6. This CTC is a narrow band-gap semiconductor: $\sigma_{rt} = 5.6 \times 10^{-2}$ Ω^{-1} cm^{-1}, the band gap width being 0.1 eV.[134] The effect of hydrogen bonding is manifested as the ability of highly unsymmetrical donors **32** and **33** to form CTC that behave as organic metals.[135,136] In particular, CTC (**32**)(CA) is composed of segregated donor and chloranil stacks and the degree of CT is 0.5. The hydrogen bonds and shortened S···S contacts make this system three-dimensional.[135] The value σ_{rt} = 124 Ω^{-1} cm^{-1}, *i.e.*, it is comparable with this value for the RCS (**33**)Cl·H_2O [σ_{rt} = 124 Ω^{-1} cm^{-1} (Ref. 137)], which retains the metallic properties down to 0.47 K. Complex (**32**)(CA) exhibits metallic properties down to 180 K, while below this temperature a 0.020 eV band gap appears.[135] Moore *et al.*[138] described the CTC based on TCNQ and other strong acceptors with a series of donors **34a**–**e** able to form intermolecular hydrogen bonds.

Complex (**34b**)(TCNQ) consists of mixed stacks ···DDAADD··· in which the *N*-methylthiocarbamoyl groups are hydrogen-bonded to the cyano nitrogen atoms of the acceptor. The CT value was estimated as 0.5.[138] Acceptor **35** forms with donor **34d** the CTC (**34d**)$_2$(**35**), which also has the mixed-stacked structure ···DDADDA··· but a very low degree of CT. In this case, the dipole–dipole

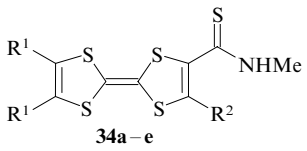
Structures 32–35



32

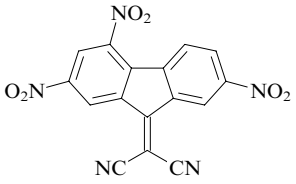


33



34a–**e**

$R^1 = R^2$ = H (**a**), Me (**e**);
R^1 = SMe, R^2 = H (**b**);
R^1–R^1 = $S(CH_2)_2S$, R^2 = H (**c**);
R^1 = Me, R^2 = H (**d**)

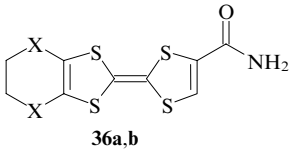


35

interaction predominates over the intermolecular hydrogen bonds.[138]

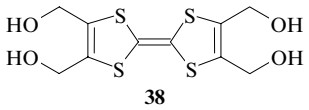
Carbamoyl derivatives **36a**,**b**, although having similar structure and slightly differing donor properties [the oxidation potential of **36a** is −0.40 V *vs.* saturated calomel electrode (SCE); the oxidation potential of **36b** is −0.50 V (SCE)] [139] are complexed with F_4TCNQ to form CTC that differ in the composition and structure. Indeed, the CTC (**36a**)$_2$(F_4TCNQ)$_2$ is composed of mixed stacks comprising alternating radical cation and radical anion dimers. The absence of interaction between the dimers accounts for the dielectric properties of this CTC. Donor **36b** forms 2 : 1 CTC, which is actually a radical ion salt: $\{(\mathbf{36b})_2\}^{+\bullet}(F_4TCNQ^{-\bullet})$.[139] In this CTC, the separate chains of dimers $\{(\mathbf{36b})_2^{+\bullet}\}_\infty$ are parallel to the chains of non-interacting radical anions.

Structures 36–38

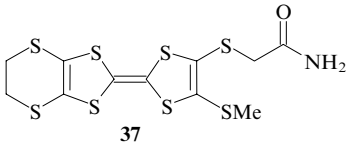


36a,**b**

X = O (**a**), S (**b**)



38



37

In the CTC of carbamoylmethylthio-substituted tetrathiafulvalene **37** with F_4TCNQ, the donors form face-to-face dimers and the acceptor and donor planes are nearly perpendicular (Fig. 15).[140]

As can be seen from this Figure, the intermolecular NH···O=C hydrogen bonds connect the donor dimers. However, judging by the length (2.96 Å), these bonds are rather weak. It is evident that this structure does not favour high conductivity; hence, this CTC is a semiconductor, $\sigma_{rt} = 1.4 \times 10^{-5}$ Ω^{-1} cm^{-1}.

Hydrogen bonds can also hamper the formation of conducting structures. Thus tetrakis(hydroxymethyl)tetrathiafulvalene **38** forms CTC (**38**)(F_4TCNQ) in which the CT is almost complete. Although the CTC crystal consists of segregated stacks, the planes of the donor and the acceptor in the neighbouring stacks are mutually perpendicular.

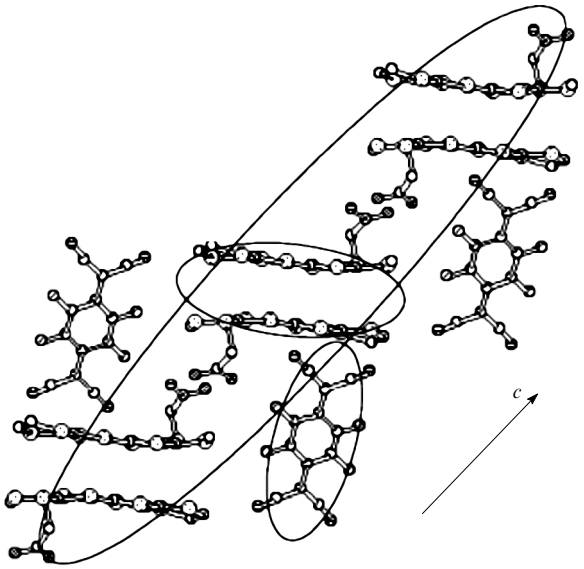
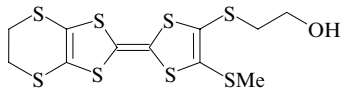
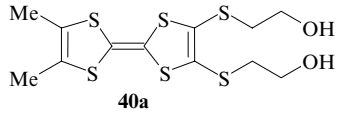


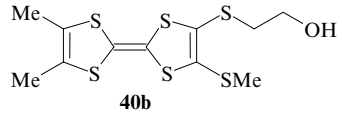
Figure 15. Crystal structure of the complex (**37**)(F_4TCNQ) projected along the *c* axis.[140]
The donors form a stepped structure with face-to-face overlap, the acceptor planes are perpendicular to the donor planes; some fragments are enclosed in ovals for clarity.

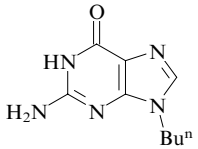
Strong hydrogen bonds connect radical cations **38** to form dimers. The radical anions are also dimerized. As a result, this CTC is a diamagnetic dielectric.[141] Hydroxyl-containing donor **39** able to form intermolecular hydrogen bonds reacts with TCNQ to give a mixed-stacked CTC with a very low electrical conductivity ($\sim 10^{-6}\ \Omega^{-1}\ cm^{-1}$).[142] The TCNQ complexes with other hydroxyl-containing donors **40a**,**b** are also dielectrics.[143] This is attributable to the formation of mixed stacks with almost complete CT.

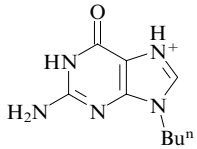
Structures 39–41


39


40a

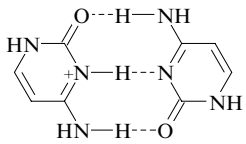

40b

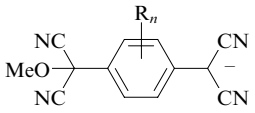

41 (Bu-G)


Bu-GH$^+$

The CTC with biologically active donors capable of forming intermolecular hydrogen bonds are of interest from the biochemical standpoint. Thus butylguanine (**41**, Bu-G) and fluorotetracyanoquinodimethane (FTCNQ) form a CTC representing a radical ion salt because it contains both neutral and cationic forms, the butylguaninium ion. The complex (Bu-G)(Bu-GH$^+$)(FTCNQ$^{-\bullet}$) is a dielectric due to the strong antiferromagnetic interaction of radical anions, the arising pairs being separated by butyl groups.[144] The same type of CTC is formed by cytosine, which reacts with 2,5-diethyltetracyanoquinodimethane to give the complex (CHC$^+$)(Et_2TCNQ$^{-\bullet}$) (CHC$^+$ is hemiprotonated cytosine pair, **42**).

Structures 42, 43


42 (CHC$^+$)


(**43**)$^-$
(R-TCNQ-OMe)$^-$
R_n = H, F_4, CF_3, 2,5-F_2, F

The structure of this CTC is composed of CHC$^+$ cationic layers constructed *via* complementary hydrogen bonds and π-electron interaction, and intermolecular hydrogen bonds with Et_2TCNQ$^{-\bullet}$ give rise to segregated bilayers.[145] Thus, this CTC contains uniform segregated stacks of Et_2TCNQ$^{-\bullet}$ radical anions, which are retained down to helium temperatures: they exhibit neither Mott instability nor spin-Peierls instability.[145] Magnetic measurements demonstrate strong antiferromagnetic coupling ($J/k_B = -500$ K), which is much weaker than in the similar complex (CHC$^+$)(TCNQ$^{-\bullet}$) ($J/k_B = -700$ K).[145] This can be attributed to a decrease in the overlap integrals in the stacks due to steric influence of the ethyl groups.

More detailed investigation of the cytosine CTC with various TCNQ derivatives and anion **43** has been reported.[146] The authors distinguish three groups of CTC: group I comprises ionic salts containing anion (**43**)$^-$

Table 2. Composition and electrophysical properties of CTC based on cytosine (C).[146]

Group	CTC	$\sigma_{rt}/\Omega^{-1}\ cm^{-1}$ (Δ/eV)
I	(CHC$^+$)(F_4TCNQ-OMe)(H_2O)	see [a]
I	(CHC$^+$)(CF_3TCNQ-OMe)(H_2O)$_{0.5}$	see [a]
I	(C_2HC$^+$)(F_2TCNQ-OMe)(H_2O)$_{0.5}$	see [a]
I	(CHC$^+$)(FTCNQ-OMe)(H_2O)	see [a]
I	(CHC$^+$)(TCNQ-OMe)(H_2O)$_{0.9}$	see [a]
I	(CHC$^+$)(MeTCNQ-OMe)(H_2O)$_{0.3}$(MeCN)	see [a]
II	(CHC$^+$)(F_4TCNQ$^{-\bullet}$)	$(5.3-6.4)\times10^{-9}$ (0.17)
II	(CHC$^+$)(F_2TCNQ$^{-\bullet}$)	$(1.0-1.4)\times10^{-3}$ (0.21)
II	(CHC$^+$)(FTCNQ$^{-\bullet}$)	5.8×10^{-4} (0.17)
II	(CHC$^+$)(TCNQ$^{-\bullet}$)	$(2.7-3.2)\times10^{-2}$ (0.14)
II	(CH$^+$)(TCNQ$^{-\bullet}$)(H_2O)$_{0.5}$	1.1×10^{-4} (0.12)
II	(CHC$^+$)(Et_2TCNQ$^{-\bullet}$)	$(0.4-1.3)\times10^{-4}$ (0.18)
III	(CHC$^+$)(MeTCNQ$^{0.5-\bullet}$)$_2$	27–72 (see [b])
III	(C_2HC$^+$)$_2$(Me_2TCNQ$^{2/3-\bullet}$)$_3$(H_2O)	$(2.6-4.7)\times10^{-2}$ (0.081–0.085)

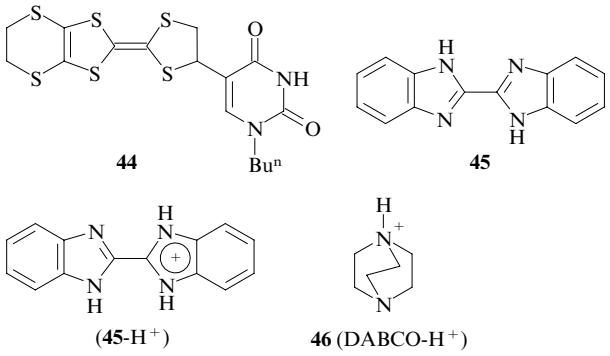
[a] Dielectric; [b] metal, T_{max} = 273–289 K.

(formed upon methanolysis of TCNQ); group II includes fully ionic radical anion salts; and group III includes CTC with partial CT and uniform or non-uniform charge distribution. The properties of these CTC are summarized in Table 2.

As can be seen from Table 2, minor structural and electronic modifications of TCNQ can be utilized to vary the electrophysical properties of the cytosine CTC over a broad range, from dielectrics to metals. The CTC $(CHC^+)(MeTCNQ^{0.5-\bullet})_2$ has the highest conductivity among the CTC based on biomolecules, being superior to another high-conductivity CTC formed by donor **44** with an *N*-butyluracil moiety.

Owing to the presence of complementary hydrogen bonds and π–π and S···S interactions, the complex $(\mathbf{44})_2$(TCNQ) acquires a structure favourable for high electrical conductivity (σ_{rt} = 2.1 Ω^{-1} cm^{-1}).[147]

Structures 44–46

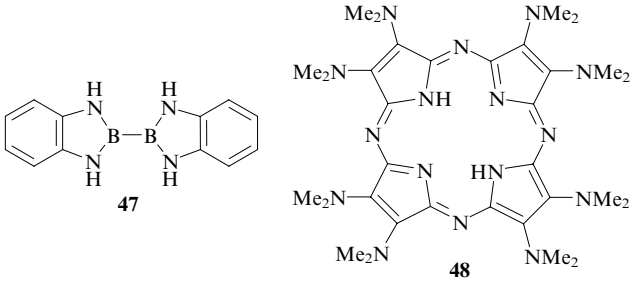


Fascinating supramolecular structures are formed by CTC based on 2,2′-bi(1*H*-benzimidazole) (**45**).[148–149] Owing to neutral bi(benzimidazole), the supramolecular salt $(\mathbf{45})(\mathbf{45}\text{-}H^+)_2Cl_2$ exhibits donor properties with respect to TCNQ. As a result, the supramolecular product $(\mathbf{45})(\mathbf{45}\text{-}H^+)_2(TCNQ)Cl_2$ is formed. The degree of CT in this complex was estimated as 0.5.[148] At room temperature, $\sigma_{rt} = 10\ \Omega^{-1}\ cm^{-1}$, and on cooling the conductivity increases. The metallic state is retained down to 250 K. At temperatures above 200 K, the superionic (proton) conductivity also appears.[149] Thus, the system of hydrogen bonds facilitates the hybrid electron–proton conductivity.

Hydrogen bonds influence considerably the electrophysical properties of the CTC $(DABCO\text{-}H^+)_2(TCNQ)_3$ (DABCO-H$^+$ is protonated 1,4-diazabicyclo[2.2.2]octane, **46**). This CTC, which contains TCNQ species with the formal charge of −2/3, is composed of segregated stacks. At room temperature, the conductivity is $5\times10^{-3}\ \Omega^{-1}\ cm^{-1}$, while that of the deuterated analogue $(DABCO\text{-}D^+)_2(TCNQ)_3$ is $10^{-2}\ \Omega^{-1}\ cm^{-1}$; the band gap widths are 0.28 and 0.25 eV, respectively.[150] This difference can be attributed to the contribution of proton conductivity. A study of the temperature dependence of the dielectric constant revealed an order–disorder dielectric phase transition in the system of hydrogen-bonded protons. This is confirmed by the large isotope effect: in the crystals of $(DABCO\text{-}H^+)_2(TCNQ)_3$, this transition occurs at 306 K and in the crystals of $(DABCO\text{-}D^+)_2(TCNQ)_3$, it takes place at 376 K.[150]

A peculiar donor able to form intermolecular hydrogen bonds is diborane derivative **47**.

Structures 47, 48



In the complex $(\mathbf{47})(TCNQ)_2$, there are actually N–H···N bonds with the cyano nitrogen atoms of the acceptor but the structure rather corresponds to co-crystals because the degree of CT is negligibly small, resulting in dielectric properties.[151]

As regards the design of new conducting molecular magnets, noteworthy is octakis(dimethylamino)porphyr-

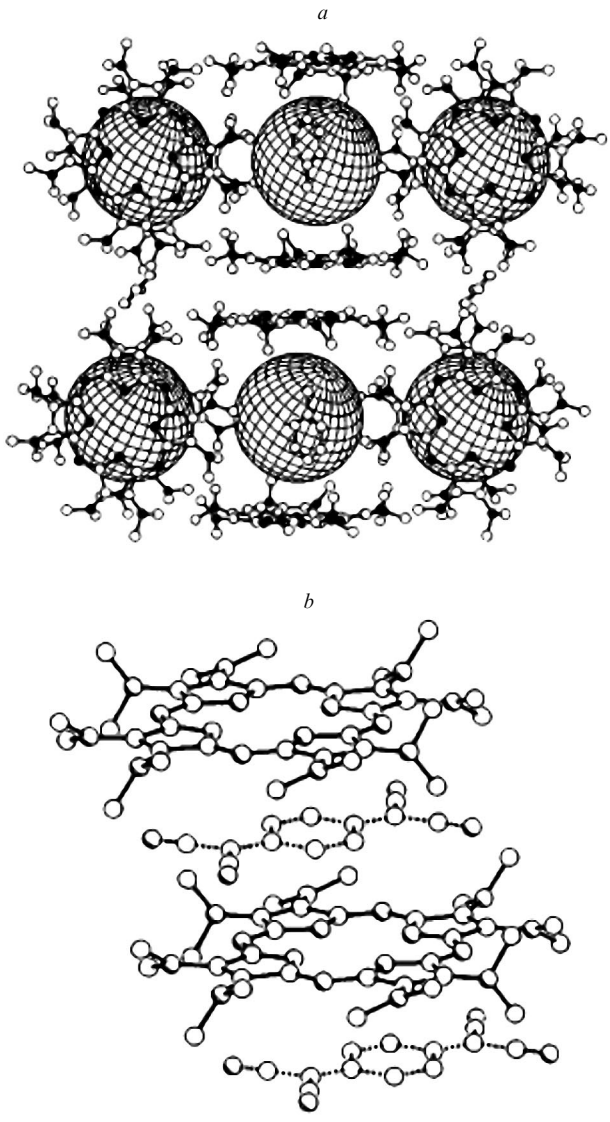


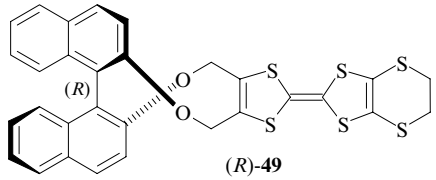
Figure 16. Packing of the donor and acceptor molecules in the crystals of CTC $(\mathbf{48})_2C_{60}$ (*a*) and (**48**)(TCNQ) (*b*).[153]

azine (**48**) reported by Mani *et al.*[152] The donor properties make this compound suitable for the synthesis of conducting CTC, and due to the ability to form complexes with transition metal cations, it can be used to fabricate magnetic materials. Porphyrazine **48** forms CTC with such acceptors as fullerene C_{60} and TCNQ. In the former case, the CTC $(\mathbf{48})_2C_{60}$ is formed, while in the latter case, the CTC is (**48**)(TCNQ).[153] The packing type in the structures of these CTC is shown in Fig. 16.

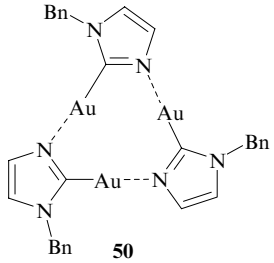
In the former CTC, the degree of CT is low but in the latter complex, the CT may be almost complete: according to the crystallographic data, the CT value is 0.17; however, analysis of the IR spectra is indicative of almost complete (1.00) CT. This is indirectly confirmed by diamagnetism of the CTC (**48**)(TCNQ), which implies strong donor–acceptor exchange coupling.[153]

Among the hybrid polyfunctional materials that combine at least two different properties, of interest are chiral conducting materials. This is related first of all to attempts to disclose the so-called electrical magnetochiral anisotropy, which was predicted theoretically and confirmed experimentally in a study[154] dealing with chiral carbon nanotubes. Currently, several conducting enantiomerically pure TCNQ-based CTC have been synthesized.[155–158] For instance, Saad *et al.*[155] described CTC based on asymmetric tetrathiafulvalene **49**.

Structures 49, 50



(*R*)-**49**



50

The oxidation potential of fulvalene **49** is 0.49 V (SCE), whereas the reduction potential of TCNQ is 0.17 V (SCE). This means that TCNQ cannot oxidize donor **49** to a radical cation. However, the reduction potential of F_4TCNQ is 0.53 V (SCE). Therefore, the researchers cited[155] prepared the enantiomerically pure CTC [(*R*)-**49**](F_4TCNQ)(CH_2Cl_2) and [(*S*)-**49**](F_4TCNQ)(CH_2Cl_2) and the corresponding racemate. The complexes were composed of segregated stacks of the acceptors and the donors, and owing to almost complete CT, they can be classified as radical ion salts. Notably, radical cations **49** are also able to be stacked despite the presence of the bulky binaphthol substituents. The strong dimerization in the stacks (indeed, the interplanar spacings within the dimers in the donor stacks are 3.35–3.43 Å, whereas those between the dimers are ~3.8 Å) results in the singlet ground state.

The trinuclear gold(I) complex **50** is an interesting example of CTC based on organometallic donors. With TCNQ, it forms the complex $(\mathbf{50})_2$(TCNQ) in which the

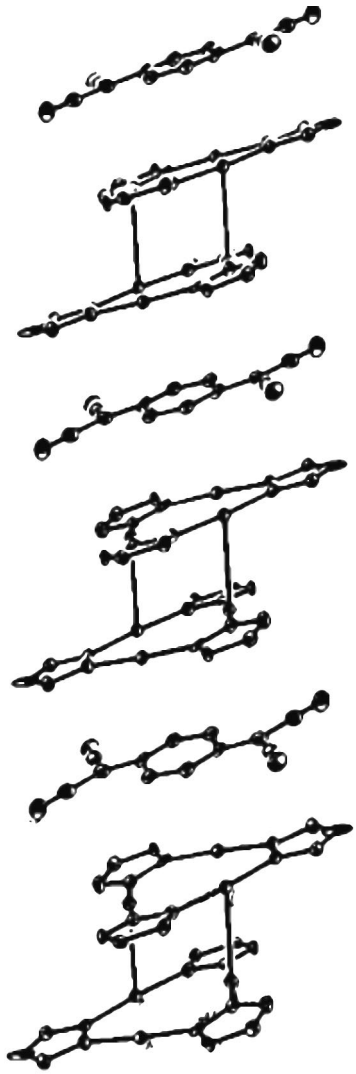


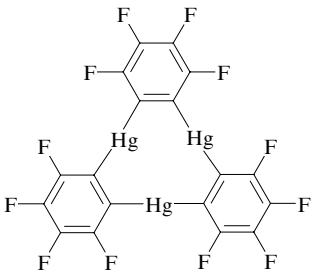
Figure 17. Packing of donor **50** and TCNQ species in the CTC $(\mathbf{50})_2$(TCNQ) (benzyl groups are omitted for the sake of simplicity).[159]

TCNQ molecule is sandwiched by dimers of the donor molecules formed through aurophilic interactions (Fig. 17).

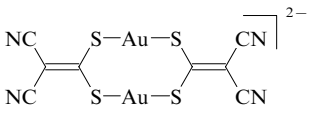
Hence, this CTC can be described by the formula (π-**50**)(μ-TCNQ)(π-**50**). Aurophilic bonds are formed between four of the six Au^I ions. These intermolecular bonds are very short (3.152 Å), being much shorter than the Au···Au distances within the molecule, which are 3.475, 3.471 and 3.534 Å. In the opinion of Rawashdech-Omary *et al.*[159] this CTC could find use in optoelectronics and as a sensor for volatile organic compounds.

A similar trinuclear mercury(II) complex also forms the complex $(\mathbf{51})_2$(TCNQ) with TCNQ; however, this cannot be classified as CTC, and compound **51** should be regarded as a Lewis acid. The plane of the TCNQ molecule is perpendicular to the planes of **51**, and therefore mercury atoms coordinate the cyano nitrogen atoms of the acceptor.[160] Note that in this case, no $Hg^{II}-Hg^{II}$ bonds are formed, which confirms the opinion[159] about the important role of the acceptor for the formation of these bonds: in complex $(\mathbf{51})_2$(TCNQ), the donor–acceptor interaction is absent.

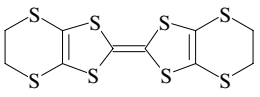
Structures 51 – 53



51



52



53 (ET)

Gold(I) complex with 1,1-dithio-2,2-dicyanoethylene, bis(μ-2,2-dicyanoethylene-1,1-dithiolato-*S*,*S*′)diaurate(I) anion (**52**), is not only a structural analogue of TCNQ but is also prone to form CTC. For example **52** and bis(ethylenedithio)tetrathiafulvalene (**53**, ET) form, the CTC [(**53**)$_2$(**52**)]. This is a complex with mixed stacks in which the complex anion is arranged between two donor molecules. Despite the mixed type of packing, this CTC is a narrow band-gap semiconductor: $\sigma_{rt} = 0.03\ \Omega^{-1}\ cm^{-1}$, the band gap being 0.38 eV.[161]

6. Metals and superconductors based on charge transfer complexes

An important area of molecular electronics is the design of new CTC-based organic metals. The charge transfer complex TTF(TCNQ) in which the metallic state is retained to 54 K is known [13] to be the first organic metal of this type. In 1978, the CTC ET(TCNQ) and PT(TCNQ) [PT is bis(propylenedithio)tetrathiafulvalene], were synthesized.[162] The electrical conductivity (σ_{rt}) measured for pellet samples proved to be higher than that of TTF(TCNQ), namely, 50 and 80 $\Omega^{-1}\ cm^{-1}$, respectively, as compared with 20 $\Omega^{-1}\ cm^{-1}$ for TTF(TCNQ). This is obviously related to the clear-cut two-dimensional character of conduction of the ET- and PT-based CTC.

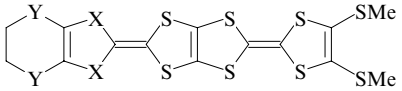
In 1986, it was found that the reaction of **53** (ET) with TCNQ gives two phases: a monoclinic phase composed of mixed stacks (···DADA···) and a triclinic phase containing one-dimensional TCNQ stacks and two-dimensional layers of ET molecules.[163] The triclinic modification behaves as an organic metal at temperatures above 330 K, while below this temperature the complex is dielectric. The nature of the metal – dielectric transition in the triclinic crystals of the CTC ET(TCNQ) is the subject of a number of publications.[164 – 166] Relying on the results of electrophysical and magnetic measurements [164] and ^{1}H and ^{13}C NMR data,[165, 166] it can be considered proven that the transition at 330 K is a Mott – Hubbard rather than a Peierls transition, *i.e.*, a transition to the magnetic dielectric state.

The influence of the pressure on the properties of CTC ET(TCNQ) was studied.[167] At a 50 kbar pressure, an irreversible transition to a new phase occurs accompanied by a change in the sign of the derivative $d\sigma/dp$. This might be the third phase of this CTC discovered in 2003.[168] It is noted that it is formed only in the presence of a catalytic amount of tetraiodoethylene. This phase, which is usually designated by β″-ET(TCNQ), is metallic and remains metallic down to helium temperature with anomalies exhibited at 170, 80 and 20 K.[168, 169]

The search for new organic metals includes the use of halogenated donors and TCNQ and modification of the proper fulvalene structure by increasing the number of chalcogen atoms in the molecules.

Aragaki *et al.*[170] described the CTC TCNQ with donors **54a – c** containing 12 chalcogen atoms.

Structures 54



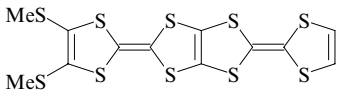
54a – c

X = Y = S (**a**); X = Se, Y = S (**b**); X = S, Y = Se (**c**)

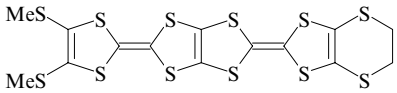
The complex (**54b**)$_2$(TCNQ) is unusual by the fact that it contains isolated $TCNQ^{-\bullet}$ radical anions, the CT value in it being 1. The structure of this CTC and the CTC (**54a**)$_2$(TCNQ) corresponds to the so-called θ-type (see, for example, Ref. 171). Thus, the electrical conductivity of the CTC is determined only by stacks of donors. The value $\sigma_{rt} = 1 - 10\ \Omega^{-1}\ cm^{-1}$ varies according to the activation law at $T < 120$ K. The nature of the semiconductor state of the complex (**54b**)$_2$(TCNQ) was studied by EPR.[170] The intensity of the EPR signal starts to decrease at temperatures below 200 K, and at 120 K the signal width sharply increases. This attests to magnetic ordering by formation of spin density waves. The temperature of this transition coincides with the metal – dielectric transition (M → I) temperature. The complex (**50a**)$_2$(TCNQ) also undergoes a M → I transition at 120 K, giving, however, a paramagnetic dielectric phase (Mott transition). This difference can be caused by the decrease in the Coulomb integral (U) upon introduction of selenium atoms having higher polarizability. The M → I transitions induced by magnetic ordering have also been observed in θ-phases such as the RCS (ET)$_2$Cs[Zn(SCN)$_4$] (20 K) and (MDT-TTF)$_2$[Au(CN)$_2$] (20 K) (MDT-TTF is methylenedithiotetrathiafulvalene).[170] Thus, the complex (**54b**)$_2$(TCNQ) has the highest temperature of transition to the magnetic dielectric state. This is important as the superconducting phase of organic conductors is usually formed at temperatures close to the temperature of the formation of the antiferromagnetic phase.

Complexes with segregated stacks are also formed from TCNQ and unsymmetrical donors **55a**,**b**. Both CTC, (**55a**)(TCNQ)(TCE) (TCE is 1,1,2-trichloroethane) and (**55b**)(TCNQ), are organic metals:[172] σ_{rt} is 200 $\Omega^{-1}\ cm^{-1}$ for the former and 14 $\Omega^{-1}\ cm^{-1}$ for the latter; the conductivity decreases on cooling, *i.e.*, a metallic type behaviour is manifested. The M → I transitions occur at 100 K.

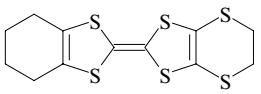
Structures 55 – 57



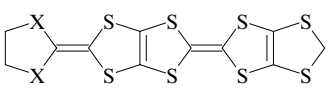
55a



55b



56



57a,**b**

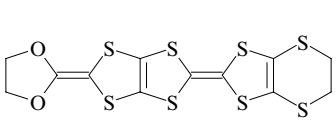
X = O (**a**), S (**b**)

Unsymmetrical donor **56** also forms segregated-stacked CTC with TCNQ. The electrical conductivity of the CTC (**56**)(TCNQ) is $0.8\ \Omega^{-1}\ cm^{-1}$ and the band gap is 50 meV.[173] The Curie type paramagnetic susceptibility is retained down to 2 K; hence, this CTC is a Mott type magnetic dielectric.

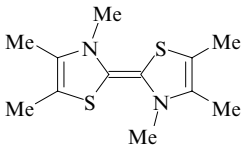
The properties of an organic metal are inherent in the CTC (**57a**)(TCNQ) with the $M \rightarrow I$ transition at 280 K, whereas the complex (**57b**)(TCNQ) is a narrow band-gap semiconductor: $\sigma_{rt} = 1.1 \times 10^{-2}\ \Omega^{-1}\ cm^{-1}$, the band gap is 200 meV.[174]

The replacement of TCNQ by a stronger acceptor, F_4TCNQ, results in a sharp increase in the electrical resistance: indeed, for the CTC (**57a**)(F_4TCNQ), $\sigma_{rt} = 8.7 \times 10^{-5}\ \Omega^{-1}\ cm^{-1}$, $\Delta = 260$ meV [for (**57a**)(TCNQ), $\sigma_{rt} = 63\ \Omega^{-1}\ cm^{-1}$]. The increase in the CT upon the use of stronger acceptor leads to an increase in the Coulomb integrals and thus facilitates the Mott–Hubbard transition.

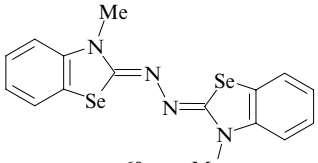
Structures 58–61



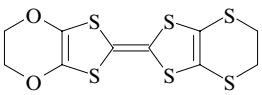
58



59



60



61

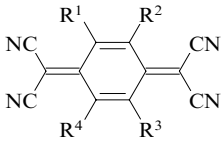
The replacement of the methylene group in **57a** by an ethylene group gives rise to donor **58**. With TCNQ it forms an CTC that shows metallic properties even when taken as pressed pellet samples ($\sigma_{rt} = 12\ \Omega^{-1}\ cm^{-1}$).[94]

Hexamethyldithiadiazafulvalene (**59**) and TCNQ form the CTC (**59**)$(TCNQ)_3$[175] containing the dication $(\mathbf{59})^{2+}$; therefore, the TCNQ oxidation state is $-2/3$. Although selenium-containing azine **60** forms an CTC with TCNQ, this CTC should rather be treated as resulting from co-crystallization, as the CT value is close to zero and no EPR signal is recorded. The CTC structure is composed of mixed-type stacks.[176] The same is true for the sulfur-containing analogue of donor **60**.[177]

Saito *et al.*[178] reported 35 CTC based on donor **61**, which is a sort of hybrid of molecules **24** and **53**. As acceptors, the authors employed TCNQ and its derivatives **62a–j**, fluoranil, chloranil, bromanil and iodanil, *p*-benzoquinone derivatives **63a–e**, naphthoquinone derivatives **64a**,**b**, fluorenes **65a–d**, hexacyanobutadiene (**66**), 4,4′-dinitrobiphenyl (**67**), 4,4′-dihydroxy-3,3′,5,5′-tetranitrobiphenyl (**68**) and fullerene C_{60}.

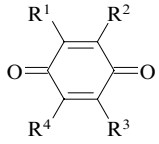
On the grounds of extensive experimental data, the authors classified all CTC into five groups in terms of their structural and electrophysical properties. Highly conducting CTC with segregated stacks and partial CT were assigned to group **A**; the CTC with partial CT but mixed-type stacks were placed into group **B**; essentially neutral clathrate-type CTC were put into group **C**; the CTC with low CT and mixed-type stacks were classified into group **D**;

Structures 62, 63



62a–j

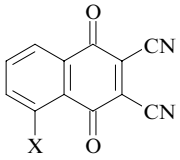
Compounds **62**	R^1	R^2	R^3	R^4
a	F	F	F	F
b	F	H	F	H
c	F	H	H	H
d	CF_3	H	H	H
e	Me	H	H	H
f	Me	H	Me	H
g	Et	H	Et	H
h	MeO	H	MeO	H
i	EtO	H	EtO	H
j	NSN		NSN	



63a–e

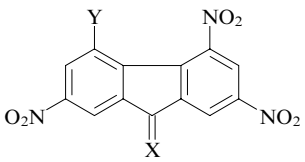
Compounds **63**	R^1	R^2	R^3	R^4
a	CN	CN	I	I
b	CN	CN	Cl	Cl
c	CN	CN	H	H
d	Cl	OH	Cl	OH
e	Br	OH	Br	OH

Structures 64, 65



64a,**b**

X = H (**a**), NO_2 (**b**)



65a–d

Compounds **65**	X	Y
a	$C(CN)_2$	NO_2
b	$C(CN)_2$	H
c	O	NO_2
d	O	H

and dielectric complexes with virtually 100% CT were in group **E**. In Table 3 presents data on the composition and electrophysical properties of CTC based on donor **61**.

The data of the cited paper[178] attest that donor **61** is capable of self-aggregation similarly to donor **24**. This is manifested in the formation of some CTC that behave as organic metals and narrow band-gap semiconductors. This capability, however, is less pronounced in compound **61** than in compound **24**. As can be seen from Table 3, only 10 out of the 35 CTC based on donor **61** behave as organic metals. Meanwhile, metallic properties were found for three-fourths of the 37 reported[179] CTC based on donor **24**. The lower ability to form self-ordered structures shows itself as the formation of mixed-type stacks in the CTC with the $(MeO)_2$TCNQ (**62h**) (group **B**) and iodanil (group **C**) acceptors. The CTC structures with fullerene C_{60} (group **D**) are also substantially different, one containing bent molecules **61** and 1D stacks of C_{60} molecules and the other containing planar molecules **61** and 2D layers of C_{60}. In the CTC with F_4TCNQ (group **E**), antiferromagnetic ordering takes place at 7 K. Interestingly, the temperature of this

Table 3. Composition and electrophysical properties of CTC based on donor **61**.[178]

Acceptor	Composition: D : A : (Solv)[a]	σ_{rt} /Ω^{-1} cm^{-1}	Δ /eV	$T_{M\to I}$ /K
66	—	12(P)[b]	—	120
66	1 : 1	$<10^{-8}$	—	—
62a (F_4TCNQ)	1 : 1	1.8×10^{-6}(P)	160	—
63b	7 : 8 : (2 H_2O)	0.67(P)	16	—
63a	2 : 1 : (0.5 H_2O)	3.6(P)	25	—
62d (CF_3TCNQ)	2 : 1	5.8(P)	—	250
62b (F_2TCNQ)	2 : 1 : (H_2O)	35(P)	—	15
64b	7 : 4 : (4 H_2O)	0.23(P)	76	—
63c	—	$<10^{-8}$	—	—
62c (FTCNQ)	1 : 1	7.7(P)		100
65a	2 : 1 : (MeCN)	0.83(P)	120	—
TCNQ	1 : 1	7.7	—	165–100
64a	2 : 1	3.5(P)	30	—
62e (MeTCNQ)	4 : 3	1.3(P)	—	100
62g (Et_2TCNQ)	2 : 1	15(P)	—	120
62f (Me_2TCNQ)	1 : 1	$<10^{-8}$	—	—
62h ($(MeO)_2$TCNQ)	2 : 1	$<10^{-8}$	—	—
FA	—	$<10^{-8}$	—	—
FA	—	3.1×10^{-3}(P)	130	—
CA	8 : 9 : (H_2O)	2.9(P)	—	200
BA	3 : 2	$<10^{-8}$	—	—
62j	3 : 2	23(P)	—	200
62j	1 : 1	$<10^{-8}$	—	—
62j	1 : 2	$<10^{-8}$	—	—
65b	1 : 1	3.2×10^{-9}	420	—
62i ($(ETO)_2$TCNQ)	2 : 1	$<10^{-8}$	—	—
IA	2 : 1	$<10^{-8}$	—	—
63e	—	14	—	260
63e	—	$<10^{-8}$	—	—
63d	—	1.8(P)	24	—
65c	—	$<10^{-8}$	—	—
65d	4 : 3	$<10^{-8}$	—	—
C_{60}	1 : 1 : (PhH)	$<10^{-8}$	—	—
68	—	$<10^{-8}$	—	—
67	6 : 5	$<10^{-8}$	—	—

[a] Solv is solvent; [b] (P) means measurements on a polycrystalline sample.

transition is intermediate between the transition temperatures in the CTC (**24**)(F_4TCNQ) (5.4 K) and (**53**)(F_4TCNQ) (14 K).[178]

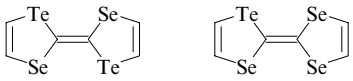
Donor **24** forms the CTC (**24**)$_2$(CF_3TCNQ) consisting of segregated stacks of the donor and the acceptor radical anions, the CT being 0.5. The compressed pellet samples exhibit the metallic type of dependence of electrical resistance down to 1.8 K.[180]

It is known[12,181] that the replacement of all sulfur atoms in TTF by selenium (TSeF) and tellurium (TTeF) atoms increases the stability of the metallic state and increases the conductivity of the TCNQ-based CTC.

CTC	σ/Ω^{-1} cm^{-1}	$T_{M\to I}$/K
TTF(TCNQ)	500	54
TSeF(TCNQ)	800	28
TTeF(TCNQ)	2200	2

Of interest are donors in which the selenium atoms are partly replaced by tellurium. In particular, the CTC of compounds **69a** and **69b** with TCNQ have been studied.[182] The σ_{rt} values for the CTC (**69a**)(TCNQ) and (**69b**)(TCNQ) are 1400 and 2000 Ω^{-1} cm^{-1}, respectively. However, they show different temperature dependences of resistance: in the CTC (**69b**)(TCNQ), the M → I transition occurs at 85 K, whereas the second CTC remains metallic down to 4.2 K. Both structures are built of segregated stacks of donors and acceptors. The introduction of tellurium atoms having high polarizability and more susceptible to intermolecular contacts stabilizes the metallic state. The higher M → I transition temperature of (**69b**)(TCNQ) compared with unsubstituted donors (TTF and TSeF) is attributable to structural disorder of unsymmetrical donor **69b**.

Structure 69



69a **69b**

The complex (HMTTeF)(Et_2TCNQ)(THF)$_x$ (HMTTeF is hexamethylenetetratellurafulvalene) contains mixed stacks and, therefore, it is expected to behave as a semiconductor. However, with a relatively low electrical conductivity (σ_{rt} = 0.1–10 Ω^{-1} cm^{-1} for a series of crystals), it shows metallic behaviour down to 200 K.[182,183] Two types of disorder occur in the structure of this CTC: the positional disorder of the THF molecules and the orientational disorder of the ethyl groups of the Et_2TCNQ species. Some intermolecular contacts of the tellurium and nitrogen atoms (3.61 Å) are shortened with respect to the sum of the van der Waals radii. On the basis of measurements of the temperature dependence of conductivity, thermal emf, magnetic susceptibility and optical properties, Saito *et al.*[183] proposed a mixed neutral-ionic model for this complex in which the fraction of neutral DA complexes is about 0.2–0.4 and the fraction of ionic $D^{+1}A^{-1}$ complexes is 0.6–0.8.

$$\underline{D^+A^-D^+A^-D^+}\,|\,A^0D^0A^0D^0A^0\;D^0A^0D^0A^0D^0A^0D^0\,|\,\underline{A^-D^+A^-D^+A^-}$$

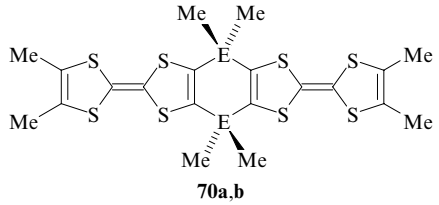
Here $\underline{D^+A^-}$ and $\underline{A^-D^+}$ are dimerized pairs, D^+ and A^- are solitons and the vertical bars are the domain walls. The metallic type of conductivity at temperatures above 200 K is attributable to the increase in the soliton concentration with temperature rise. At 200 K, their fraction is about 3%. The properties of this CTC are fairly sensitive to the content of THF; a decrease in the THF content promotes the appearance of metallic properties.[183]

Above we considered the CTC of TCNQ with difulvalene **6** bridged by two tellurium atoms. Charge transfer complexes with donors **70a**,**b** and **71** containing two single-atom bridges of Group IVA and VA element atoms have been reported.[184,185]

The addition of a solution of TCNQ to a solution containing a mixture of isomers *cis*-**71** and *trans*-**71** gives the CTC (*cis*-**71**)(TCNQ) [185] the molecular packing of which is shown in Fig. 18.

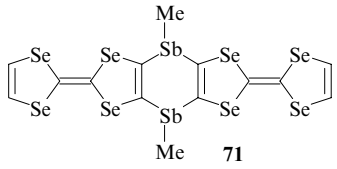
X-Ray diffraction data were used to determine the charges on type A and B TCNQ species, which were found

Structures 70, 71



70a,b

E = Si (**a**), Ge (**b**)



71

to be 0.41 and 0.20, respectively. The TSeF fragments of donor *cis*-**71** overlap in the face-to-face mode with TCNQ species of both types (see Fig. 19). The TCNQ species of type A are bound to donors *cis*-**71** along the crystallographic axis *b* by N···Sb contacts (3.34 Å), which are substantially shortened with respect to the sum of the van der Waals radii (3.8 Å).[186] Along this direction, the temperature dependence of the electrical resistance was measured. At room temperature, $\sigma_{rt} = 2\ \Omega^{-1}\ cm^{-1}$, and this value increases down to 150 K, the complex exhibiting the metallic behaviour (below this temperature measurements were not carried out).

Compound **70a** is a weaker donor than compound **70b**. Therefore, CTC based on **70a** was prepared using a mixture of TCNQ and F_4TCNQ. The CTC (**70a**)$(TCNQ)_{0.5}(F_4TCNQ)_{0.5}$ and (**70b**)(TCNQ), respectively, were isolated. Both CTC are narrow band-gap semiconductors, the conductivity of the latter being sharply increased upon pressure increase: $\sigma_{rt} = 3 \times 10^{-3}\ \Omega^{-1}\ cm^{-1}$ under ambient pressure and $0.2\ \Omega^{-1}\ cm^{-1}$ at 22 kbar.[184]

Unsymmetrical donors **72a**–**c** form 1 : 1 CTC with TCNQ; two of these complexes are organic metals, while the third one — (**72b**)(TCNQ) — is a narrow band-gap semiconductor (Table 4).[187] As can be seen from Table 4, the CTC (**72c**)(TCNQ) has the highest room-temperature conductivity among the known organic metals.

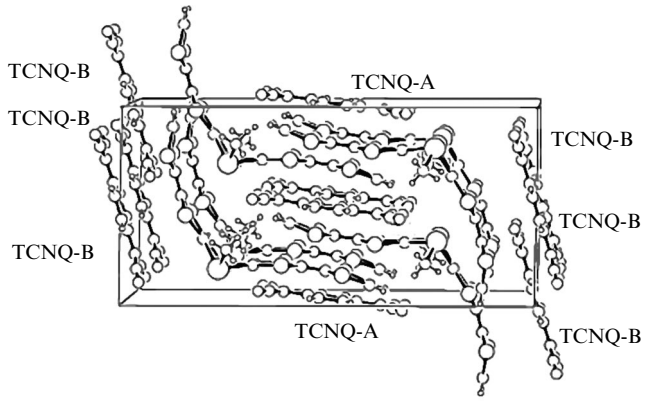


Figure 18. Molecular packing in the crystals of the CTC (*cis*-**71**)(TCNQ).[185]
Two crystallographically non-equivalent TCNQ molecules are shown. The donor molecules are V-shaped along the line connecting the antimony atoms.

Table 4. Electrophysical properties of the CTC formed by donors **72a**–**c** with TCNQ (conductivity in $\Omega^{-1}\ cm^{-1}$).[187]

Complex	Ground state	σ_{rt}	T_{max}/K	σ_{max}	$\sigma_{4.2\,K}$
(**72a**)(TCNQ)	metal	150	110	270	0.064
(**72b**)(TCNQ	semiconductor	0.2	—	—	—
(**72c**)(TCNQ)	metal	2700	40	9800	4700

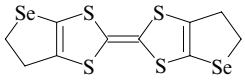
As noted above, the attempts to prepare new organic metals and superconductors based on CTC are often associated with introduction of halogen atoms into the molecules of both donors and acceptors.[188–191] Iyoda *et al.*[188,189] reported TCNQ-based CTC with unsymmetrical donors **73a**–**c** in which some of the hydrogen atoms have been replaced by halogen atoms. In particular, the CTC (**73c**)(TCNQ) shows metallic behaviour, $\sigma_{rt} = 152\ \Omega^{-1}\ cm^{-1}$. Donors **74a**,**b** reported by Batsanov *et al.*[190] form 1 : 1 CTC with TCNQ; these CTC contain mixed stacks, which accounts for their low conductivity (10^{-7}–$10^{-9}\ \Omega^{-1}\ cm^{-1}$).

Tetrafluoro-substituted fulvalene **75** has a too high oxidation potential [0.79 V (SCE)]; therefore, no CTC are formed with TCNQ or F_4TCNQ. However, difluoro-substituted unsymmetrical fulvalenes **76a**,**b** have lower oxidation potentials [0.59 and 0.48 V (SCE), respectively] and do form CTC with F_4TCNQ. The structure of these CTC refers to so-called κ-type.[171] An important role in the formation of radical cation and radical anion dimers is played by the C–H···(N,F) hydrogen bonds. The consequences of strong dimerization of the stacks of these CTC are the diamagnetism of complex (**76a**)(F_4TCNQ) and the thermally activated paramagnetism of CTC (**76b**)(F_4TCNQ) (singlet–triplet excitation, $|J|/k = 950$ K).[191]

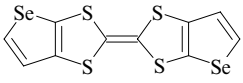
More impressive results come from partial halogenation of the TCNQ itself.[192] Complexes of the donor **53** — (**53**)(FTCNQ) and (**53**)$(F_2TCNQ)_x(TCNQ)_{1-x}$ ($x \approx 0.5$) — are organic metals and retain metallic properties down to 2 K. Disubstituted tetracyanoquinodimethane molecules (Me_2TCNQ, ClMeTCNQ and Cl_2TCNQ) form CTC with donors **53** and **24** composed of mixed stacks similar to those in TTF(CA).[193–195] The CT values for (**53**)(Me_2TCNQ) and (**53**)(ClMeTCNQ) are close to zero, whereas the CTC (**24**)(Cl_2TCNQ) is nearly ionic.[194] In these CTC, the side-to-side contacts between the stacks are comparable with the face-to-face interaction in the stacks of donors and acceptors. This suppresses the spin-Peierls instability. The complex (**24**)(Cl_2TCNQ) is a magnetic insulator, the dependence $\chi^{-1}(T)$ being linear down to 120 K, whereas below this temperature a sharp jump of χ^{-1} occurs with a large hysteresis. This definitely attests to a first-order phase transition, related apparently to the lattice deformation. The presence of phase transition is also confirmed by EPR.[195]

The studies of CTC based on halo-substituted TCNQ culminated in the discovery of superconductivity of crystals of the CTC $(\mathbf{77})_2(Cl_2TCNQ)$.[196–198] The structure of this complex consists of two-dimensional conducting layers of the donor, while the TCNQ stacks do not interact with one another. This CTC is an organic metal, its conductivity increasing down to the helium temperature at a pressure of up to 3.5 kbar. The transition to the superconducting state

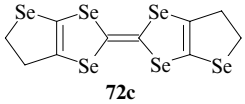
Structures 72–77



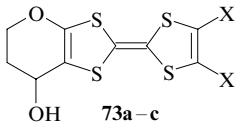
72a



72b

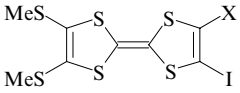


72c



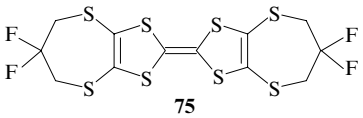
73a–c

X = Cl (**a**), Br (**b**), I (**c**)

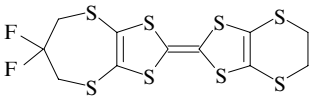


74a,b

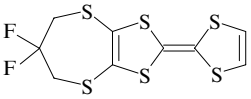
X = H (**a**), Me (**b**)



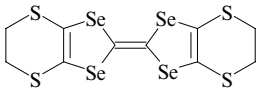
75



76a



76b



77

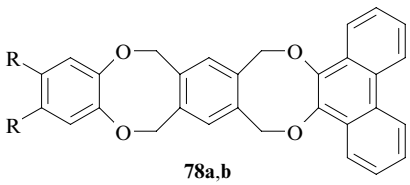
occurs at 1.6 K.[196] It is noteworthy that the pressure effect is non-monotonic: at $p > 6$ kbar, the resistivity of crystals increases at $T < 22$ K, and the superconductor transition occurs at $T \leqslant 0.8$ K. At a pressure of 8.5 kbar, no superconductivity is detected at least down to 0.5 K.

The superconductivity at elevated pressure is observed in iodanil (IA) crystals.[129,199] At ambient pressure, $\sigma_{rt} = 10^{-12}\ \Omega^{-1}\ cm^{-1}$ and the band gap is rather large: 1.37 eV. At 350 kbar, iodanil becomes a metal, while at > 520 kbar, it passes to the superconducting state at 2 K.[199] However, the superconductivity is not related to the acceptor properties of iodanil: hexaiodobenzene also becomes a superconductor at a pressure of 330 kbar and a temperature of 0.6–0.7 K.[199]

7. Charge transfer complexes with other acceptors

Among the CTC based on other strong acceptors, note first of all those in which non-covalent interactions play an important role for the development of synthetic receptors. These CTC are exemplified by so-called molecular tweezers containing two aromatic chromophore groups, for example, dioxa[2.2]orthocyclophanes **78a**,**b**,[200–202] hydrocarbons **79a**,**b** [203] and **80**–**82**.[204]

Structures 78



78a,b

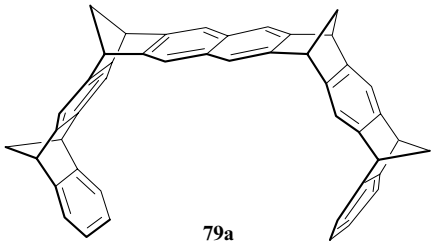
R = H (**a**), R–R is benzo (**b**)

All of the listed molecules are weak donors but they form CTC with strong acceptors such as TCNQ, TCNB (1,2,4,5-tetracyanobenzene) and pyromellitic dianhydride (PMDA) not only in the crystalline state but also in solution. Indeed, donors **78a**,**b** react with these acceptors in acetone to give CTC with stability constants presented below (in litre mol^{-1}).[200]

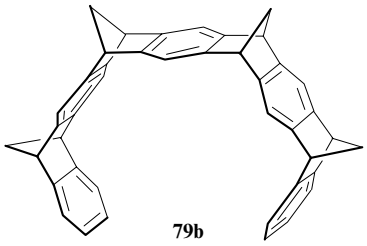
Acceptor (guest)	Donor (host)	
	78a	**78b**
TCNQ	35	130
PMDA	60	1000
TCNB	73	1000

According to X-ray diffraction data,[200] the donor molecules acquire the shape of molecular tweezers, thus binding the acceptor molecule. The shape of the complexes is similar to that presented in Fig. 9.

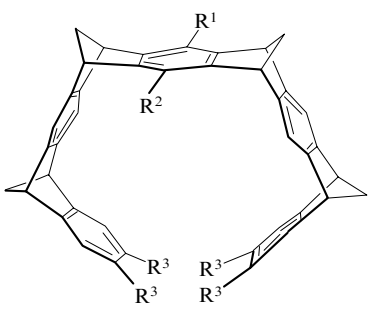
Structures 79–82



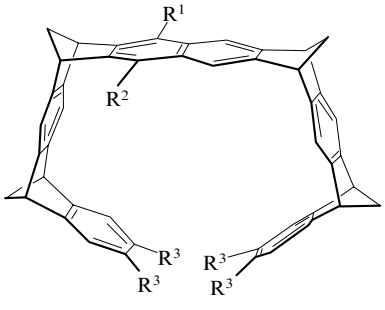
79a



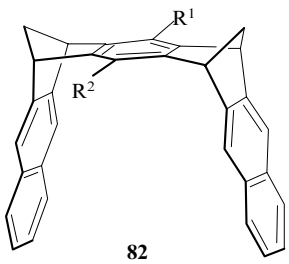
79b



80



81

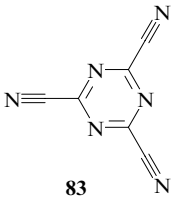


82

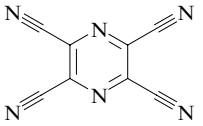
R^1, R^2, R^3 = H, OAc, OMe, CO_2Me, OCH_2CO_2Et

The compound TCNB is a weaker acceptor than TCNQ [the reduction potential is −0.64 V (SCE)]; however, it still forms the strongest CTC with the molecular tweezers **78a**,**b**. Evidently, an important role is played by not only the donor–acceptor interaction of the components but also intermolecular interaction. With other donors, TCNB forms CTC with a low CT value and with the alternating stacking.[205, 206] Nevertheless, some CTC involving TCNB are characterized by a high degree of CT. Indeed, tetrakis-(dimethylamino)ethylene (TDAE) is capable of reversible oxidation to the radical cation and the dication at potentials of −0.68 and −0.53 V (SCE), respectively. The reaction of TCNB with TDAE in acetonitrile forms the CTC $(TDAE)(TCNB)_3(MeCN)$ [207] containing the $TDAE^{2+}$ dication and the $\{(TCNB)_3\}^{2-}$ trimeric anion.

Structures 83, 84



83



84

2,4,6-Tricyano-*sym*-triazine (**83**) is irreversibly reduced at −0.39 V (SCE), which hampers the preparation of CTC based on this compound. Nevertheless, by using donors with low oxidation potentials, for example, TTF and tetramethyl-*p*-phenylenediamine, it is possible to obtain crystalline 1 : 1 CTC.[208] These complexes consist of mixed-type stacks. Although acceptor **83** can in principle oxidize these donors, the CT in both complexes is close to zero.

Tetracyanopyrazine (**84**) oxidizes TDAE to the dication, thus forming the CTC $(TDAE)^{2+}(\mathbf{84})_2^{2-}$ containing dimerized radical cations $(\mathbf{84})^{-\bullet}$ in which the species are rotated through 30° with respect to each other and unusual quasi-quinoid distortions of the radical anion structures are observed.[209]

Several TCNQ derivatives **85**, **86**, **87a**,**b** have been reported.[210–213] Acceptor **85** served for the preparation of organic metals in which the metallic state is stable down to 130 K;[131] while highly conducting RCS are formed by acceptor **86**. The dithiophene analogue of TCNQ (**87a**) is a rather weak acceptor but the introduction of nitrogen atoms into the thiophene rings enhances the acceptor properties and, consequently, acceptor **87b** forms semiconducting CTC with a number of donors (below the σ_{rt} values measured for compressed pellet samples are given; TMTSF is tetramethyltetraselenafulvalene, TTT is tetrathiotetracene).[213]

Donor	$\sigma_{rt}/\Omega^{-1}\,cm^{-1}$
TTF	2.1×10^{-3}
TMTSF	3.1×10^{-5}
ET (**53**)	3.6×10^{-8}
TTT	7.7×10^{-3}

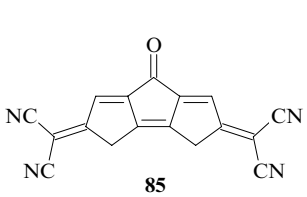
Takahashi *et al.*[214] described heterocyclic derivatives of [3]radialenes **88** and **89**. Complexes of these acceptors with TTF and TTT possess high conductivity: for single-crystalline samples of the CTC formed by acceptor **88** with TTF, $\sigma_{rt} = 420\ \Omega^{-1}\,cm^{-1}$, and with TTT, $450\ \Omega^{-1}\,cm^{-1}$. These CTC exhibit metallic behaviour down to 182 and 80 K, respectively.

2,5-Bis(cyanimino)-2,5-dihydrothieno[3,2-*b*]thiophene (**90**) reacts with TTF to give segregated-stacked CTC ($\sigma_{rt} = 20\ \Omega^{-1}\,cm^{-1}$); with TMTSF, this acceptor forms two CTC, one being dielectric (alternating stacking) and the other being highly conductive ($\sigma_{rt} = 200\ \Omega^{-1}\,cm^{-1}$).[215]

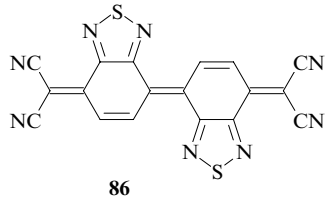
In 1984, *N*,*N*′-dicyanodiimino derivatives of benzoquinone (DCNQI), naphthoquinone (DCNNI) and anthraquinone (DCNAI), compounds **91a–c**, respectively, were synthesized.[216]

These acceptors attracted considerable attention, as RAS based on them possess high conductivity, which is strongly affected by temperature and pressure, which allows them to be used in various electronic devices (see Section III). Of interest are also CTC based on them. Depending on the number and the nature of substituents R, both segregated- and mixed-stacked CTC are formed. For example, the CTC TTF(DCNQI) composed of segregated stacks has $\sigma_{rt} = 10\ \Omega^{-1}\,cm^{-1}$, whereas in the case of

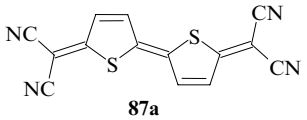
Structures 85–91



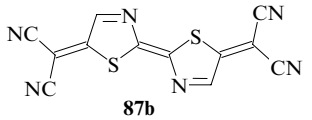
85



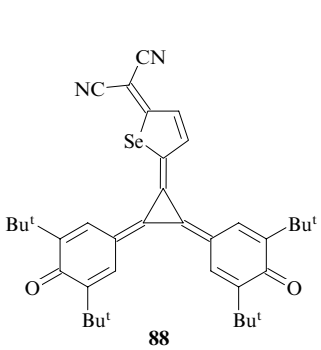
86



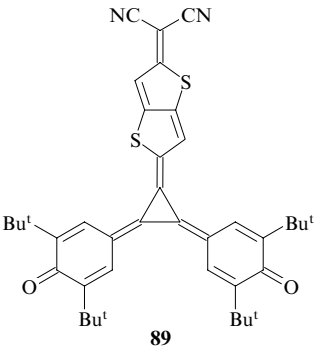
87a



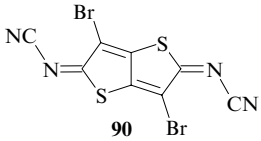
87b



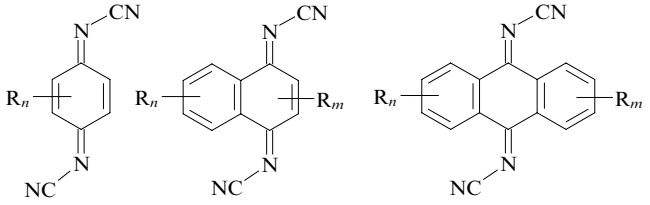
88



89



90

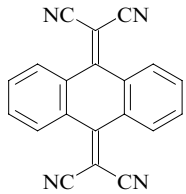


91a **91b** **91c**

91a: R_n = 2-Cl, 2-MeS, 2,5-$(MeO)_2$, 2,5-Bu^t_2, 2-Me-5-CF_3, *etc.*;
91b: R_m = 2-Me, 2-Cl, Cl_2, Br_2, $S(CH_2)_2S$, *etc.*; R_n = H, benzo;
91c: R_m = 1-Cl, 2-Me, 2-Et, 1,2-benzo, *etc.*; R_n = H, 5-Cl

TTF(TCNQ), $\sigma_{rt} = 500\ \Omega^{-1}\ cm^{-1}$.[216] For TTF(DCNNI), $\sigma_{rt} = 20-30\ \Omega^{-1}\ cm^{-1}$; the conductivity increases on cooling to 130 K, while below this temperature, the metal–dielectric transition takes place. The complex $(TMTSF)_2$(2,5-Br_2-DCNQI) is an organic conductor in which the hopping conduction mechanism operates. The complex TTF(2,5-Me_2-DCNQI) consists of mixed stacks. In this complex, as in TTF(CA), the L → H type transition occurs at $p \approx 10$ kbar.[216] Mixed stacks are formed in the CTC (ClMePD)(2,5-Me_2-DCNQI) (ClMePD is 2-chloro-5-methyl-*p*-phenylenediamine).[217] The room-temperature CT value is 0.3 and by 80 K it smoothly increases to 0.6. 11,11,12,12-Tetracyano-9,10-anthraquinodimethane (**92**) has less clear-cut acceptor properties than TCNQ.[218] However, its first and second reduction potentials are very close (−2.06 and −2.58 V, respectively), whereas in the case of TCNQ, they considerably differ (−0.09 and −0.75 V).

Structure 92



92

Furthermore, radical anion $(\mathbf{92})^{-\bullet}$ is substantially nonplanar. For this reason, the CTC it forms are dielectric.[218]

The nitration of 4,4′-dihydroxybiphenyl yields 3,3′,5,5′-tetranitro-4,4′-dihydroxybiphenyl (**68**). This rather strong acceptor can form CTC in which it occurs as the $(\mathbf{68}-2\,H)^{2-}$ dianion or $(\mathbf{68}-H)^{-}$ monoanion. Two CTC may be formed with donor **53** (ET), namely, $(ET)_4$(**68**) and $(ET)_2$(**68**).[219] The former is organic metal in which the metal–dielectric transition does not take place down to 3 K, $\sigma_{3\,K} = 2800\ \Omega^{-1}\ cm^{-1}$. The 2 : 1 complex was prepared only as a powder but according to the data obtained for compressed pellets,[219] it is also highly conducting. This is in poor agreement with the formula $(ET^{+})_2(\mathbf{68}-2\,H)^{2-}$, as in this case, the CTC should be the Mott dielectric. Therefore, a more likely formula is $(ET^{0.5+})_2(\mathbf{68}-H)^{-}$. Magnetic measurements[219] support this assumption: the magnetic susceptibility of this CTC is similar to those for most of $ET^{0.5+}$ compounds, which are highly correlated spin systems.

Lately, attention has been attracted by acceptors based on benzoquinone derivatives, in particular, hydroxy derivatives. This is caused by the potential possibility of hydrogen bond formation in the CTC based on these acceptors, which enables investigation of the hydrogen bond effect on the physical properties of CTC. In 2004, the first organic metal, a CTC formed by imidazolyl-substituted TTF (**93a**) and CA was obtained in which the composition and the CT were determined by hydrogen bonds.[134] The complex $(\mathbf{93a})_2$CA is composed of uniform stacks extended along the *a* axis with an interplanar distance of 3.46 Å in the donor stacks and 3.19 Å in the CA stacks. The S···S side-to-side contacts between the donor stacks along the *b* axis give rise to 2D layers of molecules **93a** parallel to the *ab* plane. Hydrogen bonds with the acceptor stacks finally produce a 3D electronic structure. The value $\sigma_{rt} = 124\ \Omega^{-1}\ cm^{-1}$ is comparable with the conductivity of TTF(TCNQ). It increases on cooling to 180 K; below this temperature a 20 meV band gap is formed. Thus, the CTC $(\mathbf{93a})_2$CA is an organic metal, exhibiting the narrow band-gap semiconductor behaviour at low temperature.[134]

Similar supramolecular structures were also discovered in the CTC formed by donor **93b** with chloranilic and cyananilic acids.[220]

A cooperative intermolecular proton transfer in an CTC with hydrogen-bonded donor and acceptor stacks may give rise to ferroelectric properties. The electric polarization is caused by the proton transfer between the crystal components combined by strong hydrogen bonds. When chloranilic (**63d**) or bromanilic (**63e**) acid reacts with phenazine, ferroelectric CTC are formed,[221] whereas 4,4′-dimethyl-2,2′-bipyridine (**94**) forms an antiferroelectric CTC with chloranilic acid and a ferroelectric complex with iodanilic acid (**95a**)[222] (Fig. 19).

Cyananilic acid (**95b**) forms CTC in which it can exist as either the $(\mathbf{95b}-H)^{-}$ monoanion or the $(\mathbf{95b}-2\,H)^{2-}$ dianion. The CTC formed by **95b** with the ET donor (**53**) has the composition $(ET)_2(\mathbf{95b}-H)$ and the CT value of 0.5.[223] The structure of this CTC corresponds to the α′-type characteristic of ET-based CTC. The value $\sigma_{rt} = 0.20-0.83\ \Omega^{-1}\ cm^{-1}$ varies according to the activation law, the activation energy being 0.15 eV.

Uracil derivatives **96a**,**b** react with cyananilic acid or TCNQ to form CTC in which the uracil moieties of the neighbouring donor molecules are linked by complementary double hydrogen bonds. The complex with compound **95b** is a dielectric, while the CTC (**96a**)(TCNQ) and (**96b**)(TCNQ) are narrow band-gap semiconductors.[224]

The simplest analogue of TCNQ — tetracyanoethylene (TCNE) — forms numerous CTC and radical ion salts (RIS), which have been under vigorous research in recent years. Like TCNQ, TCNE forms CTC with TTF; however, its properties sharply differ from the properties of TTF(TCNQ). In 1996, two polymorphs of TTF(TCNE) (α and β) were described, both being dielectrics.[225] One more

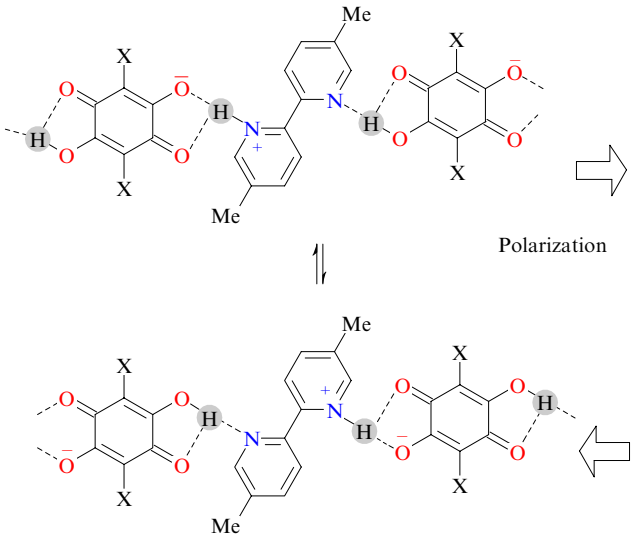
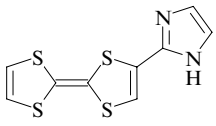
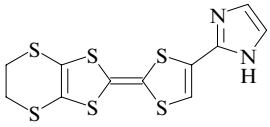


Figure 19. Formation of the polar chains of the alternating acid and base molecules linked by hydrogen bonds (dashed lines) and polarization inversion caused by collective proton transfer.[222]

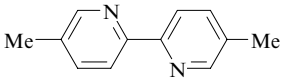
Structures 93–96



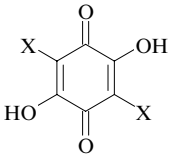
93a



93b

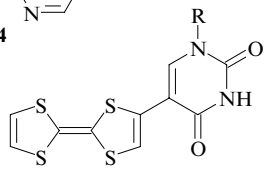


94



95a,b

X = I (**a**), CN (**b**)



96a,b

R = H (**a**), Bu^n (**b**)

phase (δ-modification) of this CTC was reported in 2011.[226] The α and β phases contain mixed stacks consisting of $(TTF)_2$ and $(TCNE)_2$ dimers, which form the sequence

...$(TTF)_2$–$(TCNE)_2$–$(TTF)_2$ –$(TCNE)_2$–...

The dyads $(TTF)_2$ and $(TCNE)_2$ interact very strongly, as indicated by small interplanar spacing: 3.13 Å in the α-phase and 3.15 Å in the β-phase. The degree of ionicity was estimated for both phases as 0.54, which does not differ much from 0.59 found for TTF(TCNQ).[225] This difference between the structures of TTF(TCNE) and TTF(TCNQ) can be interpreted in terms of the anticomplementarity principle:[88] the structures of TTF and TCNQ are anticomplementary; therefore, the formation of mixed stacks is energetically unfavourable. The structures of TTF and TCNE are complementary and the formation of mixed stacks becomes favourable. A consequence of this structure is high electrical resistance of the TTF(TCNE) crystals, which is higher than 10^9 Ω cm.

The diamagnetic dimeric anions $(TCNE)_2$ can be described in terms of two-electron four-centre bonds ($2e^-$/4c-bonds) (Fig. 20).

As can be seen from this Figure, unusually long C–C bonds (2.88 Å) are present in this dimer. A similar diamagnetic heterodimer, π-$[TTF]^{\delta+}$–$[TCNE]^{\delta-}$, in which

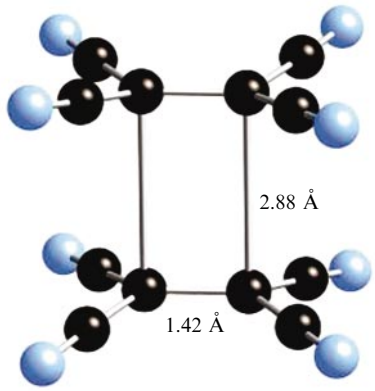
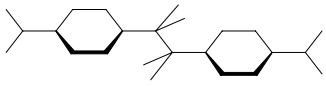


Figure 20. Structure of the dimeric $(TCNE)_2$ anion.[226]

$\delta \approx 0.5$ can be considered as a zwitter-ion.[226] The formation of unusually long C–C bonds is due to the competition of two interactions: electrostatic repulsion of likely charged radical ions and tendency of the unpaired electrons to form a covalent bond. The problem of theoretical interpretation of C–C bonds with bond lengths of 2.8–3.4 Å is the subject of a number of publications.[207, 227–234] According to the results of a publication,[230] the isolated dimeric dianion $(TCNE)_2^{2-}$ is unstable; therefore, it cannot be detected by electrospray ionization mass spectrometry. Nevertheless, it can exist in some solvents such as THF[230] or dichloromethane.[233] In particular, the barrier for fragmentation of $(TCNE)_2^{2-}$ into two radical anions in THF is only 9 kcal mol^{-1}.[230] Dimeric anions of this type with unusually long C–C bonds are also formed by such acceptors as TCNQ, F_4TCNQ and 2,3-dichloro-5,6-dicyanobenzoquinone.[227] In this case, however, σ-dimers are formed, which can generally be depicted as structure **97**. The formation of dimers of this type with unusually long C–C bonds are also possible for radical cations.[235]

Structure 97

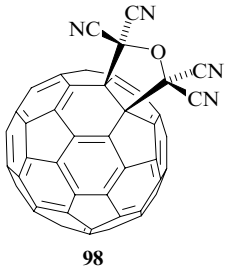


97

8. Chemical reactivity of strong π-electron acceptors

Tetracyanoethylene readily condenses with unsaturated hydrocarbons giving new strong electron acceptors. The condensation with fullerene C_{60} oxide gives acceptor **98** (TCNEO-C_{60}), which is stronger than the initial C_{60}.[236]

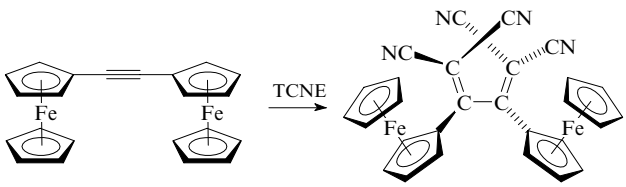
Structure 98



98

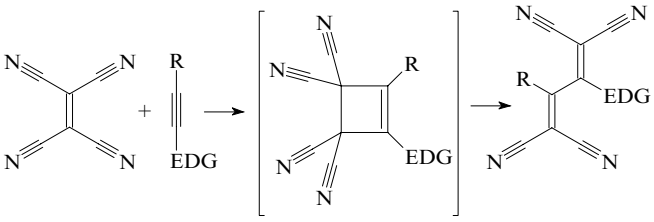
Bis(ferrocenyl)acetylene reacts with TCNE to give a 1 : 1 adduct (Scheme 2).[237] This adduct can find use as a material for nonlinear optics.

Scheme 2



The reaction of TCNE with alkynes containing electron-donating groups (EDG) gives a high product yield (nearly 100%) and is an example of [2 + 2]-cycloaddition followed by electrocyclic opening of the cyclobutene thus formed (Scheme 3).[238, 239] The resulting adducts can find use in optoelectronic devices.

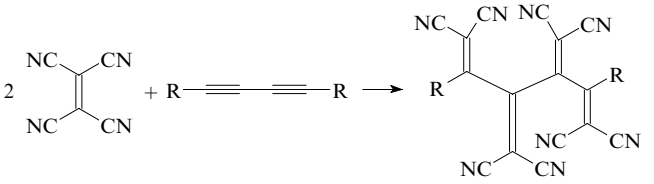
Scheme 3



R = H, $SiPr^i_3$, *etc.*; EDG = 4-$Me_2NC_6H_4$, 2-$Me_2NC_6H_4$, 3-$Me_2NC_6H_4$, *etc.*

Substituted buta-1,3-diynes react with TCNE according to the double [2+2]-cycloaddition route to give so-called octacyano[4]dendralenes (Scheme 4).[240] These compounds can be used as p-type dopants in optoelectronic devices and as components of organic metals. They are stronger acceptors than TCNE or TCNQ and are comparable with F_4TCNQ.[240]

Scheme 4

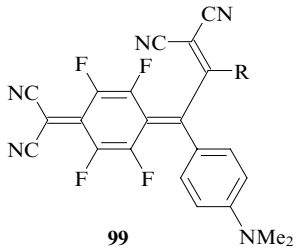


R = 4-(XYN)C_6H_4 (X = H: Y = Pr^i, Bu^n; X = Me: Y = Me, Pr^i; X = Y = Pr^i, *etc.*)

The [2+2]-cycloaddition reactions are also known for TCNQ.[241–243] Upon [2+2]-cycloaddition of *N*,*N*-dialkylaminophenyl-substituted alkynes to TCNQ followed by the retro ring opening reaction, adducts exhibiting chromophore properties are formed (Scheme 5).[241,242]

Recently,[243] methods for the synthesis of adducts based on TCNQ and TTF derivatives have been developed. This provides routes to so-called superacceptors, for example, adducts **99**. Indeed, for R = CN, acceptor **99** has a reduction potential of 0.00 V relative to Fc^+/Fc (Fc is ferrocene).[243]

Structure 99

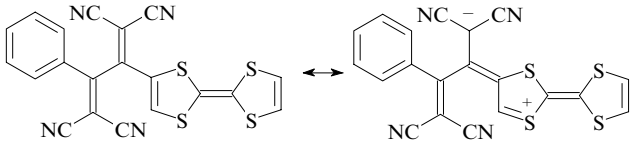


99

R = CN, CH=C(CN)$_2$, C(CN)=C(CN)$_2$

In mixed adduct **100**, the planes of the acceptor and donor moieties are nearly parallel (the torsion angle is 1.7°). This gives rise to substantial donor–acceptor interaction, which allows assigning this adduct to autocomplexes (Scheme 6).[244]

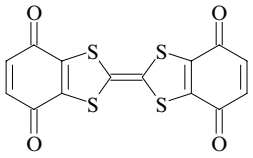
Scheme 6



100

Among other hybrid (D–A) organic molecules containing strong donor and acceptor moieties, note the complexes in which these moieties are directly linked. The D–A hybrid **101** in which the TTF molecule forms a fused system with two benzoquinone molecules (Q) has been reported.[244,245] The structure of Q-TTF-Q was not presented in the studies cited[244,245] but, judging by its properties, it is highly nonplanar.

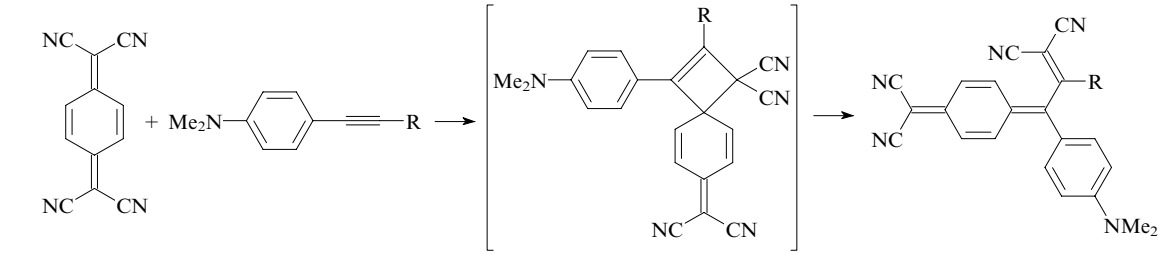
Structure 101



101 (Q-TTF-Q)

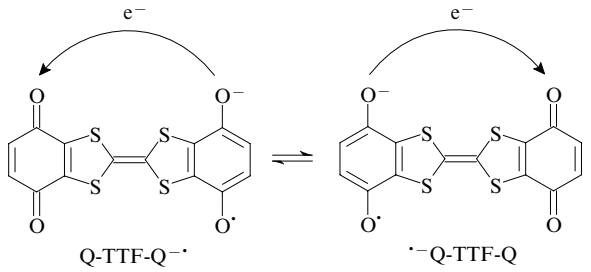
Indeed, the cyclic voltammogram was found to exhibit two waves corresponding to the reversible one-electron oxidation at the potentials $E^\circ_{ox1} = +0.99$ V and $E^\circ_{ox2} = +1.36$ V (*vs.* silver chloride electrode) typical of TTF and two clearly discernable waves of reversible one-electron reduction at the potentials $E^\circ_{red1} = -0.20$ V and $E^\circ_{red2} = -0.28$ V corresponding to the stepwise reduction of each benzoquinone moiety. The slight difference between the potentials ($\Delta E = 0.08$ V) implies that the reduction of the second Q-moiety is affected by the charge state of the first one. Thus, the TTF moiety is weakly conjugated with other acceptor centres. An EPR study of the radical anion $(Q\text{-}TTF\text{-}Q)^{-\bullet}$ demonstrated the existence of thermally activated electron exchange between the two acceptor centres (Scheme 7).

Scheme 5



R = H, Bu^n, Ph, $C_6H_4NMe_2$, C≡CSiMe$_3$

Scheme 7



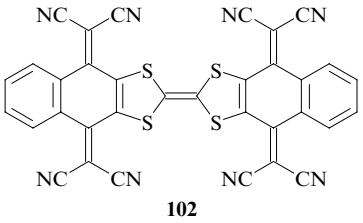
Hybrid complex **102** in which the TTF molecule is fused to two benzo-TCNQ molecules is also known. Molecule **102** has a boat conformation,[246] which prevents conjugation of the donor and acceptor moieties. In this case, thermally activated intramolecular electron transfer

described by the Arrhenius equation with the parameters $E_a = 1.13$ kcal mol^{-1} and $\log A = 7.53$ was also detected. The rate of the electron transfer in molecule **102** is an order of magnitude lower than in Q-TTF-Q,[246] which can be attributed to a more pronounced deviation from a planar structure in the case of **102**.

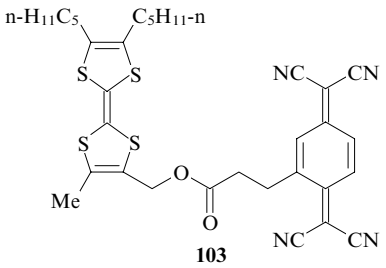
Perepichka *et al.*[247] described the hybrid complex **103** in which the acceptor and the donor moieties are separated by a bridge that precludes conjugation. The lack of conjugation results in that molecule **103** can exist in five charge states (from -2 to $+2$), each having its own colour: the dark-brown starting compound **103** becomes light-blue upon one-electron reduction or red upon two-electron reduction. Radical cation $(\mathbf{103})^{+\bullet}$ is green-coloured and dication $(\mathbf{103})^{2+}$ is orange. Thus, this compound is suitable as a multichannel electrochromic material, the more so because it forms high-quality Langmuir–Blodgett films.[247]

The reaction of dendrimers **104**, resulting from condensation of TCNE with a triethynyl benzene derivative, with TTF gives even more intricate donor–acceptor structures **105** (Scheme 8).[243]

Structures 102, 103



102

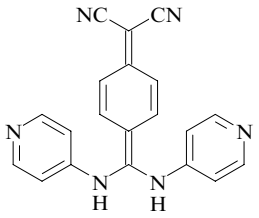


103

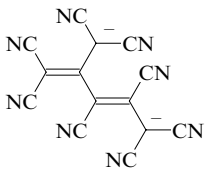
Thus, cycloaddition of a strong electron acceptor to unsaturated organic compounds opens up the way to the synthesis of new functional materials.

Non-electrocyclic condensation reactions are also known for TCNQ and TCNE. For example, 3- or 4-aminopyridines react with TCNQ to give the greenish-coloured CTC (Py-NH_2)TCNQ (Py is pyridyl). The colour rapidly changes to reddish-brown, as liberation of hydrogen cyanide affords condensation product **106**.[248]

Structures 106, 107

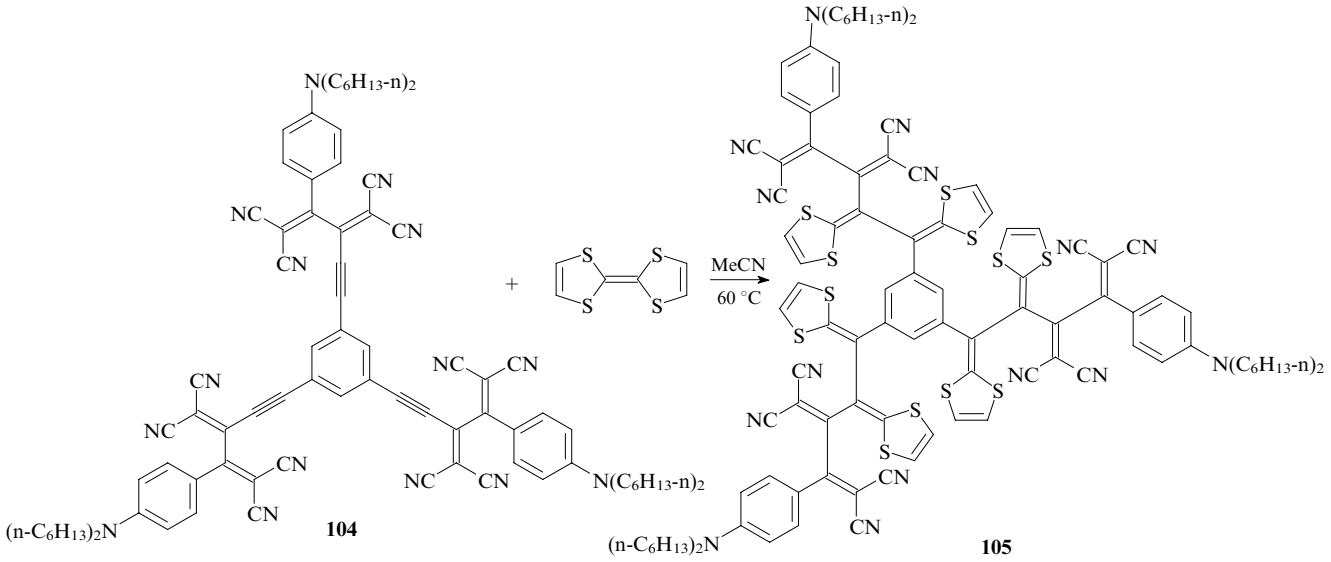


106



$(\mathbf{107})^{2-}$

Scheme 8



Similarly, TCNE reacts with aniline to give the condensation product as follows:[248]

$$PhNH_2 + C_2(CN)_4 \longrightarrow PhNH[C_2(CN)_3] + HCN$$

To conclude the section, note that some polycyano-substituted hydrocarbons can form CTC with segregated stacks; some of these complexes behave as organic metals. Thus hexacyanobutadiene and tetramethyltetrathiafulvalene form a segregated-stacked CTC.[249] The 2-dicyanomethylene-1,1,3,4,5,5-hexacyanopentene dianion (**107**) with donors **53** and **24** forms highly conducting CTC, which behave as organic metals down to 1.3 and 4.3 K, respectively.[250]

III. Radical anion salts based on TCNQ and other strong acceptors

1. Fusible conducting RAS based on TCNQ

Most of the known organic metals decompose on heating without melting. This is caused by the high cohesion energy in the crystals of these compounds, as they actually form mixed-type, molecular-ionic crystals. This circumstance precludes extensive use of organic metals and semiconductors. The first fusible conducting organic materials were obtained in the second half of the 1980s.[18, 19, 251] The melting points of these RAS were > 196 °C. The combination of fusibility and considerable electrical conductivity makes these RAS suitable as solid electrolytes for the manufacture of porous electrodes, components of new type of capacitors.

A radical anion salt melt has a high viscosity at the melting point; to reduce the viscosity, the melt is to be heated by 40 – 50 degrees above the melting point. However, stability of the melt against decomposition sharply decreases with temperature rise. To ensure effective impregnation of the porous electrode with a melt of conducting RAS, the use of dielectric additives, in particular, γ-butyrolactone, was proposed in patents.[18, 19] The melting point of this composite can be reduced to 150 °C. However, the addition of a dielectric increases the dielectric loss tangent, which deteriorates the performance of the capacitor.

In our patent,[251] a noticeable decrease in the melting point of conducting RAS based on TCNQ was achieved by using *N*-alkylquinaldinium cations (*N*-Alk-Qd). Table 5 presents the room temperature resistivity values and the melting points for pellet samples of radical anion salts. It can be seen that the use of alkylquinaldinium RAS provides a considerable (by up to 30 °C) decrease in the melting point, while maintaining a high (for organic semiconductors) electrical conductivity.

Even more pronounced decrease in the melting point of TCNQ-based conducting RAS is attained by using composite RAS comprising TCNQ and MeTCNQ (**62e**).[252] The presence of a methyl substituent in the MeTCNQ molecule results in the formation of looser stacks, and this entails a decrease in the conductivity and in the melting point of RAS based on this acceptor. We found that the electrical conductivity of the MeTCNQ-based RAS is about an order of magnitude lower compared to the salts based on TCNQ.[252] Composites of TCNQ salts with MeTCNQ salts should have obvious advantages over the composites in which dielectric additives are used. Studies of these composites revealed a remarkable feature — the presence of clear-cut eutectics of the composites $(N\text{-}R^1\text{-iso-Qn})_x(TCNQ)_{2x}(N\text{-}R^2\text{-iso-Qn})_{1-x}(MeTCNQ)_{2-2x}$ (iso-Qn is isoquinolinium). The eutectics are observed at $x = 0.1$. This provided conductive organic materials with the uniquely low melting point of 80 °C (Table 6). The specific conductivity values presented in Table 6 were determined for pressed samples using push contacts and, therefore, they are underestimated but can serve for investigation of the regular variation of this parameter in the series. Considering the value $\sigma_{rt} = 0.8\ \Omega^{-1}\ cm^{-1}$ obtained for single crystalline samples of the RAS (N-Bu^n-iso-Qn)(TCNQ)$_2$ *versus* the value $\sigma_{rt} = 8.9 \times 10^{-3}\ \Omega^{-1}\ cm^{-1}$ for pressed samples[253] provides an idea of relationship between these results and true values.

It was proposed[18, 19] to estimate the stability of a conducting RAS by the temperature at which the RAS decomposes at a noticeable rate. However, this value cannot serve as a measure of stability because its definition is ambiguous and because it depends on the heating rate. In addition, according to our data, melts of the TCNQ salts decompose with time. The decomposition time is temperature-dependent. Having a broad range of composites with different melting points at our disposal, we found that the half-life $\tau_{1/2}$ (the time during which the resistance of a molten sample irreversibly doubles) does not depend on the cation and is thus related to the destruction of TCNQ stacks. The $\tau_{1/2}$ value exponentially decreases with temperature rise:

$$\tau_{1/2} = \tau_{1/2}^{(0)} \exp(-\alpha T) \quad (1)$$

In Eqn (1), $\ln \tau_{1/2}^{(0)} = 34.23$ (τ in s), $\alpha = 0.069$.[253] Using relation (1), it is possible to find $\tau_{1/2}$ for the RAS reported in

Table 5. Room temperature resistivity and melting points of the RAS (N-Alk-Qd)(TCNQ)$_2$.[251]

Parameter	Alk							
	Me	Pr^n	Pr^i	Bu^n	Bu^i	iso-C_5H_{11}	All	n-C_6H_{13}
ρ /Ω cm	12.2	14.3	16.8	22.4	10.3	19.4	18.4	13.1
T_m /°C	188	189	182	171	177	167	185	195

Table 6. Room temperature conductivity ($\Omega^{-1}\ cm^{-1}$) and melting points (°C) of the composites $(N\text{-}R^1\text{-iso-Qn})_x(TCNQ)_{2x}(N\text{-}R^2\text{-iso-Qn})_{1-x}(MeTCNQ)_{2-2x}$.[252]

R^1	R^2	Parameters	x				
			0	0.1	0.2	0.4	1.0
Pr^n	Pr^n	T_m	105	–	105	109	190
		σ_{rt}	0.33	–	0.40	1.4	8.2
Bu^n	Bu^n	T_m	126	–	136	142	196
		σ_{rt}	1.4	–	5.9	6.2	36
Pr^n	Me	T_m	105	80	95	115	see [a]
		σ_{rt}	0.33	0.5	7.4	35	100
Pr^n	NMP	T_m	105	97	105	see [a]	see [a]
		σ_{rt}	0.33	7.7	10	–	300

[a] Decomposes.

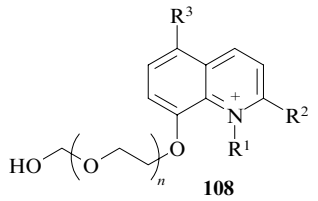
the cited publications[18,19] to be 5–10 s. Obviously, when the melt temperature is >190 °C, the use of these materials is impossible. Meanwhile, for the composites included in Table 6, the time $\tau_{1/2}$ reaches 6 h, and this means that the melts can be repeatedly used for moulding of electronic products or for impregnation of porous electrodes; this makes them suitable for fabrication of electrolytic capacitors of a new type.[252]

Low-melting conducting RAS can also be used to solve a theoretically important problem. The electrophysical properties of these RAS are highly anisotropic and, hence, they can be assigned to quasi-one-dimensional conductors. In the framework of the band theory, the properties of metals are dictated by the presence of a long-range order.[254] On melting, the long-range order is violated but in usual 'three-dimensional' metals, melting does not induce an abrupt change in the conductivity, only a slight decrease (by 15%–20%) being observed. This is related to essentially three-dimensional character of electron motion. However, in a quasi-1D material, melting can induce a sharp (by several orders of magnitude) decrease in the conductivity, as after destruction of regular stacks, motion of the carriers can occur only by thermally activated electron jumps and tunelling from one site of the distorted stack to another.

Using a composite with a melting point of 80 °C, we studied the temperature dependence of its conductivity in the temperature range of 17–147 °C.[253] According to the obtained data, melting is accompanied by some decrease in the conductivity; however, the activation energy in the melt is even lower than in the solid sample: 1323 and 1647 K, respectively. This result suggests that the conducting stacks are retained in the melt (the E_a value refers particularly to TCNQ stacks). The melt may have the liquid-crystalline nature: the long-range order is retained in the stacks and disappears in the perpendicular directions.

At the early stage of research of organic metals, it was assumed that the metallic state is possible only provided that its components have planar structure and a symmetry not lower than D_{2h}.[88] However, the subsequent studies demonstrated that this is not an obligatory condition. For example, Bunzel *et al.*[255] described the TCNQ RAS with highly unsymmetrical cations **108**.

Structures 108



108

R^1, R^2 = H, Me; R^3 = H, Cl; n = 0, 1

The electrical conductivity of these RAS reaches 7.4×10^{-2} Ω^{-1} cm^{-1}. Since the conducting state is retained even in the melt, a sufficient condition is merely the existence of the segregated TCNQ stacks. The presence of long-chain substituents in the cation structure substantially weakens the interstack interaction, which is expected to decrease the RAS melting point.

This possibility was verified in our work[256] dealing with the properties of the RAS (N-C_nH_{2n+1}-iso-Qn)$(TCNQ)_2$ (n = 1–16) most of which were synthesized in this study for the first time. All these RAS melt without decomposition. The dependence of T_m on the alkyl chain length is non-monotonic: it changes from the maximum value of 201 °C (n = 3) to 155 °C (n = 16) passing through a broad minimum at $n \approx 11$ (T_m = 152 °C). Therefore, the RAS (N-C_nH_{2n+1}-iso-Qn)$(TCNQ)_2$ (n = 9–12) can be used in electronic engineering without any additives. Their electrical conductivity depends little on n and at room temperature, it is in the range of 0.1–0.01 Ω^{-1} cm^{-1}.[256]

The radical anion salt (N-Me-iso-Qn)$(TCNQ)_2$ is an organic metal, while all other RAS of this series are narrow band-gap semiconductors. The highest activation energy (0.262 eV) was found for the RAS with the butyl substituent, while the lowest value (0.140 eV) was found for the salt with the dodecyl substituent. Thus, this study confirms the conclusion that the cation structure is not crucial for the electrophysical properties of the TCNQ RAS. This conclusion is also confirmed by optical measurements.[256]

It is known[12] that the IR spectra of conducting TCNQ RAS have specific features caused by the electron–phonon interaction (EPI). They are manifested as substantially broadened (half-width of about 100–200 cm^{-1}) absorption lines corresponding to the fully symmetrical TCNQ vibrations, which would be forbidden in the IR spectra without the EPI. In the framework of the Fano model,[257] they are interpreted as being due to the interaction of intramolecular fully symmetrical vibrations with excitation of conduction electrons having wave vectors polarized along the stack axis.[258–260] In the IR spectrum of (N-$C_{12}H_{25}$-iso-Qn)$(TCNQ)_2$, these features are even more pronounced than in the IR spectrum of the organic metal, the RAS (N-Me-iso-Qn)$(TCNQ)_2$,[256] which is consistent with conclusions about the crucial role of the TCNQ stacks. One more interesting result of the above-cited work[256] is the discovered ability of simple TCNQ salts to melt without decomposition. For example, the RAS (N-$C_{12}H_{25}$-iso-Qn)TCNQ melts at 100 °C! According to the obtained results,[256] RAS of a complex composition have about 50 °C lower T_m than salts of complex composition.

The issue of the nature of the melt was addressed in our publication.[261] Three composites x[(N-Me-iso-Qn)$(TCNQ)_2$] + (1 − x)[(N-Pr^n-iso-Qn)$(MeTCNQ)_2$] (x = 0.1, 0.2 and 0.3) were studied by IR spectroscopy. The results for the three composites were similar. The measurements were performed in the temperature range of 28–177 °C, *i.e.*, both in the solid phase and in the melt. The results can be interpreted in the following way: in the melt, the TCNQ stacks gradually (as the temperature is raised) fall apart into segments, resulting in electron localization. After cooling of the melt to room temperature, an conducting amorphous phase is formed. High conductivity of the melt can be attributed to the existence of conducting paths both in the melt and in the amorphous state. These paths are formed due to strong interaction of TCNQ species with one another.[261]

In 2005, the change in the electrophysical properties of fusible TCNQ salts of simple composition upon transition into the melt and back was also studied.[262] In particular, the RAS (EMI)(TCNQ) and (BMI)(TCNQ) were considered (EMI is 3-ethyl-1-methylimidazolium, BMI is 1-n-butyl-3-methylimidazolium). The melts of these RAS are stable under a nitrogen atmosphere up to 200 °C. The radical complex anion salts formed with the same cations have higher melting points than the simple RAS,[262] which is in line with our data.[256] The replacement of TCNQ

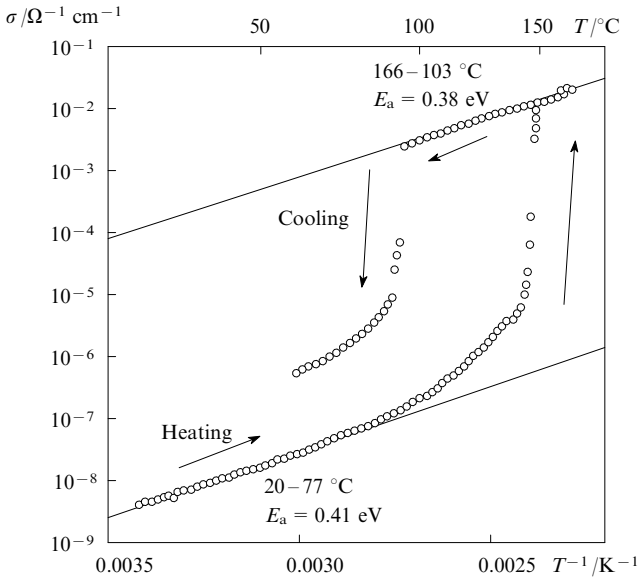


Figure 21. Temperature dependence of the electrical conductivity of the RAS (EMI)(TCNQ).[262]
E_a is the activation energy.

by MeTCNQ in the RAS (EMI)(TCNQ) and (BMI)(TCNQ) induces a decrease in T_m by 12 degrees, whereas the replacement by EtTCNQ leads to an increase in T_m by 4 degrees. An interesting result[262] was obtained upon the electrical conductivity measurements in the temperature range covering the T_m: on melting, the conductivity increases by four orders of magnitude, while on freezing of the melt, it decreases by three orders of magnitude, thus exhibiting a hysteresis (Fig. 21).

This hysteresis is related to the presence of the supercooled liquid phase. The sharp increase in the conductivity was explained by examining the EPR spectra in the solid and liquid phases.[262] The solid phase is diamagnetic with a thermally activated paramagnetic state, which is related to dimerization of stacks caused by the Peierls instability of the systems with the half-filled band.[12] In the liquid phase, dimers dissociate, which sharply increases the concentration of the carriers. The conductivity of the liquid phase ($\sim 10^{-2}$ Ω^{-1} cm^{-1}) is much higher than that of most usual TCNQ salts of simple composition ($< 10^{-4}$ Ω^{-1} cm^{-1}). As in our studies, in the work by Nishimura and Saito,[262] the decrease in the activation energy was noted from 0.41 eV in the solid phase to 0.38 eV in the liquid phase. When a constant voltage was applied, the current intensity did not change in the solid phase but decreased during 3 h in the liquid phase from 0.01 to 10^{-5} A. The authors[262] attributed this finding to the fact that the conductivity of the liquid phase is determined by contributions of both electronic and ionic conduction.

Studies of the TCNQ salts with *N*-alkylpyrazinium cations (*N*-Alk-Pz) demonstrated that these salts of both simple and complex composition do not melt without decomposition.[263]

Meanwhile, the RAS (*N*-Alk-Pz)(MeTCNQ)$_n$ (n = 1 or 2) can melt without decomposition.[264] Table 7 gives comparative characteristics of the TCNQ and MeTCNQ RAS with pyrazine-based cations. As can be seen from the Table,

Table 7. Comparative characteristics of the radical anion salts of TCNQ[263] and MeTCNQ.[264]

Cation	Composition	TCNQ		MeTCNQ	
		ρ_{rt} /Ω cm	Δ /eV	T_m /°C	ρ_{rt} /Ω cm
N-Me-Pz	1 : 1	100	< 0.05	182	2.63
N-Me-Pz	1 : 2	66.7	0.06	167	0.72
N-Et-Pz	1 : 1	78.7	0.2	159	2.94
N-Et-Pz	1 : 2	79.4	0.2	170	0.75
N-Pr^i-Pz	1 : 1	7.58×10^3	0.3	198	1.75×10^2
N-Pr^i-Pz	1 : 2	5.96×10^3	0.3	see [a]	3.57×10^2
N-Bu^i-Pz	1 : 2	2.94×10^5	0.3	see [a]	7.69×10^3

[a] Decomposes.

the melting point of the RAS (*N*-Alk-Pz)(MeTCNQ)$_n$ is higher compared to analogous RAS with isoquinolinium cations. In view of the fact that the RAS (*N*-Alk-iso-Qn)(MeTCNQ)$_2$ melt at 40–50 °C lower temperatures than the corresponding TCNQ salts and considering the data of Table 7, it can be concluded that the RAS (*N*-Alk-Pz)(MeTCNQ)$_n$ have melting points of > 210 °C.

2. Quasi-2D conductors based on TCNQ radical anion salts

Yet another unexpected feature of the RAS (*N*-Alk-Pz)(MeTCNQ)$_n$ is substantially (by 1–2 two orders of magnitude) higher electrical conductivity as compared with analogous TCNQ salts (see Table 7). This unexpected result is attributable to the fact that properties of the RAS (*N*-Alk-Pz)(MeTCNQ)$_n$ are essentially two-dimensional, unlike those of any RAS known before based on both TCNQ and MeTCNQ. The temperature dependence of the electrical resistance of these RAS is described by the variable range hopping model.[254]

$$\rho(T) = A \exp\left[\left(\frac{T_0}{T}\right)^{1/\alpha+1}\right]$$

where α is the system dimensionality. For the RAS (*N*-Alk-Pz)(MeTCNQ)$_n$ (Alk = Et, Pr^i), the logarithm of the resistivity can be expressed by the relation

$$\ln \rho = \ln A + \frac{B}{T^{1/3}}$$

with the coefficient B in the range of 140–178. The ability of TCNQ to form quasi-2D structures is probably related to the nature of the cation, a pyrazine derivative. Indeed, in 2005, we synthesized a RAS of an unusual composition — (*N*-Et-Pz)(TCNQ)$_{2.5}$.[265] Note that the RAS NMP(TCNQ) (NMP is *N*-methylphenazinium) is an organic metal, whereas NEP(TCNQ) (NEP is *N*-ethylphenazinium) is a typical dielectric with a 14 orders of magnitude lower conductivity.[266] This is related to the formation of σ-$(TCNQ)_2^{2-}$ dimers with unusually long C–C σ-bonds (1.71 Å) in the structure of this RAS.

Meanwhile, as shown in another of our publication[263] the RAS (*N*-Me-Pz)(TCNQ) is organic metal in which the temperature of the metal–dielectric transition is uniquely low for a TCNQ RAS (120 K). The replacement of the methyl group by an ethyl group results in RAS (*N*-Et-Pz)(TCNQ)$_{2.5}$, the structure of which is depicted in Fig. 22.

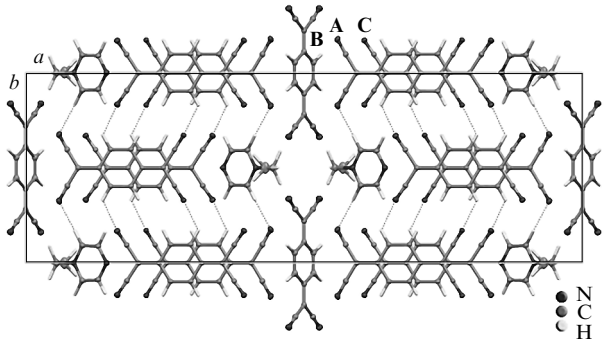


Figure 22. Structure of the RAS (*N*-Et-Pz)(TCNQ)$_{2.5}$ projected along the *c* axis (see the text).[265]

As can be seen from this Figure, the structure of the RAS is formed by stacks composed of alternating TCNQ species (**A** and **C** type), whereas **B** type species are arranged between the stacks at a 117.7° angle. The cations (*N*-Et-Pz)$^+$ are positioned in such a way that the free pyrazine nitrogen atom is located between two nitrile groups of molecule **C** (see Fig. 22). According to the charge distribution, the highest negative charge occurs on species **C** (−0.56 e); type **B** species also have a noticeable negative charge (−0.31 e). The IR spectrum of this RAS shows continuous absorption starting from $\nu = 1750$ cm^{-1}. From this, the activation energy for the conduction can be estimated as 0.22 eV. The structural features of the RAS (*N*-Et-Pz)(TCNQ)$_{2.5}$ suggest quasi-2D conduction, which is confirmed by electrophysical measurements:[265] the temperature dependence of the logarithm of the relative resistance is described by the variable range hopping mechanism with the expected value of $\alpha = 2$.

$$\ln\frac{R}{R_{rt}} = -21.85 + \frac{175.20}{T^{1/3}}$$

The spectral and magnetic investigations of this RAS performed in our work[267] suggest that this is a spin ladder — a material with intermediate properties between those for 1D chain and 2D structures.

A certain extent of 2D character was found for the physical properties of the RAS (*N*-Et-2,5-Me$_2$-Pz)(TCNQ)$_2$, prepared in our work.[268] This RAS has a layer structure in which the conducting layers formed by TCNQ species alternate along the *a* axis with non-conducting layers consisting of cations (Fig. 23).

As can be seen from Fig. 23, the TCNQ species are hydrogen-bonded to the cations (shown in Fig. 23 by dashed lines). This provides the possibility of charge transfer not only along the stacks but also in the perpendicular direction, which makes the electronic system of the RAS somewhat two-dimensional. The IR spectrum of this RAS exhibits continuous absorption starting from $\nu = 850$ cm^{-1}; from this, the activation energy for conduction can be estimated as $\Delta \approx 0.105$ eV. The room temperature conductivity is low: $\sigma_{rt} = 1.4 \times 10^{-4}\ \Omega^{-1}\ \text{cm}^{-1}$; the simple activation model poorly describes the temperature variation of the electrical resistance, which is due to highly non-uniform charge distribution in the stacks. For description of the temperature dependence of the relative resistance, the hopping model for the 2D case is most adequate.[268]

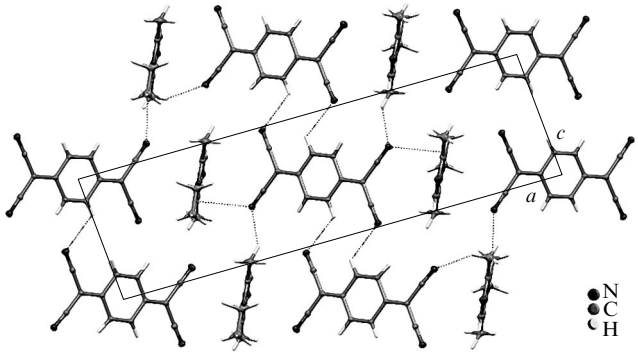


Figure 23. Structure of the RAS (*N*-Et-2,5-Me$_2$-Pz)(TCNQ)$_2$ projected along the *b* axis.[268]

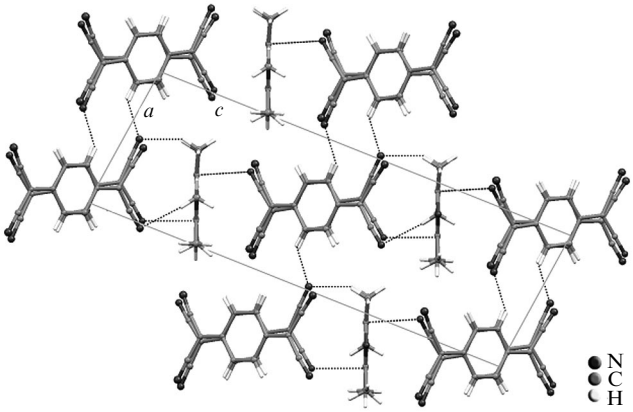
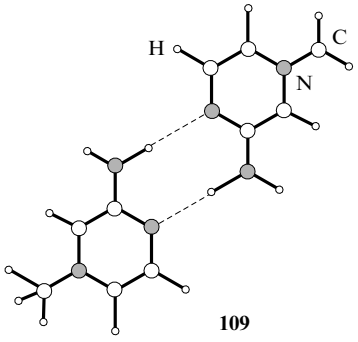


Figure 24. Structure of the RAS (*N*-Me-Me$_4$-Pz)(TCNQ)$_2$ projected along the *b* axis.[269]

$$\ln\frac{R}{R_{rt}} = -14.18 + \frac{93.43}{T^{1/3}}$$

In the crystals of the RAS(*N*-Me-Me$_4$-Pz)(TCNQ)$_2$ that we synthesized,[269] there is interaction between the TCNQ stacks (Fig. 24). In addition, some contacts between the cations and TCNQ species are shortened with respect to the sum of the van der Waals radii. However, the temperature dependence of the electrical resistance of this RAS is described by the simple activation model, and, hence, one cannot consider the possible quasi-2D character of its electronic structure.

Structure 109



109

The crystals of the RAS [*N*-Me-$(NH_2)_2$-Pz]$(TCNQ)_2$ are unusual because they contain the dimeric cation $[N\text{-Me-}(NH_2)_2\text{-Pz}]_2^{2+}$ formed through a hydrogen bond (structure **109**).[269]

The heterogeneity of the charge distribution in the TCNQ stacks (−0.37 and −0.68 e) accounts for the semiconductor properties of this RAS.[269]

3. The structure and electrophysical properties of other radical anion salts of TCNQ and other strong acceptors

The radical anion salt $[Cl_2Bn(3\text{-Me-Qn})](TCNQ)$, [$Cl_2$Bn(3-Me-Qn) is 1-(3,4-dichlorobenzyl)-3-methylquinolinium] has an unusual structure.[270] This RAS is composed of the segregated stacks of the cations $Cl_2Bn(3\text{-Me-Qn})^+$ and the radical anions. The cations have a Λ-like structure and form dimerized stacks in which π–π interaction of the quinoline rings occurs (Fig. 25).

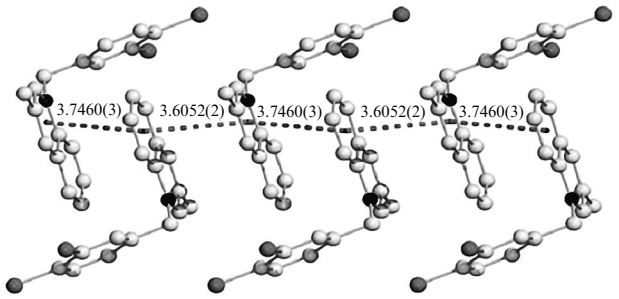


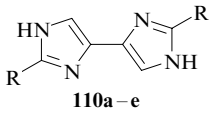
Figure 25. Packing of the cations in the RAS [Cl_2Bn(3-Me-Qn)](TCNQ) (hydrogen atoms are omitted, the distances are in Å).[270]

The TCNQ stacks are also dimerized, as was to be expected for simple RAS with a half-filled band. The unusual feature of this structure is that the Peierls distortion is very high: the interplanar spacing inside the dimers is 3.438 Å, whereas that between the dimers is 4.156 Å.

Protonated 2,2′-disubstituted 4,4′-biimidazoles **110a–e** form RAS of two types with TCNQ: one type contains one-dimensional chain structures, while the other type contains two-dimensional layers composed of alternating segregated stacks of cations and radical anions.[271] The electronic structure of these RAS is determined by the system of hydrogen bonds between the radical anions and imidazolium cations, which gives rise to a non-uniform charge distribution in the radical anion stacks. Indeed, in the RAS $(\mathbf{110b})^{2+}(TCNQ)_3(MeOH)_2$ and $(\mathbf{110c})^{2+}(TCNQ)_3(MeOH)_2$ (the first type), the stacks contain molecules and radical anions ordered in the following way: $-TCNQ^{-\bullet}-TCNQ^{-\bullet}-TCNQ-$, *i.e.*, pinning of the charge density takes place. In the RAS $(\mathbf{110d})^{2+}(TCNQ)_3(MeOH)_2$ (the second type), the charge distribution is different: $-TCNQ^{0.5-}-TCNQ^{0.5-}-TCNQ^{-\bullet}$.[271] This difference is caused by the architecture of intermolecular hydrogen bonds in the RAS of various types (chains and layers).

The crystals of the RAS $DBA(TCNQ)_2$ (DBA is di-n-butylammonium) undergo reversible phase transition involving the transformation of dimerized TCNQ stacks at $T > 270$ K into a tetramerized structure in the low-temperature phase. This transition is accompanied by cleavage of

Structures 110



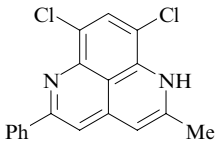
110a–e

R = H (**a**), Me (**b**), Et (**c**), Ph (**d**), 2-Th (**e**)

the intermolecular $DBA^+\cdots TCNQ$ hydrogen bonds and a sharp change in the conductivity and magnetic susceptibility.[272] The band gap is 0.526 eV in the hydrogen-bonded high-temperature phase and 0.286 eV in the low-temperature phase. At 267 K, the sample resistance considerably (1.8-fold) decreases, while on heating to 272 K, the resistance sharply (23.4-fold) increases, thus manifesting a hysteresis caused by a structural phase transition.[272]

An important role belongs to the hydrogen bonds between the cations and $TCNQ^{-\bullet}$ radical anions in the crystals of RAS based on phenalene and diazaphenalene.[273, 274] Indeed, 7,9-dichloro-2-methyl-5-phenyldiazaphenalene (**111**) forms a RAS of unusual 2 : 1 composition described as $(\mathbf{111})(\mathbf{111})^+(TCNQ^{-\bullet})(H_2O)_2$.[273]

Structure 111



111

This RAS is composed of segregated stacks, the N–H···N≡C hydrogen bonds arising between them connect the stacks into the D–A–D type triads (Fig. 26).

In the crystals of RAS with tris(alkylamino)phenalene (TAP) cations, the N–H···N≡C hydrogen bonds connect the segregated stacks of cations and radical anions to form layers (Fig. 27).[274]

A mixed proton–electron conductor was prepared from 2,2′-biimidazole (H_2Bim). The structure of the RAS $(H_3Bim^+)(TCNQ^{0.5-})(Cl^-)_{0.5}(H_2O)$ consists of segregated stacks of cations and TCNQ; channels partially filled by disordered chloride ions and water molecules run between the stacks of the H_3Bim^+ cations. The proton conduction occurs along these channels. At room temperature, the electron conduction ($\sigma_{rt} = 10\ \Omega^{-1}\ cm^{-1}$) is four orders of magnitude higher than the proton conduction. The conductivity of the crystals of this RAS changes from metallic

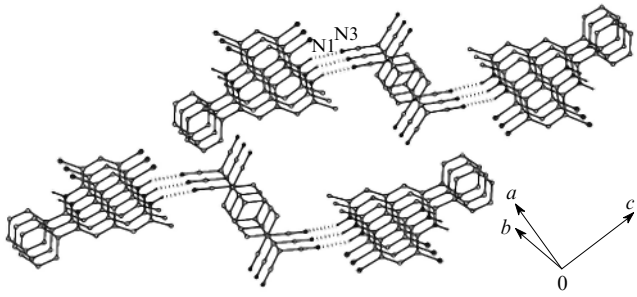


Figure 26. Triads of the segregated stacks D–A–D in the structure of the RAS $(\mathbf{111})(\mathbf{111})^+(TCNQ^{-\bullet})(H_2O)_2$.[273]

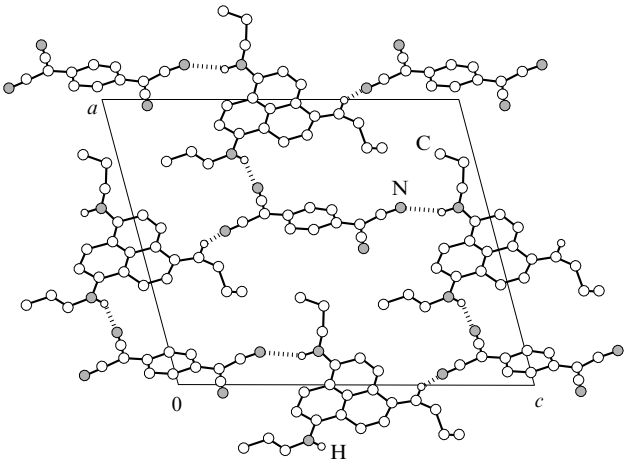


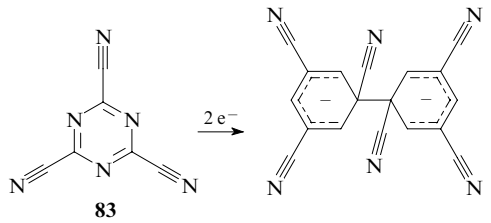
Figure 27. Structure of the RAS TAP(TCNQ) projected onto the (010) plane.[274]

($T > 250$ K) to semiconductor (in the range of $250 > T > 100$ K) and dielectric ($T < 100$ K).[149] The proton contribution to the conduction becomes noticeable at temperatures of >200 K; at 100 K, the Mott transition takes place.[149]

Among RAS with other radical anions, noteworthy is the salt (**24**)$_4$(C_4N_6)(H_2O) ($C_4N_6^{2-}$ is *N*,*N*′*N*″-tricyanoguanidinate anion), which is an organic metal.[275] The species **24** form layers through C—H···O, S···S and S···O intermolecular contacts; the *N*,*N*′*N*″-tricyanoguanidinate ions are also connected by hydrogen bonds through water molecules thus forming layers complementary to the cation layers. This RAS exhibits metallic properties down to 8 K, while below this temperature the metal–dielectric transition takes place.[275]

The reduction of 2,4,6-tricyano-1,3,5-triazine (**83**) to the radical anion is accompanied by dimerization to the dianion $(\mathbf{83})_2^{2-}$ (Scheme 9).[276]

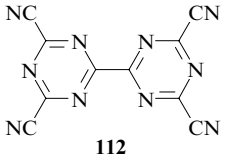
Scheme 9



83

This dianion with a somewhat elongated central C—C bond (1.57 Å) decomposes with elimination of two cyanide ions to give 4,4′,6,6′-tetracyano-2,2′-bitriazine (**112**). The latter forms a CTC with tetramethyl-*p*-phenylenediamine (TMPD), which has a radical ion structure (TMPD$^{+\bullet}$)[(**112**)$^{-\bullet}$]. The length of the central C—C bond in the radical anion (**112**)$^{-\bullet}$ is 1.492 Å, which is indicative of a considerable contribution of the sp^2-hybrid orbitals to the formation of this bond.[276] Acceptor **83** forms CTC with strong electron donors — (TTF)(**83**) and (TMPD)(**83**).[277] The structure of the CTC (TTF)(**83**) consists of mixed-type stacks with the ···DADA··· sequence; the CT value is very low, as far as one can infer from the crystallographic data: the lengths of the central C—C bond and the internal C—S bond are 1.348 and 1.756 Å, respectively, which are close to these lengths in neutral TTF (~1.35 and ~1.76 Å). Although no crystals of the complex (TMPD)(**83**) suitable for X-ray crystallography was obtained in the cited work,[277] the spectral data indicate that it also consists of virtually neutral donor and acceptor molecules.

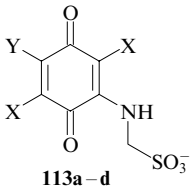
Structure 112



112

Akutsu *et al.*[277] reported four new anionic acceptors (**113a–d**) containing acceptor (1,4-benzoquinone) and anionic (sulfonate ion) components.

Structures 113



113a–d

X = Y = Cl (**a**), Br (**b**); X = Br: Y = Cl (**c**), Br_yCl_{1-y} (**d**)

Each of them forms two complexes with donor **53** (ET), differing in the composition and the type of the structure: the β-phase crystals $(ET)_5(\mathbf{113})_2(DCE)(H_2O)_z$ and the λ-phase crystals $(ET)_2(\mathbf{113})(MeOH)$. They all are narrow band-gap semiconductors, their σ_{rt} values being in the range of 0.14–0.67 Ω^{-1} cm^{-1}. The band gap for the β-phase salts is ~0.08 eV, while for the λ-phase salts it is approximately twice larger.

IV. Magnetic exchange interactions in the TCNQ radical anion salts

1. Ferromagnets based on TCNQ and other strong acceptors

The early stage of investigations of the TCNQ RAS (1960s and the early 1970s) was mainly related to attempts to fabricate organic superconductors. This accounts for the fact that little attention was paid to magnetic properties of these salts. The situation started to change in the mid-1990s when the first TCNQ-based organic ferromagnets were obtained. Before that, most researchers had considered the ferromagnetic state in purely organic objects to be impossible. Back in 1928, Heisenberg[278] formulated the statement that ferromagnetic ordering is possible only in systems containing heavy atoms, *i.e.*, metals, metal oxides and other metal compounds.

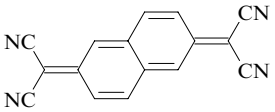
A A Ovchinnikov was the first to cast doubt on this statement. He proposed a topological ferromagnet model.[279,280] In 1987, the first organic ferromagnet, substituted polyacetylene poly[1,4-bis(2,2,6,6-tetramethyl-5-piperidyl-1-oxyl)butanediyne] (poly-BIPO), was obtained under his supervision.[281] The Curie temperature of this ferromagnet $T_C \approx 420$ K; however, the saturation magnetization (M_s) was very low (<0.1%). In 1991, an organic ferromagnet with $T_C = 16.1$ K was obtained, namely, the fullerene C_{60} complex with tetrakis(dimethylamino)-ethene.[282]

In this connection, the ability of TCNQ salts to form magnetically ordered structures, in particular, ferromagnetic ones, discovered in 1996 appears impressive.[20] This behaviour was detected for the long known compound $Cs_2(TCNQ)_3$ described back in the review by Melby *et al.*[1] and the salt $(Me_4N)_2(TCNQ)_3$. These RAS exhibit ferromagnetic properties even at room temperature; for the former, M_s reaches 1.46 emu mol^{-1}, the coercive force (H_c) is 100 Œ, while for the latter, these values are 0.79 emu mol^{-1} and 300 Œ, respectively. The RAS $(Me_4N)_2(F_4TCNQ)_3$ is also ferromagnetic.[283] For this RAS, H_c is even lower ($\sim$25 Œ) and the magnetic moment is very low (10^{-3} μ_B). This low characteristics (as compared with the expected value of 5580 emu mol^{-1}) was attributed[20] to polymorphism. For example, two crystalline forms are known for the RAS $(Me_4N)_2(TCNQ)_3$ — plates and needles. It is stated that ferromagnetic properties are inherent only in needle crystals the content of which does not exceed 0.1%. All these RAS have low conductivity ($\sigma_{rt} \approx 10^{-3}$–$10^{-5}$ Ω^{-1} cm^{-1}).[20,283]

Surprising was the preparation of TCNQ RAS that were ferromagnetic at room temperature and, moreover, had high electrical conductivity:[21] $(Me_4N)_2(DMTCNQ)_3$ and $(Me_4P)_2(DMTCNQ)_3$ (DMTCNQ = **62f**).

The ferromagnetic properties of these RAS were described in detail above and the conductivities at room temperature were 15 and 37 Ω^{-1} cm^{-1}, respectively.

Structure 114



114 (TNAP)

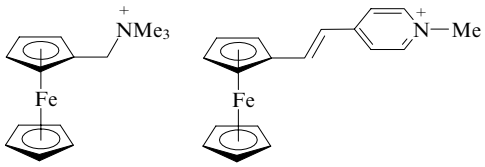
Similarly, noticeable conductivity ($\sigma_{rt} \approx 0.1$ Ω^{-1} cm^{-1} for compressed pellet samples) and ferromagnetic properties were found for the RAS Cs_2(**62g**)$_3$, Cs_2(**114**)$_3$,[284] and also (Me$_4$N)(**62g**), (Me$_4$P)(**62g**) and $(Me_4As)_2$(**62g**)$_3$.[285]

The first RAS containing a transition metal cation and capable of magnetic ordering was synthesized in 1979.[286] The compound $(FeCp_2^*)^{+\bullet}(TCNQ)^{-\bullet}$ (Cp* is pentamethylcyclopentadienyl) exhibits metamagnetic properties: at $T < 6$ K, antiferromagnetic transition occurs in fields below 1.5 kŒ and a ferromagnetic transition occurs at >1.5 kŒ. Subsequently, a ferromagnetic ordering with the Curie temperature of $\sim$16 K was found[287,288] in the crystals of the RAS $(FeCp_2^*)^{+\bullet}(TCNE)^{-\bullet}$. The magnetic susceptibility of the RAS $[Fe(\eta^5\text{-}C_5Et_5)_2]^{+\bullet}(A)^{-\bullet}$ (A = TCNQ, TCNE) is described by the Curie–Weiss equation with the Weiss constants $\theta = 6.1$ and 7.5 K, respectively, which implies the tendency toward ferromagnetic ordering.[289] The effect of the substituent nature and the symmetry of ferrocenium cations was demonstrated in a study[290] dealing, in particular, with the TCNQ salts with unsymmetrical cations **115a**,**b**.

All three synthesized RAS, (**115a**)(TCNQ), (**115a**)$(TCNQ)_2$MeCN and (**115b**)(TCNQ), are diamagnetic.

In 1991, the RAS $V(TCNE)_x(CH_2Cl_2)_y$ ($x \approx 2$, $y \approx 0.5$) with a high Curie temperature ($T_C \approx 400$ K) was prepared.[291,292] The presence of non-coordinated dichloromethane molecules does not affect the Curie temperature but

Structures 115



115a **115b**

increases the structural disorder, which results in a decrease in the coercive force at room temperature. The solvent-free molecular magnet $V(TCNE)_x$ can be prepared by co-deposition of a TCNE and $V(CO)_6$ gas mixture as films onto a glass substrate.[293,294] These films have a high degree of structural ordering, which has been employed to develop the first organic film magnet operating at room temperature.[295] This discovery stimulated further studies of TCNE RAS with other d- and f-metals. Vickers *et al.*[296] described the RAS $Ni(TCNE)_2(CH_2Cl_2)_x$ with $T_C = 13$ K and studied the influence of vanadium replacement by nickel in the systems $V_xNi_{1-x}(TCNE)_y(CH_2Cl_2)_z$. When $x > 0.05$, the T_C value does not change significantly but the magnetic moment (M) increases, and the properties of the molecular magnet can thus be varied by chemical methods.

The molecular magnet of a similar composition based on iron — the RAS $Fe(TCNE)_2(CH_2Cl_2)_x$ — shows ferromagnetic properties at $T < 100$ K.[297] The lanthanide-based salts — $Ln(TCNE)_3$ (Ln = Gd, Dy) — demonstrate ferrimagnetic properties at low temperatures (3.5 and 8.5 K, respectively).[298] When TCNE reacts with manganese(II) iodide, mixed salts containing the $TCNE^{-\bullet}$ radical anion and iodide ions, $Mn^{II}(TCNE)_{3/2}(I_3)_{1/2}$ and $Mn^{II}(TCNE)(I)(H_2O)$, are formed.[299,300] The former salt undergoes transition to the ferrimagnetic state caused by the three-dimensional antiferromagnetic interaction of the manganese ions ($S = 5/2$) with the bridging μ_4-TCNE ions. The salt $Mn^{II}(TCNE)(I)(H_2O)$ is a 2D antiferromagnet with $T_C = 171$ K. Thus, magnetic ordering of different types is possible in the salts $M(TCNE)_n$ depending on the nature of the metal, which opens up broad opportunities for their application.

Naturally, attempts were made to obtain magnetically ordered structures based on other acceptors. Vickers *et al.*[301] reported a series of RAS of the composition $V(R_2TCNQ)_2(CH_2Cl_2)_z$ (R = H, Br, Me, Et, Pr^i, OMe, OEt, OPh). Magnetic ordering was observed in all of these salts; the T_C value varies over a broad range: from 7.5 (R = Me) to 106 K (R = OEt). Ferromagnetic phases were also found in the TCNQ RAS with other d-metals: $M(TCNQ)_2$ (M = Mn, Fe, Co, Ni).[302,303] The Curie temperatures are relatively low as compared with similar RAS based on TCNE, the coercive forces are also small (the values at 2 K are given).

RAS	T_C/K	H_c/G
$Mn(TCNQ)_2$	44	20
$Fe(TCNQ)_2$	28	750
$Co(TCNQ)_2$	7	190
$Ni(TCNQ)_2$	24	270

In the heterospin system containing 3d- and 4f-metal ions, $[\{CuL\}_2Gd(TCNQ)_2](TCNQ)(MeOH)(MeCN)_2$ [L^{2-}

is *N*,*N*′-propylenebis(3-methoxysalicylideneiminate) ion], radical anions make no contribution to the magnetic susceptibility due to dimerization to give diamagnetic σ-dimers $\{(TCNQ)_2\}^{2-}$.[304] Therefore, the magnetic properties of this RAS are determined by virtually isolated [Cu_2Gd] triads (9 unpaired electrons).

The radical anion salt $\{[Gd_2(TCNQ)_5(H_2O)_9][Gd(TCNQ)_4(H_2O)_3]\}\cdot 4H_2O$ containing only gadolinium cations is an interesting example of the cation–anion complex formed upon coordination of the radical anion $TCNQ^{-\bullet}$.[305] The structure of this RAS is composed of alternating cationic and anionic layers in which the Gd^{3+} cations coordinate the radical anions $TCNQ^{-\bullet}$ in different stoichiometry. In the cationic layers, the Gd^{3+} cations have the coordination number of 9: one sort of cations coordinates 5 radical anions and 4 water molecules, while the other coordinates 4 radical anions and 5 water molecules (Fig. 28 *a*). In the anionic layers, the Gd^{3+} cations coordinate 6 nitrogen atoms of the nitrile groups and three water molecules (Fig. 28 *b*). The magnetic moment slightly decreases from 14.84 μ_B at room temperature to 14.37 μ_B at 50 K, and at $T_C = 3.5$ K, transition to the ferromagnetic phase takes place.[305]

A series of lanthanide RAS based on TCNQ and F_4TCNQ have been reported.[306, 307] Zhang *et al.*[306] discovered a unique transition from the magnetically disordered RAS $[Gd_2(TCNQ)_4(H_2O)_{10}](TCNQ)_2\cdot 3H_2O$ to the magnetically ordered RAS $[Gd_2(TCNQ)_6(H_2O)_5]$ with $T_C = 4$ K. Among the series of RAS $[M(F_4TCNQ)_2(H_2O)_x](F_4TCNQ)\cdot 3H_2O$ (M = La, Pr, Nd, Sm, Eu, Gd, Dy, Ho, Er, Yb), only in the samarium salt, does the ferromagnetic ordering take place at $T_C = 4.4$ K.[308] In the gadolinium and dysprosium salts, this ordering occurs upon partial dehydration at $T_C = 3.7$ and 4.3 K, respectively. The salt $[Ce_2(TCNQ)_4(H_2O)_{10}(MeOH)_2](TCNQ)_2\cdot 2H_2O\cdot 2MeOH$ contains non-interacting cerium ions, and no magnetic ordering is observed.[308] Nevertheless, the ferromagnetic ordering does take place when TCNQ is replaced by its 2,5-dihalo derivatives: the RAS $[Ce_2(Br_2TCNQ)_4(H_2O)(MeOH)_9](Br_2TCNQ)_2$ and $[Ce(Cl_2TCNQ)_2(H_2O)(MeOH)_9](Cl_2TCNQ)_2$ switch to the ferromagnetic state at $T_C = 5.4$ and 7.1 K, respectively.[308] The influence of slight modification of the acceptor on the magnetic properties of RAS found in this work opens up broad prospects for the design of new magnetic materials from RAS with 4f-elements.

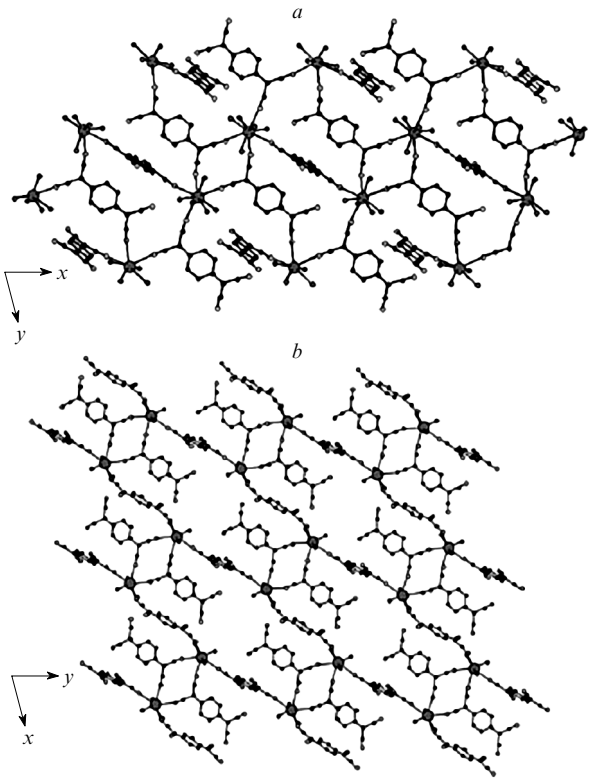


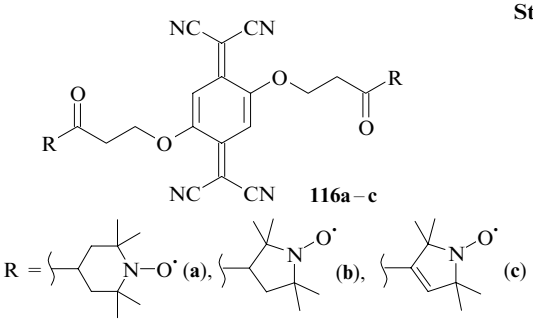
Figure 28. Structure of the cationic (*a*) and anionic (*b*) layers in the RAS $\{[Gd_2(TCNQ)_5(H_2O)_9][Gd(TCNQ)_4(H_2O)_3]\}\cdot 4H_2O$.[305]

The synthesis of a new molecular magnet with $T_C = 205$ K from dicyanoperfluorostilbene [*trans*-1,2-dicyano-bis(perfluorophenyl)ethylene, DCPFS) was unexpected.[83] The compound $V(DCPFS)_2$ is a 'soft' ferromagnet with a very small coercive force, which does not exceed 20 G at 5 K. Tetracyanopyrazine (TCNP) also forms a ferromagnetic RAS with vanadium, $V(TCNP)_2(CH_2Cl_2)_y$ with $T_C = 200$ K.[309] The reaction of 1,2,4,5-tetracyanobenzene (TCNB) with vanadium hexacarbonyl in dichloromethane or trifluoromethylbenzene gave the RAS $V^{II}(TCNB^{-\bullet})_{1.5}(TCNB^0)_{x-1.5}[V^{-I}(CO)_6]_{0.5}(Solv)_z$ (Solv is solvent, $4 > x > 3.5$). This RAS is a ferromagnet with $T_C = 325$ K.[310] The reaction of TCNB with $V(PhMe)_2$ in dichloromethane gives the ferromagnet $V^{II}(TCNB^{-\bullet})_2(CH_2Cl_2)_z$ with $T_C = 200$ K.[310] It can be seen that the addition of diamagnetic TCNB and partial replacement of the RAS $V^{II}(TCNB^{-\bullet})_2$ by hexacarbonylvanadate ion results in a sharp increase in the Curie temperature.

The salts Ni(TCNQ) and $Ni_3(TCNQ)_2$ were synthesized by an electrochemical procedure.[311] The former salt contains paramagnetic Ni^{II} cations and diamagnetic $TCNQ^{2-}$ anions, while the latter salt consists of diamagnetic Ni^{II} cations and paramagnetic $TCNQ^{3-}$ anions with the spin of 0.5. Note that the TCNQ oxidation state of −3 is known only for this salts and can be attained only by electrochemical reduction. Both salts exhibit ferromagnetic properties at high temperatures (the effective magnetic moment increases with temperature decrease) and antiferromagnetic behaviour at low temperatures. The Curie temperatures are 28.3 and 8.6 K, respectively.

Suzuki *et al.*[312] studied the so-called one-component complexes of compounds **116a–c** (actually, autocomplexes) in which the TCNQ nucleus serves as the acceptor and nitroxide radicals of the substituent are the donors.

Structures 116



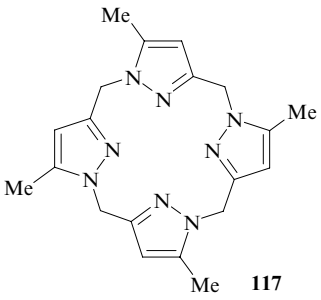
In the crystals of these autocomplexes, supramolecular ordering takes place, resulting in the formation of very short contacts between neighbouring molecules, the oxygen atom of one molecule being directed towards the centre of the quinoid ring of the adjacent molecule (the distance from the oxygen atom to the midpoint of the plane is 2.906 Å). All of the studied autocomplexes are weak antiferromagnets (the Weiss constants $\theta \approx -1$ K). Study of two-component CTC, for example, with TTF, is in prospect.

Thus, studies of CTC-based molecular magnets formed by strong electron acceptors are still at their infancy and quite a few surprises are to be expected.

2. Antiferromagnetic radical anion salts

The radical anion salt $[Cu(\mathbf{117})]_2(TCNQ)_7$ contains paramagnetic $[Cu(\mathbf{117})]^{2+}$ cations.[313]

Structure 117



117

As regards the TCNQ species, one is a radical anion (species **A** in Fig. 29), while the other six have a charge of $-1/2$. The TCNQ species are stacked and the metal-containing macrocycles are sandwiched between the stacks (see Fig. 29). The magnetic susceptibility of this RAS is determined by two contributions, one from paramagnetic ions $[Cu(\mathbf{117})]^{2+}$ (spin 0.5) and one from TCNQ species, which undergo strong antiferromagnetic interaction in the stacks. At 300 K, the magnetic moment is 3.12 μ_B, which corresponds to two unpaired electrons (one from the cations and one from the radical anions), while at $T = 3$ K, $\mu_{eff} = 1.82$ μ_B, which implies one unpaired electron (no contribution of the radical anions).

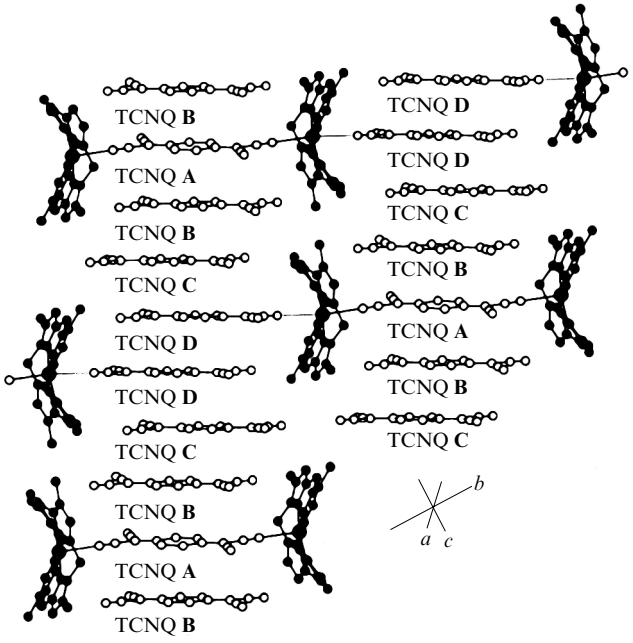
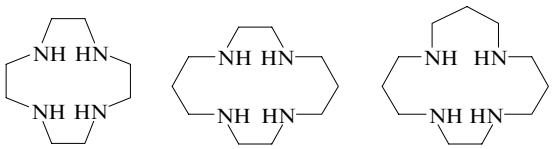


Figure 29. TCNQ stacks in the RAS $[Cu(\mathbf{117})]_2(TCNQ)_7$. Four crystallographically non-equivalent TCNQ species, **A**, **B**, **C** and **D**, are shown.[313]

Weak antiferromagnetic interaction was detected in TCNQ salts with cations based on macrocyclic polyimines **118a–c**.[314]

Structures 118



118a **118b** **118c**

In the complexes $[Cu(\mathbf{118a})](TCNQ)_2$, the copper atom has a coordination number of 6 upon coordination of four polyimine nitrogen atoms and two $TCNQ^{-\bullet}$ nitrogen atoms. The overlap of the π-orbitals of neighbouring $TCNQ^{-\bullet}$ radical anions gives rise to diamagnetic dimeric dianions $(TCNQ)_2^{2-}$. The thus arising structure represents chains of metal-containing macrocyclic cations and dianions. According to magnetic measurements,[314] the bond in dimers can be cleaved only at about room temperature, which is manifested as an increase in the magnetic moment at temperatures above 150 K.

In the crystals of the RAS $(IBnNH_2Py)(TCNQ)$ [$IBnNH_2Py$ is 4-amino-1-(4-iodobenzyl)pyridinium], the cations and the radical anions form segregated stacks; between the cations and the radical anions, strong hydrogen bonds arise involving the TCNQ cyano groups and the amino groups of the cations.[315] This could impart some two-dimensional character to the electronic system of the RAS; however, electrophysical measurements were not carried out in the study cited [315] and the magnetic susceptibility is described by the Curie–Weiss law. Meanwhile, the RAS $(BrBnQi)(TCNQ)_2$ [BrBnQi is 1-(4-bromobenzyl)quinolinium] is a spin gap system.[315]

Analogous RAS of the composition (IBnMePy)TCNQ, $(IBnMe_2Py)TCNQ$, $(BrBnMe_2Py)TCNQ$ and $(CNBnMe_2Py)TCNQ$ [IBnMePy is 1-(4-iodobenzyl)-3-methylpyridinium, $IBnMe_2Py$ is 1-(4-iodobenzyl)-3,5-dimethylpyridinium, $BrBnMe_2Py$ is 1-(4-bromobenzyl)-3,5-dimethylpyridinium, $CNBnMe_2Py$ is 1-(4-cyanobenzyl)-3,5-dimethylpyridinium] have been reported.[316] Hydrogen bonds and π–π-interactions form a complex three-dimensional crystal structure of these RAS containing one-dimensional channels. Strong antiferromagnetic interactions of the $TCNQ^{-\bullet}$radical anions result in dimerization. Finally, the temperature dependence of the magnetic susceptibility is described by the spin gap model:

$$\chi = \frac{\chi_{dimer}}{1 - (zJ'/Ng^2\beta^2)\chi_{dimer}} + \frac{C}{T}$$

$$\chi_{dimer} = \frac{Ng^2\beta^2}{k_B T} \frac{1}{3 + \exp(\Delta/k_B T)} \qquad (2)$$

where N is Avogadro' number, g is the Lande g-factor, β is the Bohr magneton, C is the Curie constant. The fitting parameters of Eqn (2) for these RAS are as follows:[316]

Cation	Δ/k_B/K	zJ'/k_B/K	C/emu mol^{-1}	g
IBnMePy	1723	−11	1.8×10^{-3}	2.0063
$IBnMe_2Py$	1689	− 7	2.2×10^{-3}	2.0067
$BrBnMe_2Py$	1682	− 6	1.5×10^{-3}	2.0060
$CNBnMe_2Py$	1684	− 8	2.3×10^{-3}	2.0064

The singlet – triplet model describes also the temperature dependence of the RAS $(NO_2BnPy)TCNQ$ and $(NO_2BnPy)(TCNQ)_2$ [NO_2BnPy is 1-(4-nitrobenzyl)pyridinium] with the parameters $\Delta/k_B = 1813$ K, $zJ'/k_B = -6$ K and $\Delta/k_B = 1882$ K, $zJ'/k_B = -11$ K, respectively.[317] Transition from the paramagnetic state in the high-temperature phase to the spin gap state in the low-temperature phase was also observed for the RAS $AP(TCNQ)(H_2O)$ [AP is 4-amino-1-n-butylpyridinium),[318] $AB(TCNQ)$, $(CP)_2(TCNQ)_3$ and $(BQ)_2(TCNQ)_2(MeCN)$ [AB is 4-amino-1-benzylpyridinium, CP is 1-(2-chlorobenzyl)pyridinium, BQ is 1-(4-bromobenzyl)quinolinium];[319] $(CNQi)_2(TCNQ)_3$ and $(CNPy)_2(TCNQ)_3$ [CNQi is 1-(4-cyanobenzyl)quinolinium, CNPy is 1-(4-cyanobenzyl)pyridinium];[320] $(IBnQi)(TCNQ)_2$ [IBnQi is 1-(4-iodobenzyl)quinolinium];[321] and $(Bbzim)(TCNQ)_{1.5}(MeCN)$ [Bbzim is 1,3-bis(4-cyanobenzyl)-1*H*-imidazolium].[322]

The supramolecular architecture of TCNQ RAS with cations based on nickel and copper complexes with polyamines has been considered in detail.[323]

In 1974, it was demonstrated[324] that a spin-Peierls transition can take place in 1D systems, *i.e.*, at $T < T_{SP}$ (T_{SP} is the spin-Peierls transition temperature), the uniform antiferromagnetic Heisenberg chains (high-temperature phase) are converted to a system of dimerized alternating antiferromagnetic chains (low-temperature phase). Note that the spin-Peierls transition is the magnetic analogue of the electronic Peierls transition.[8] As soon as a year later this theoretical prediction received experimental proof for the crystals of $(TTF)[Cu\{S_2C_2(CF_3)_2\}_2]$ ($T_{SP} = 12.4$ K) and $(TTF)[Au\{S_2C_2(CF_3)_2\}_2]$ ($T_{SP} = 2.06$ K).[325] Soon, in 1979, the spin-Peierls transition was detected in a study of the RAS $(MEM)(TCNQ)_2$[326] ($T_{SP} = 18$ K; MEM is *N*-methyl-*N*-ethylmorpholinium).

Copper germanate $CuGeO_3$ is also a magnet in which the spin-Peierls transition occurs at $T_{SP} = 14$ K; furthermore, it was found[327] that the spin-Peierls transition is affected by the magnetic field: the magnetic moment near T_{SP} increases with increase in the field strength. This effect is not unique to this inorganic compound but has been shown[328] to be inherent in any magnet with spin-Peierls instability.

The compound $(DEM)(TCNQ)_2$ (DEM is *N*-diethylmorpholinium) also exhibits spin-Peierls instability with $T_{SP} = 23$ K.[329] It can be seen that the spin-Peierls transition temperatures are very low. However, back in 1978 the opinion was stated[330] that the phase transition observed in the crystals of the RAS K(TCNQ) at 396 K is a spin-Peierls transition. This transition is accompanied by a change in the band gap width and involves a sophisticated structural rearrangement of one-dimensional chains with simultaneous change in the spin structure of the salt. According to microwave conductivity measurements for K(TCNQ), the activation energy for conduction in the low-temperature spin-Peierls phase is 0.26 eV, while above T_{SP} it is 0.13 eV.[331]

It was proposed[332, 333] that all of the salts described as $Ct^+(TCNQ^{-\bullet})$ (Ct is an alkali metal or ammonium cation) are spin-Peierls systems with unusually high temperatures T_{SP} (200 – 400 K). This suggestion is confirmed by spectral investigations of these salts[334] and by heat capacity measurements of $(NH_4^+)(TCNQ^{-\bullet})$.[335] The spin-Peierls transition in this salt is manifested as a sharp endothermal peak at 300 K without noticeable hysteresis. The same T_{SP} value was found by differential scanning calorimetry, IR spectroscopy and X-ray diffraction[335] and by magnetic susceptibility measurements.

The spin-Peierls instability was also found in the RAS $(N\text{-Me-2,5-Me}_2\text{-Pz})(TCNQ)_2$ synthesized in our work.[268, 336] It follows from the optical studies of these RAS[336] that the band splitting is either absent or insignificant. However, we still detected a spin-Peierls transition[337] in a study of the temperature dependence of the magnetic susceptibility and the heat capacity (C). The temperature dependences of $\chi(T)$ and $C(T)$ are adequately described by the one-dimensional dimerized Heisenberg spin-1/2 chain:

$$\widehat{H} = -J\sum_{i=1}^{n/2}\left[\widehat{S}_{2i}\widehat{S}_{2i-1} + \widehat{S}_{2i}\widehat{S}_{2i+1}\right]$$

where $\widehat{H}$ is the Hamilton operator, J is the exchange parameter describing the antiferromagnetic interaction of the neighbouring spins of the chain, $\widehat{S}$ is the spin operator, i is the unit number. According to the calculations,[337] dimerized chains have a gap the width of which depends appreciably on the applied field strength. In low fields ($0 \leqslant H \leqslant 500$ mT), a second low-temperature susceptibility peak is expected and is actually observed.

The experimental and theoretical research indicate that at $T_{SP} = 36$ K, the dimers in the TCNQ stack are combined in tetramers, which corresponds to the spin-Peierls transition. In magnetic fields of > 50 mT, the gap collapses and the susceptibility increases at low temperatures. This is a new feature of behaviour of the spin-Peierls phase in the magnetic field predicted theoretically and observed experimentally in the purely organic system $(N\text{-Me-2,5-Me}_2\text{-Pz})(TCNQ)_2$.[337]

In the crystals of the salt containing the isomeric cation $(N\text{-Me-2,6-Me}_2\text{-Pz})$, two types of stacks exist: those formed by TCNQ species located in general position (species **A**) and those formed by the species located in special centrosymmetric positions (species **B** and **C**). In the stacks containing species **A**, the neighbouring anions are shifted relative to each other along the longitudinal axis by the C=C bond length, while in the stacks of species **B** and **C** the overlap is almost absent (Fig. 30).[338]

The electrophysical properties of this salt are described by a two-dimensional model. However, a study of the magnetic properties and the heat capacity over a broad temperature range (300 – 2 K) provides the conclusion that this is a spin ladder.[22] Neither one- nor two-dimensional Heisenberg antiferromagnetism models are suitable for describing the temperature dependence of the magnetic susceptibility. However, over the whole temperature range it is described quite satisfactorily by the empirical formula with the parameters $C_1 - C_6$ proposed[339] for spin ladders:

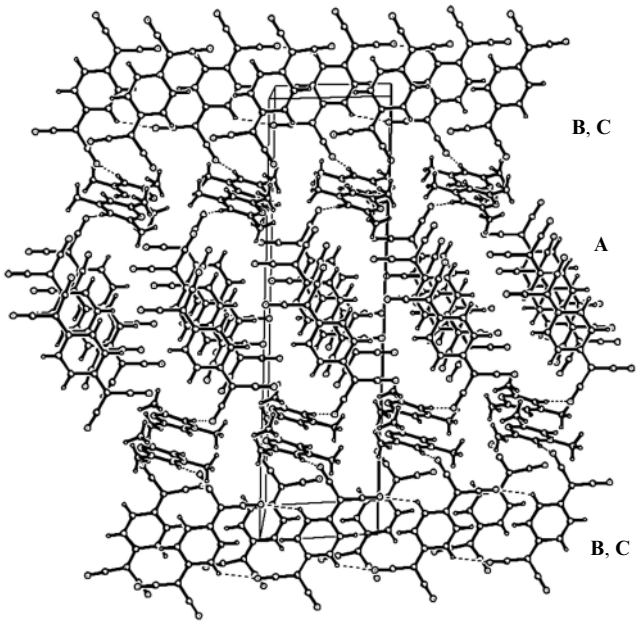


Figure 30. Fragment of the crystal structure of the RAS (*N*-Me-2,6-Me_2-Pz)$(TCNQ)_2$.[22]

$$\chi(T) = \frac{C_1}{T}\,\frac{1}{1+(T/C_2)C_3(\mathrm{e}^{C_4/T}-1)}\,\frac{1}{1+(C_5/T)C_6}$$

The model chosen for the theoretical description of the temperature dependence of the magnetic susceptibility and the magnetic heat capacity is presented in Fig. 31.[22] The calculations were carried out with a model Hamiltonian for a two-stack spin ladder using the program reported by Cheranovskii *et al.*[340]

$$\widehat{H} = J_{\mathrm{rung}}\sum_{j=1}^{N/2} S_{1,j}S_{2,j} + J_{\mathrm{leg}}\sum_{i=1}^{N/2}\sum_{j=1}^{N/2} S_{i,j}S_{i,j+1} - h\sum_{i,j} S_{i,j}^{z}$$

Here J_{rung} is the constant of exchange along the ladder rungs, J_{leg} is that along the ladder legs and h is the external magnetic field.

The temperature dependence of the magnetic heat capacity calculated with this Hamiltonian is described by the Maxwell function

$$C_{\mathrm{magn}} = \alpha T^2 \exp(-\beta T^2)$$

The measured heat capacity value is the sum of magnetic and lattice contributions. At low temperatures, the latter depends on temperature according to a cubic law. Then in the spin ladder model, the experimental value for heat capacity C can be expressed as follows:

$$C_{\mathrm{magn}} = \alpha T^2 \exp(-\beta T^2) + \gamma T^3$$

This value adequately describes the experimental results at $T \leqslant 20$ K. The spin ladder parameters are as follows: $J_{\mathrm{rung}}/k_{\mathrm{B}} = 28$ K; $J_{\mathrm{rung}}/J_{\mathrm{leg}} = 40$; $h/k_{\mathrm{B}} = 50$. These parameters correspond most closely to both the magnetic susceptibility and the magnetic heat capacity of the salt (*N*-Me-2,6-Me_2-Pz)$(TCNQ)_2$. Thus, it is quite probable that this salt is a spin ladder.[22]

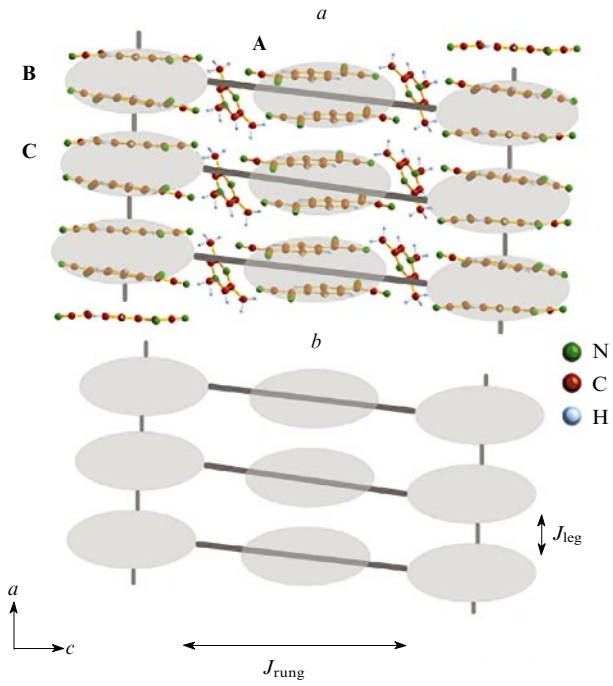


Figure 31. Crystal structure of the RAS (*N*-Me-2,6-Me_2-Pz)$(TCNQ)_2$.[22]
The cationic and anionic layers alternate along the *c* axis; two different types of overlap of the TCNQ species along the *a* axis can be seen (*a*) and schematic view of the spin ladder: antiferromagnetic interactions are shown by lines, and ellipses designate the effective spins of 1/2 of the TCNQ dimer (*b*).

In 2010, we reported[341] the crystal structure determination and measurement of magnetic properties of the RAS [*N*-Me-3,5-Me_2-Py](TCNQ)$_2$ (*N*-Me-3,5-Me_2-Py is *N*-methyl-3,5-dimethylpyridinium). The structure of this salt is formed by the TCNQ radical anions of four types (**A**, **B**, **C** and **D**) and two crystallographically independent cations. This salt has a layered structure in which the layers formed by cations alternate along the *a* axis with the layers consisting of TCNQ species. The latter form irregular stacks along the *b* axis and layers along the *c* axis (Fig. 32 and 33). In the stacks, **A**–**B** and **C**–**D** dimers can be distinguished. The interplanar spacings in the **A**–**B** dimers are 3.19 Å and those in the **C**–**D** dimers are 3.28 Å. Both types of dimers have spins of 1/2; therefore, upon temperature lowering, further ordering in the stacks is expected, resulting in the formation of spinless $(TCNQ)_4^{2-}$ tetramers upon spin-Peierls transition. The temperature dependence of the magnetic susceptibility is described by the formula

$$\chi(T) = \frac{A_1}{T}\exp\left(-\frac{\Delta_1}{T}\right) + \frac{A_2}{T}\exp\left(-\frac{\Delta_2}{T}\right)$$

with the parameters $\Delta_1 = 74.1$ K, $\Delta_2 = 26.6$ K. The existence of this unusual dependence is related to the presence of two types of stacks and, hence, two gaps in the magnetic excitation spectrum. Since the exchange integral exponentially decreases with increase in the distance, the greater gap can be attributed to the **A**–**B** dimers and the smaller one may correspond to the **C**–**D** dimers. Note that previously a two-gap magnetic structure was observed only for the crystals of the inorganic compound $(VO)_2P_2O_7$.[342] Thus,

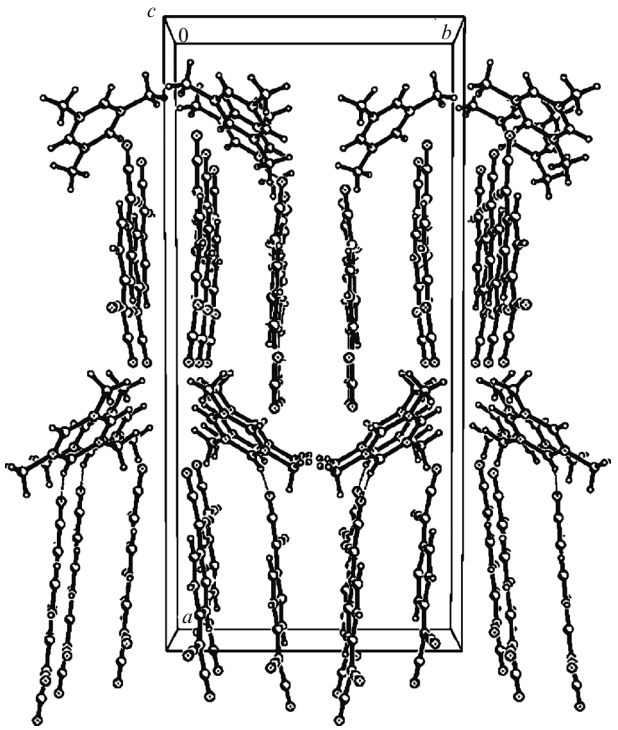


Figure 32. Crystal structure of the RAS (*N*-Me-3,5-Me_2-Py)$(TCNQ)_2$.[341]

the RAS (*N*-Me-3,5-Me_2-Py)$(TCNQ)_2$ is the second example of a two-gap spin-Peierls system.

Yet another example of a spin-Peierls system is apparently the RAS AP(TCNQ)$\cdot H_2O$ (AP is 4-amino-1-n-butylpyridinium) reported by Liu *et al.*[318] Its structure is formed by uniform stacks composed of the $TCNQ^{-\bullet}$ radical anions and cations (segregated stacking). The distance between the radical anions in the stack (4.054 Å) is too long for the conducting state to exist. Although electrophysical measurements were not performed in the study in question,[318] the IR spectrum of the salt indicates that it is a dielectric. Nevertheless, in this system, the spin-Peierls transition should take place if the period is doubled, which is likely to actually take place: the magnetic susceptibility increases on cooling down to ~100 K; below this temperature sharp transition to the diamagnetic phase takes place. (The researchers cited[318] explained this in a different way: by the repulsion of radical anions, hydrogen bonding between the cations and radical anions, spin–lattice and spin–spin interactions.) In the low-temperature region the susceptibility is described by a formula with a magnetic gap:

$$\chi(T) = \frac{\alpha \exp(-\Delta/k_B T)}{T} + \frac{C}{T} + \chi_0$$

where α is the dispersion of excitation energy, Δ is the spin gap, χ_0 is the van Vleck paramagnetism contribution. The Δ value was taken[318] to be 299 K.

V. Practical application of the radical anion salts of TCNQ

The unique properties of TCNQ and other related electron acceptors account for the broad applicability of these compounds.

Back in the second half of the 1980s, the discovery of fusible conducting TCNQ RAS opened up the unique opportunity of using them as solid electrolytes in the electrolytic capacitors of a new type. A melt of conducting RAS can be used for impregnation of porous electrodes based on aluminium, niobium and tantalum.[18, 19, 251, 252, 343] These capacitors have an obvious advantage over capacitors with a liquid electrolyte, which become useless as the electrolyte has dried. They are also preferred over the capacitors in which inorganic semiconductor materials such as manganese dioxide serve as the solid electrolyte. Manganese dioxide is applied onto a porous electrode the surface of which has an electrolytically pre-formed oxide layer. Upon the deposition of the conducting layer and during the operation, the dielectric layer is damaged resulting in increasing leakage current and loss of serviceability of the capacitor. The capacitors with TCNQ RAS have the unique capability of self-healing of dielectric layer defects.[251] Some researchers (see, *e.g.*, Ref. 343) attribute this feature to the fact that atmospheric oxygen can diffuse

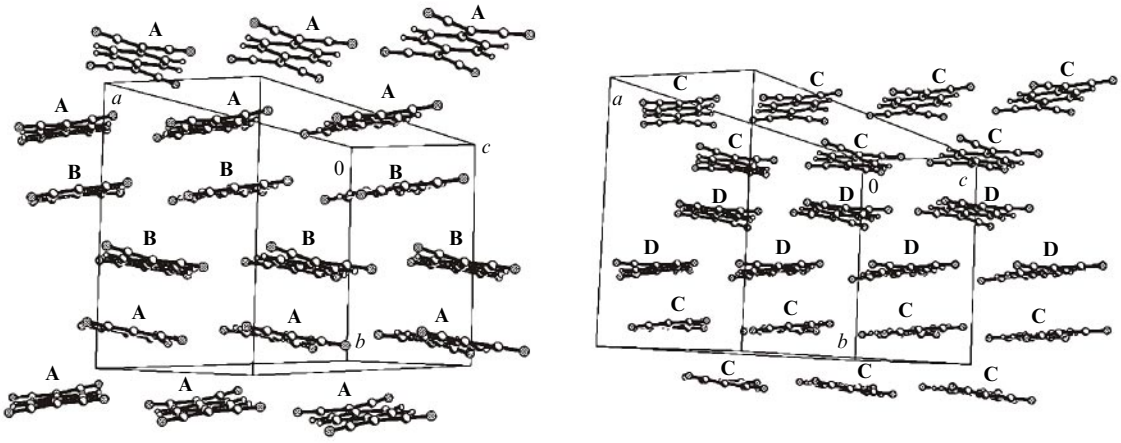


Figure 33. Two types of TCNQ layers in the RAS (*N*-Me-3,5-Me_2-Py)$(TCNQ)_2$ formed by different anions.[341]

through a layer of the organic conductor. It appears more likely that a radical anion salt of the complex composition can act as an oxidant with respect to the metal. In the case of oxide layer damage, the metal, for example aluminium, is brought into direct contact with the salt and then the reaction

$$Al + 3\,Ct^{+}(TCNQ)_2 \longrightarrow Al(TCNQ)_3 + Ct^{+}(TCNQ)^{-}$$

is possible resulting in restoration of the dielectric layer.

Other possibilities of application of the TCNQ salts appeared with the production of ultrathin conducting Langmuir–Blodgett films based on them. For example, the films of compound (**24**)($C_{10}H_{21}$-TCNQ) have the monolayer conductivity of $\sim 0.6\ \Omega^{-1}\ cm^{-1}$.[114] As the number of layers increases, the conductivity increases up to saturation at $\sim 10\ \Omega^{-1}\ cm^{-1}$, when the number of layers is 20. The conductivity also increases as the hydrostatic pressure grows at room temperature. The temperature dependence of the electrical conductivity is described by the formula taking into account the electron scattering.[344]

$$\sigma = AT^{-\alpha}\exp\left(-\frac{E_a}{kT}\right)$$

Relying on the measurements of the temperature dependence of thermal emf, Isotalo *et al.*[114] suggested the existence of structuring in the films with the formation of semiconducting domains.

Ultrathin films of this type can also be obtained based on the RAS (*N*-$C_{22}H_{45}$-Qn)(TCNQ).[345] The usual size of silicon-based electronic devices is about 1 μm, whereas the Langmuir–Blodgett films based on TCNQ RAS are suitable for the fabrication of electronic devices with dimensions comparable with molecular size. A significant advantage of such films is the possibility of accurate control of their thickness, which was demonstrated by Kim *et al.*[345] In addition, film thickness is very sensitive to temperature variation. For example, the thickness of the RAS (*N*-$C_{22}H_{45}$-Qn)(TCNQ) film deposited on the silicon surface sharply decreases on heating above 100 °C, and at temperatures of >120°C its thickness does not exceed 20% of the initial value measured at room temperature.[345] This is undoubtedly related to the flexibility of the hydrophobic alkyl substituent.

Jeszka *et al.*[346] demonstrated the possibility of using conducting TCNQ RAS for the fabrication of effective junctions in silicon or cadmium sulfide-based semiconductor devices. They can be used for both n- and p-type silicon semiconductors. Comparison with the junctions based on other molecular metals or conducting polymers attests to better characteristics of the TCNQ RAS-based junctions. It was shown[347] that the electronic properties of the TCNQ single crystals can be modified by vapour deposition of TTF layers on its surface. This modification occurs upon the formation of thin films of the CTC TTF(TCNQ) on the single crystal surface.

The adsorption of TTF, TCNQ and the complex TTF(TCNQ) on the Au(111) surface and the structures thus arising in the adsorption layer have been studied.[348] In the adsorption layers of both TTF and TCNQ, ordered structures (6×3) and (4×7), respectively, are formed. The adsorption layers of TCNQ are sensitive to the electrical potential applied: at 0.08 V (*vs.* reversible hydrogen electrode), structural transition into a new phase with the structure $(3\sqrt{3}\times12)$ occurs in these layers. The complex TTF(TCNQ) is capable of self-organization: domains with a lamellar structure differing from the structure of adsorption layers of pure TTF and TCNQ are formed on the Au(111) surface. An important role in the formation of the lamellar structure is played by π–π interactions.[348] These results are important for development of the preparation strategy of organic conducting films to be used in molecular electronics.

Tetracyanonaphthoquinodimethane (TNAP) is a stronger electron acceptor than TCNQ. When adsorbed on the Au(111) surface, it gives rise to weakly structured islets of virtually neutral TNAP molecules, *i.e.*, in this case, adsorption is mainly physical. However, adsorption of TNAP together with TTF affords highly ordered structures of alternating TNAP and TTF layers which substantially interact with the surface. It is of interest that TNAP species accept more than one electron, which reflects its high electron affinity.[349]

Owing to the ability to form intensely coloured CTC with many electron donors, TCNQ and other similar acceptors can be used for analytical purposes for spectrophotometric determination of various drugs. Table 8 gives examples of such assays many of which are applicable directly to pharmaceutical products.

The ability of TCNQ and other strong acceptors to form highly conducting CTC, which change properties in the presence of particular donor or acceptor compounds, can also be used for analytical purposes. For example, it is possible to manufacture a glucose-sensitive electrocatalytic biosensor based on the CTC TTF(TCNQ);[364] a polyvinyl chloride and TTF(TCNQ) composite can be used to fabricate an ion selective electrode to determine the concentrations of both cations and anions[365] and ascorbic acid.[366, 367] The complex TTF(TCNQ) can be used as a mediator of biosensors for glucose[368] and for simultaneous

Table 8. Examples of analytical applications of TCNQ and other acceptors.

Analyte	Reagent	Ref.
β-Adrenergic agents [a]	TCNQ, TCNE, BA, DDQ,[b] CA	350
Quinolones [c]	TCNQ	351
Lisinopril	TCNQ, CA	352
Gabapentin	TCNQ, DDQ, CA, TCNE	353
Azelastin	DDQ, CA, TCNQ	354
Pregabalin	DDQ, CA, TCNE, TCNQ	355
Cefotaxime	DDQ, CA, TCNE, TCNQ	356
Morpholine	TCNQ, CA	357
Domperidone, doxycycline	TCNE, TCNQ	358
Sodium alendronate	TCNQ, DDQ	359
Sitagliptin, vildagliptin	TCNQ, DDQ, CA	360
Amino acid derivatives [d]	TCNQ	361
Zolmitriptan	TCNQ	362
Mirtazapine	TCNE, TCNQ, DDQ	363

[a] Atenolol, timolol maleate, propranolol hydrochloride, metoprolol tartrate, betaxolol hydrochloride, levobunolol hydrochloride and bisoprolol fumarate; [b] DDQ is 2,3-dichloro-5,6-dicyano-1,4-benzoquinone (**63b**); [c] floxacin, levofloxacin, lomefloxacin, pipemidic acid; [d] carbocisteine, aminobutyric acid, dihydroxyphenylalanine.

determination of ascorbic and uric acids.[369] The ability of TCNQ to electron transfer in an external electric field can be used in pharmacokinetics and to develop biomembranes and chemical sensors.[370]

The possibility of preparing highly oriented conducting films based on strong organic acceptors stimulates vigorous research in the field of organic electronics, in particular, in nanotechnology. The progress achieved along this line implies creation of single-molecule-based electronics,[371] and in the future this may lead to the fabrication of computers assembled only from organic components.

The classical organic chemical vapour deposition (OCVD) technique provides highly oriented films of the CTC TTF(TCNQ) on glass and potassium chloride surface.[372, 373] The conductivity of these films ($\sigma_{rt} = 8\ \Omega^{-1}\ cm^{-1}$) is lower than that of single crystals but much higher than the conductivities of other organic films. It is noteworthy that the Peierls transition occurs in these films at $T \approx 58$ K, which is close to the values found for single crystals. The highly oriented films of TTF(TCNQ) and other CTC can favourably compete with thin-film pentacene-based transistors.[374]

Using TCNQ, the first *n*-channel single-crystalline and film organic transistors were fabricated.[375, 376] Field effect transistors were also fabricated based on CTC TTF(TCNQ) and TMTSF(TCNQ) films (TMTSF is tetramethyltetraselenafulvalene) consisting of three molecular layers. The transistor effect is observed when the potential changes from -15 to $+15$ V.[377, 378] Deposition of TTF(TCNQ) films from solution to appropriate substrates allows for the fabrication of thin-film field effect transistors of both p and n type.[379] The mobility of carriers reaches 0.16 $cm^2\ V^{-1}\ s^{-1}$, and the transistor effect is observed at potentials below -4 V.

The research concerned with TCNQ-based organic transistors have been developing rather vigorously in the last decade.[380–393] It was demonstrated[381] that the orientation of molecules in the TTF(TCNQ) fields can be controlled by an electric field. A high carrier mobility ($\sim 1\ cm^2\ V^{-1}\ s^{-1}$) was achieved in an n-type field effect transistor produced by a combination of the semiconductor CTC [DBTTF(TCNQ), DBTTF is dibenzotetrathiafulvalene] with a metallic CTC [TTF(TCNQ)].[382] By doping a thin-film transistor based on pentacene with F_4TCNQ, an equal mobility was attained, while the current increased more than 10^5-fold.[383] The possibility of fabrication of nanowires and nanotransistors by using joint evaporation and subsequent deposition of TTF and TCNQ in an alternating electric field was demonstrated.[387] An ambipolar field effect transistor based on the CTC (**53**)(TCNQ) was described.[390]

On the basis of TCNQ, it is possible to manufacture light-activated transistors favourably distinguished by high sensitivity and low noise.[394] Nanostructures based on graphene and TCNQ were described.[393] The interaction of graphene with the metallic substrate varies from very strong [*e.g.*, Ru(0001)] to weak [Ir(111)]. Doping of graphene films deposited on the iridium surface with acceptors (TCNQ and F_4TCNQ)[393–395] gives rise to holes in the graphene structure, the CT value being as high as ~ 0.3 for TCNQ and 0.4 for F_4TCNQ. The calculations by the density differential method for the graphene–F_4TCNQ system give a CT value of 0.3 electrons per acceptor molecule,[4] which is close to the experimental value. The TCNQ molecules form compact layers on the graphene surface. These molecular-size film structures can find numerous applications in the electronic and optoelectronic devices — field effect transistors, light emitting diodes and photovoltaic cells of solar panels.[393]

The electronic properties of the epitaxial layers of graphene (mono- or bimolecular) on the SiC(0001) surface can be precisely changed by adsorption of F_4TCNQ either from the gas phase or in solution.[396] The deposition of thin films of F_4TCNQ on the surface of various substrates [2,2′,7,7′-tetrakis(*N*,*N*-diphenylamino)-9,9-spirobifluorene, 4,4′,4″-tris(*N*-3-methylphenyl-*N*-phenylamino)triphenylamine, *N*,*N*′-bis(1-naphthyl)-*N*,*N*′-diphenyl-2,2′-dimethylbenzidine] may change the performance of these substrates.[397] The performance increases with increase in the F_4TCNQ layer thickness up to 7 nm and then reaches saturation.

Development of fabrication methods of micro- and nanowires (including molecular wires) based on organic materials has played an important role in extension of the scope of applicability of organic acceptors.[398–404] Back in 2002, long needle crystals of the CTC TTF(TCNQ) with a thickness of several tens of micrometres were obtained.[399] Whisker-like crystals of the same CTC were formed upon electric field assisted evaporation (EFAE) of the components.[400] The same method was used in another study[401] to prepare the nanowires of TTF(TCNQ); it was demonstrated that initially connected nanowires can be disconnected due to the Joule heat generated in the point contact. Linear and helical nanowires have been obtained by the two-phase method:[402]

$$\text{TTF (hexane)} + \text{TCNQ (MeCN)} \longrightarrow \text{TTF(TCNQ)}\downarrow$$

These nanowires can find use in new types of microelectronic devices. In the TTF(TCNQ) nanowires with a diameter of ~ 130 nm, the Peierls transition occurs at ~ 55 K,[403] which does not differ much from the value measured for single crystals. Oriented molecular nanowires can be grown on a mica surface.[404] A general strategy for the manufacture of nanowires of CTC using nanoelectrochemical procedures with carbon nanotubes as electrodes was developed.[405]

A method for the fabrication of microcapsules containing TTF and TCNQ was proposed.[406] These capsules were placed into microelectronic devices and in the case of contact failure in these devices, the contact can be restored by mere mechanical impact where the capsules crack and conducting grains of CTC are formed upon the reaction. The use of ionic liquids provides conducting gels of the CTC TTF(TCNQ).[407] These gels possess mixed electronic and ionic electrical conductivity.

Doping of poly(3-hexylthiophene) with the acceptor F_4TCNQ gives high-conductivity films ($\sim 1\ \Omega^{-1}\ cm^{-1}$, which is five orders of magnitude higher than for the initial polythiophene); this could find use for the fabrication of electrodes[408] (so-called plastic electrodes).

The TCNQ radical anion salts with alkali metal cations can reversibly add iodine from the gas phase. The 1 : 1 radical ion salts give the RAS Ct(TCNQ)I (Ct = Li, Na, K); in the case of rubidium, the salt has the composition $Rb_2(TCNQ)_3I_2$. The initial salts are diamagnetic and have low conductivity, whereas the iodine-saturated salts are paramagnetic and have conductivities of up to 0.1 $\Omega^{-1}\ cm^{-1}$.[409] This phenomenon can be employed for the design of highly sensitive sensors for iodine. Note that the RAS Na(F_4TCNQ) does not show such behaviour.

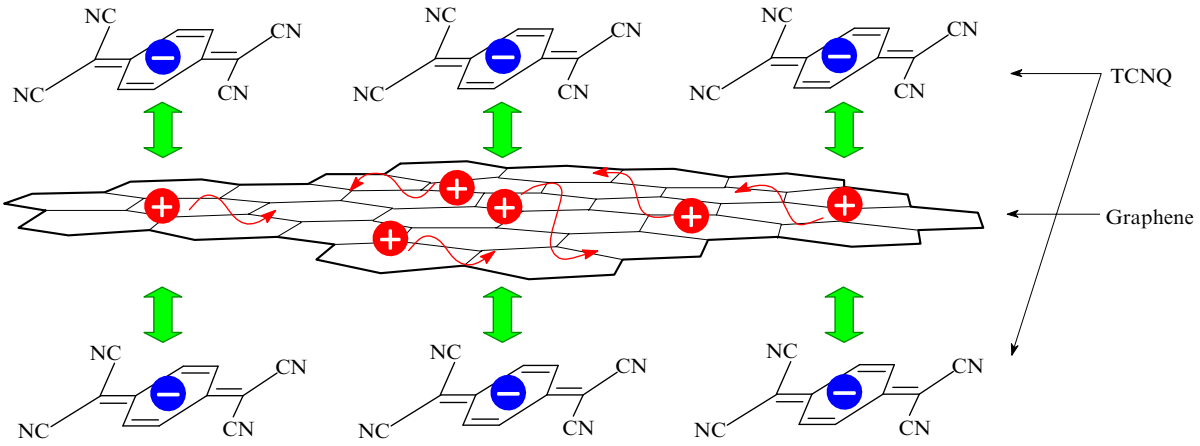
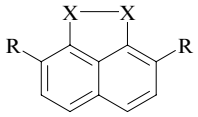


Figure 34. Scheme of graphene doping with adsorbed TCNQ molecules.[418]

Structures 119

The complexes of TCNQ with strong electron donors based on *peri*-dichalcogen naphthalenes **119** can be used to generate low-energy photons (down to 0.8 eV).[410]

A series of TCNQ derivatives, molecules and zwitter ions, that show nonlinear optical properties have been reported.[411] In particular, the CTC (**24**)$_9$($C_{14}H_{29}$-TCNQ) is suitable for the use in ink-jet printers for continuous ink



119

X = S, Se, Te; R = H, OMe

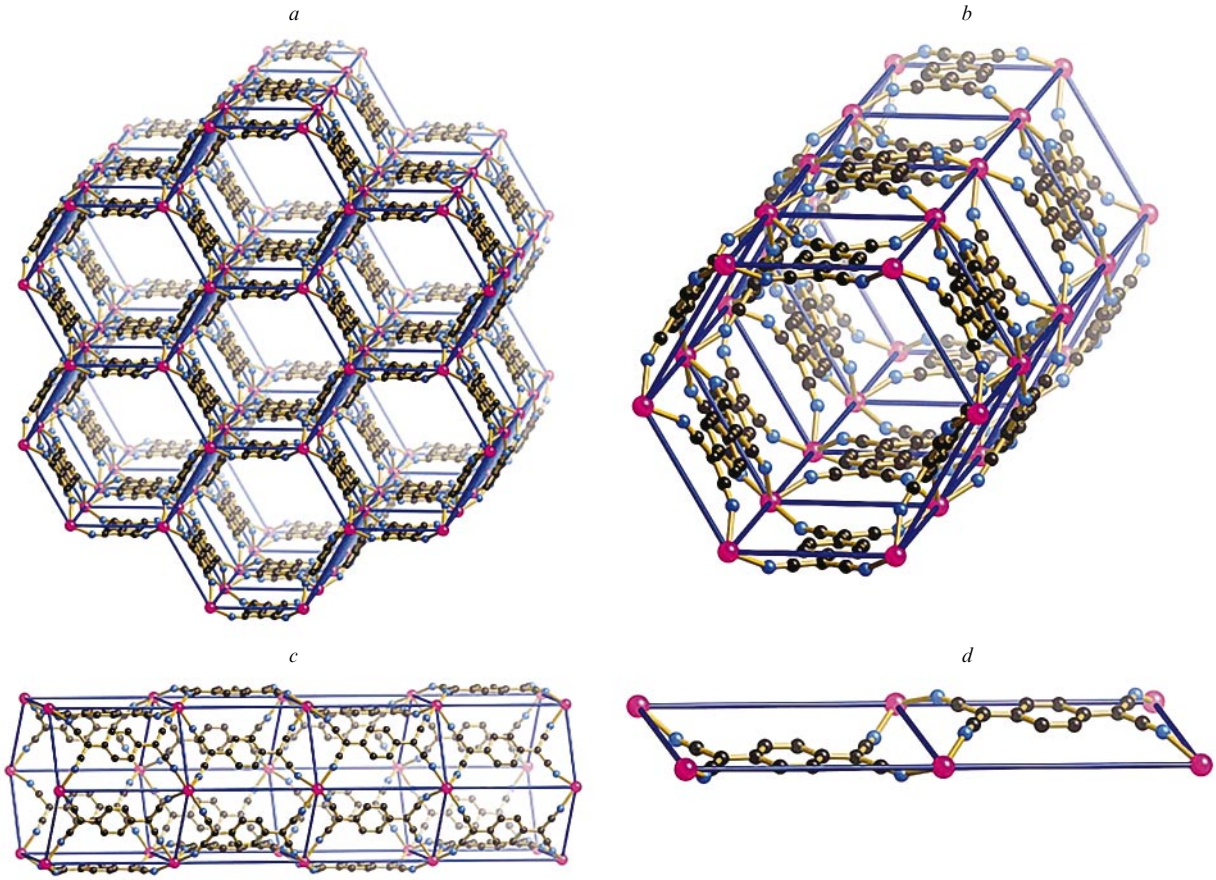


Figure 35. Structure of the RAS [Mn(bipy)$_3$][Mn_2(TCNQ)$_3$] (bipy is 2,2′-bipyridine).[420]
(*a*) Hexagonal channels formed by the $[Mn_2(TCNQ)_3]^{2-}$ anions; (*b*) enlarged image of a separate channel; (*c*) side view of a separate channel; (*d*) $TCNQ^{2-}$ dianions arranged parallel to the channel axis.

supply as an ink-jet printed organic electrode.[412] Treatment of silver nanoparticles as TCNQ generates a large positive charge on the nanoparticle surface, which sharply increases their affinity for alkenes. Therefore, these materials can be used to separate alkene–alkane mixtures.[413]

Radical anion salts, in particular, $(Bu^n_2NH_2)(TCNQ)_2$,[414] $(Et_3NH)(TCNQ)_2$,[415] and salts with morpholine-based cations,[416] can be used for information recording. The method is based on thermochemical hole burning (THB) in the RAS.

Charge transfer complexes based on acceptors capable of hydrogen bonding can exhibit ferroelectric properties.[82] These include 2,5-dihydroxy-*p*-benzoquinone, cyananilic and squaric acids. The possibilities of using RAS based on strong acceptors as materials for solar cells are being investigated.[417,418] For example, doping of graphene with TCNQ under controlled conditions results in the formation of p-doped films (Fig. 34).[418] Low amounts of TCNQ considerably improve the resistive properties of these films without deteriorating their optical transparency. These conducting transparent films can find numerous applications including flat panel displays, light emitting diodes and solar cells.

Of particular interest are the TCNQ RAS with inorganic cations such as Cu^I, Ag^I, Tl^I, Mn^{II}, Zn^{II} and Cd^{II}.[419–421] The structures of these salts have channels and, hence, they can be used to prepare intercalated compounds. In particular, hexagonal channels are present in the TCNQ salt based on Mn^{II} complexes (Fig. 35). These coordination polymers contain $TCNQ^{2-}$ dianions. Compounds of this type have been little studied as yet.

* * *

Radical anion salts and charge transfer complexes based on strong π-electron acceptors attracted the attention of researchers in the second half of the 1960s, as they were used to prepare the first organic metals. The second half of the 1980s witnessed a sort of renaissance in this field related to the discovery of fusible conducting organic materials and the discovery of their ability to form magnetically ordered structures (ferro-, ferri- and antiferromagnetic) and spin ladders. The vigorous development of the chemistry of RAS and CTC based on TCNQ and related acceptors in the last decade is caused by extensive scope of their applicability in microelectronics, spintronics and nanotechnologies.[418] There are grounds to believe that further studies in the TCNQ chemistry would bring quite a few discoveries.

References

1. L R Melby, R J Harder, W R Hertler, W Mahler, R E Benson, W E Mochel *J. Am. Chem. Soc.* **84** 3374 (1962)
2. L R Melby *Can. J. Chem.* **43** 1448 (1965)
3. B Milián, R Pou-Amérigo, R Viruela, E Ortí *Chem. Phys. Lett.* **391** 148 (2004)
4. H Pinto, R Jones, J P Goss, P R Briddom *J. Phys.: Condens. Matter.* **21** 402001 (2009)
5. W A Little *Phys. Rev. A* **134** 1416 (1964)
6. I F Schegolev *Phys. Stat. Sol., Ser. A* **12** 9 (1972)
7. E B Yagubskii, M L Khidekel *Russ. Chem. Rev.* **41** 2132 (1972)
8. R E Peierls *Quantum Theory of Solids* (Oxford: Oxford University Press, 1955)
9. K Krogmann, P Dodel *Chem. Ber., B* **99** 3402 (1966)
10. L Malatesta, F Canziani *J. Inorg. Nucl. Chem.* **19** 81 (1961)
11. I F Shchegolev, L I Buravov, A V Zvarykina, R B Lyubovskii *Pis'ma Zh. Eksp. Teor. Fiz.* **8** 353 (1968) [a]
12. V A Starodub, I V Krivoshei *Russ. Chem. Rev.* **51** 439 (1982)
13. L B Coleman, M J Cohen, D J Sandman, F G Yamagishi, A F Garito, A J Heeger *Solid State Commun.* **12** 1125 (1973)
14. F Wudl, D Wabschall, E J Hufnagel *J. Am. Chem. Soc.* **94** 670 (1972)
15. L I Buravov, G I Zvereva, L E Kaminskii, L P Rosenberg, M L Khidekel, R P Shibaeva, I F Shchegolev, E B Yagubskii *J. Chem. Soc., Chem. Commun.* 720 (1976)
16. L I Buravov, A I Kotov, M L Khidekel', I F Shchegolev, E B Yagubskii *Izv. Akad. Nauk, Ser. Khim.* 475 (1976) [b]
17. D Jerome, A Mazaud, M Ribault, K Bechgaard *J. Phys. Lett.* **41** L95 (1980)
18. JP P. 60-139832 (1987)
19. US P. 458055 (1986)
20. K Ueda, T Sugimoto, S Endo, N Toyota, M Kohama, K Yamamoto, Y Suenaga, H Morimoto, T Yamaguchi, M Munakata, N Hosoito, N Kanehisa, Y Shibamoto, Y Kai *Chem. Phys. Lett.* **261** 295 (1996)
21. T Sugimoto, K Ueda, S Endo, N Toyota, T Tada, K Nishimura, M Kohama, K Shiwaku, K Yamamoto, T Yamaguchi, Y Suenaga, M Munakata *Chem. Phys. Lett.* **288** 767 (1998)
22. A Radvvkovv, D V Ziolkovskiy, M Kajnakova, B Laskowska, B Barszcz, A Graja, V A Starodub, A Feher *J. Phys.: Condens. Matter* **21** 175405 (2009)
23. A Nafady, A M Bond, A Bilyk, A R Harris, A I Bhatt, A P O'Mullane, R D Marco *J. Am. Chem. Soc.* **129** 2369 (2007)
24. F H Herbstein, M Capon *Crystallogr. Rev.* **14** 3 (2009)
25. G Saito, T Murata *Philos. Trans. R. Soc. London, Ser. A* **366** 139 (2008)
26. J Huang, S Kingsbury, M Kertesz *Phys. Chem. Chem. Phys.* **10** 2625 (2008)
27. J B Torrance, J E Vazquez, J J Mayerle, V Y Lee *Phys. Rev. Lett.* **46** 253 (1981)
28. I F Golovkina, I V Krivoshei, V A Starodub, V G Aleshin, I M Gella, V V Nemoshkalenko, A I Senkevich, Yu N Surov *Teor. Eksp. Khim.* **15** 139 (1979) [c]
29. V E Kampar, O Ya Neiland *Russ. Chem. Rev.* **55** 334 (1986)
30. V V Malev, V V Kondratiev *Russ. Chem. Rev.* **75** 147 (2006)
31. S I Terashita, K Nakatsu, Y Ozaki *J. Phys. Chem.* **99** 3618 (1995)
32. H Okamoto, T Mitani, Y Tokura, S Koshihara, T Komatsu, Y Iwasa, T Koda, G Saito *Phys. Rev. B* **43** 8224 (1991)
33. M L Cointe, M H Lemée-Cailleau, H Cailleau, B Toudic *J. Mol. Struct.* **374** 147 (1996)
34. S Iwai, S Tanaka, K Fujinuma, H Kishida, H Okamoto, Y Tokura *Phys. Rev. Lett.* **88** 057402 (2002)
35. M Filatov *Phys. Chem. Chem. Phys.* **13** 144 (2011)
36. V Oison, C Katan, P Rabiller, M Souhassou, C Koenig *Phys. Rev. B: Condens. Matter* **67** 035120 (2003)
37. J B Torrance, A Girlando, J J Mayerle, J I Crowley, V Y Lee, P Batail, S J LaPlaca *Phys. Rev. Lett.* **47** 1747 (1981)
38. J Hubbard, J B Torrance *Phys. Rev. Lett.* **47** 1750 (1981)
39. A Girlando, F Marzola, C Pecile, J B Torrance *J. Chem. Phys.* **79** 1075 (1983)
40. M Masino, A Girlando, A Brillante, R G Della Valle, E Venuti *Mater. Sci. Pol.* **22** 333 (2004)
41. R Drago *Physical Methods in Chemistry* (Philadelphia: Saunders, 1977)
42. J J Mayerle, J B Torrance, J I Crowley *Acta Crystallogr., Sect. B: Struct. Crystallogr. Cryst. Chem.* **35** 2988 (1979)
43. M Le Cointe, M H Lemée-Cailleau, B Toudic, L Toupet, G Heger, F Moussa, P Schweiss, K H Kraft, N Karl *Phys. Rev. B: Condens. Matter* **51** 3374 (1995)

44. M Le Cointe, J Gallier, H Gailleau, M Gourdji, A Péneau, L Guibg *Solid State Commun.* **94** 455 (1995)
45. A Moreac, A Girard, Y Delugeard, Y Marqueton *J. Phys.: Condens. Matter* **8** 3553 (1996)
46. A Moreac, A Girard, Y Delugeard *J. Phys.: Condens. Matter* **8** 3569 (1996)
47. M Buron-Le Cointe, M H Lemée-Cailleau, H Cailleau, S Ravy, J F Bérar, S Rouzière, E Elkaïm, E Collet *Phys. Rev. Lett.* **96** 205503 (2006)
48. S Horiuchi, K Kobayashi, R Kumai, S Ishibashi *Chem. Lett.* **43** 26 (2014)
49. Y Matsubara, T Yoshida, T Ishikawa, Y Okimoto, S-Y Koshihara, K Onda *Acta Phys. Pol., A* **121** 340 (2012)
50. K Yonemitsu *Crystals* **2** 56 (2012)
51. Sh Ishibashi, K Terakura *Physica B* **405** S338 (2010)
52. K Kobayashi, S Horiuchi, R Kumai, F Kagawa, Y Murakami, Y Tokura *Photon Fact. Activ. Rep., Part B* **29** 166 (2012)
53. T Mitani, G Saito, Y Tokura, T Koda *Phys. Rev. Lett.* **53** 842 (1984)
54. G Giovannetti, S Kumar, A Stroppa, J van den Brink, S Picozzi *Phys. Rev. Lett.* **103** 266401 (2009)
55. K Kobayashi, S Horiuchi, R Kumai, F Kagawa, Y Murakami, Y Tokura *Phys. Rev. Lett.* **108** 237601 (2012)
56. J-i Nishizawa, T Tanno, T Oohashi, H Watanabe, Y Oyama *Synth. Met.* **158** 278 (2008)
57. A Wixtrom, J Buhler, S Pagola, T Abdel-Fattah, in *220th ECS Meeting (Abstracts)* (Boston, MA: Electrochemical Soc., 2011) Abstr. 1834
58. S V Rosokha, S M Dibrov, T Y Rosokha, J K Kochi *Photochem. Photobiol. Sci.* **5** 914 (2006)
59. Y Iwasa, T Koda, Y Tokura, A Kobayashi, N Iwasawa, G Saito *Phys. Rev. B: Condens. Matter* **42** 2374 (1990)
60. S Aoki, T Nakayama, A Miura *Phys. Rev. B: Condens. Matter* **48** 626 (1993)
61. Y Nogami, M Taoda, K Oshima, S Aoki, T Nakayama, A Miura *Synth. Met.* **70** 1219 (1995)
62. S Aoki, T Nakayama, A Miura *Synth. Met.* **70** 1243 (1995)
63. H Goto, H Asahi, T Inabe, H Ogata, S Miyajima, Y Maruyama *Synth. Met.* **70** 1237 (1995)
64. S Basaki, S Matsuzaki *Synth. Met.* **70** 1239 (1995)
65. S Matsuzaki, T Hiejima, M Sano *Bull. Chem. Soc. Jpn.* **64** 2052 (1991)
66. P García, S Dahaoui, P Fertey, E Wenger, C Lecomte *Phys. Rev. B: Condens. Matter* **72** 104115 (2005)
67. K Tasaki, S Matsuzaki, V M Yartsev *Phys. Status Solidi B* **203** 265 (1997)
68. P Garcna-Orduta, S Dahaoui, C Lecomte *Acta Crystallogr., Sect. B.: Struct. Sci.* **67** 244 (2011)
69. S Horiuchi, R Kumai, Y Okimoto, Y Tokura *Chem. Phys.* **325** 78 (2006)
70. S Horiuchi, R Kumai, Y Okimoto, Y Tokura *Synth. Met.* **133** – **134** 615 (2003)
71. R Sadonara, S Matsuzaki *Mol. Cryst. Liq. Cryst.* **296** 269 (1997)
72. S Horiuchi, Y Okimoto, R Kumai, Y Tokura *J. Phys. Soc. Jpn.* **69** 1302 (2000)
73. S Horiuchi, Y Okimoto, R Kumai, Y Tokura *J. Am. Chem. Soc.* **123** 665 (2001)
74. Y Iwasa, I Soga, T Koda, Y Tokura, G Saito *Synth Met.* **42** 1827 (1991)
75. Y Iwasa, N Watanabe, T Koda, G Saito *Phys. Rev. B: Condens. Matter* **47** 2920 (1993)
76. S Aoki, T Nakayama *Phys. Rev. B: Condens. Matter* **56** R2893 (1997)
77. M Masino, A Girlando, L Farina, A Brillante *Phys. Chem. Chem. Phys.* **3** 1904 (2001)
78. L Farina, A Brillante, M Masino, A Girlando *Phys. Rev. B: Condens. Matter* **64** 144102 (2001)
79. S Basaki, S Matsuzaki *Solid State Commun.* **91** 865 (1994)
80. T Hasegawa, T Akutagawa, T Nakamura, T Mochida, R Kondo, S Kagoshima, Y Iwasa *Phys. Rev. B* **64** 085106 (2001)
81. H Sakamoto, K Mizoguchi, T Hasegawa *Phys. Rev. Lett.* **93** 186401 (2004)
82. S Horiuchi, R Kumai, Y Tokura *Chem. Commun.* 2321 (2007)
83. J P Fitzgerald, Bh B Kaul, G T Yee *Chem. Commun.* **49** 49 (2000)
84. F Kagawa, S Horiuchi, H Matsui, R Kumai, Y Onose, T Hasegawa, Y Tokura *Phys. Rev. Lett.* **104** 227602 (2010)
85. A S Tayi, A K Shveyd, A C-H Sue, J M Sharko, B S Rolczynski, D Cao, T J Kennedy, A A Sarjeant, Ch L Stern, W F Paxton, W Wu, S K Dey, A C Fahrenbach, J R Guest, H Mohseni, L X Chen, K L Wang, J F Stoddart, S I Stupp *Nature (London)* **488** 485 (2012)
86. V A Starodub, Doctoral Thesis in Chemical Sciences, Khar'kov National University, Khar'kov, 1994
87. E Aharon-Shalom, J Y Becker, J Bernstein, S Bittner, S Shaik *Synth. Met.* **11** 213 (1985)
88. I V Krivoshei *Zh. Strukt. Khim.* **12** 110 (1976) [d]
89. J Y Becker, J Bernstein, M Dayan, A Ellern, L Shakal *Adv. Mater.* **6** 758 (1994)
90. E Ojima, H Fujiwara, H Kobajashi, A Kobajashi *Adv. Mater.* **11** 1527 (1999)
91. K Imaeda, T Mori, Ch Nakano, H Inokuchi, N Iwasawa, G Saito *Bull. Chem. Soc. Jpn.* **64** 2159 (1991)
92. I F Shchegolev, E B Yagubskii, in *Extended Linear Chain Compounds* Vol. 2 (Ed. J S Miller) (New York: Plenum, 1982) p. 385
93. K Takimiya, Y Aso, T Otsubo, F Ogura *Bull. Chem. Soc. Jpn.* **64** 2091 (1991)
94. J-i Yamada, H Akutsu, H Nishikawa, K Kikuchi *Chem. Rev.* **104** 5057 (2004)
95. M Iyoda, M Hasegawa, Y Miyake *Chem. Rev.* **104** 5085 (2004)
96. D Lorcy, N Bellec *Chem. Rev.* **104** 5185 (2004)
97. L Kaboub, J-M Fabre, L Vendier, J-P Legros *Acta Crystallogr. Sect. C: Cryst. Struct. Commun.* **66** o429 (2010)
98. K B Simonsen, N Svenstrup, J Lau, N Thorup, J Becher *Angew. Chem., Int. Ed.* **111** 1515 (1999)
99. M Yasutake, Y Sakamoto, S Onaka, K Sako, H Tatemitsu, T Shinmyozu *Tetrahedron Lett.* **41** 7933 (2000)
100. M Yasutake, K Araki, M Zhou, R Nogita, T Shinmyozu *Eur. J. Org. Chem.* 1343 (2003)
101. K Nielsen, J O Jeppesen, N Thorup, J Becher *Org. Lett.* **4** 1327 (2002)
102. T Poulsen, K A Nielsen, A D Bond, J O Jeppesen *Org. Lett.* **9** 5485 (2007)
103. U H F Bunz, V Enkelmann *Chem. – Eur. J.* **5** 263 (1999)
104. T Akutagawa, Y Abe, T Hasegawa, T Nakamura, T Inabe, Ch A Christensen, J Becher *Chem. Lett.* 132 (2000)
105. G Gachot, P Pellon, Th Roisnel, D Lorcy *Eur. J. Inorg. Chem.* 2604 (2006)
106. J D McKinney, P A Anderson, Th A Hamor, Ch J Jones, K Paxton, A Porch *J. Organomet. Chem.* **558** 147 (1998)
107. F de Montigny, G Argouarch, K Costuas, J-F Halet, Th Roisnel, L Toupet, C Lapinte *Organometallics* **24** 4558 (2005)
108. I V Jourdain, M Fourmigué, F Guyon, J Amaudrut *Organometallics* **18** 1834 (1999)
109. M Lohan, F Justaud, Th Roisnel, P Ecorchard, H Lang, C Lapinte *Organometallics* **29** 4804 (2010)
110. X Wu, Z Hu, A S Jeevarajan, M P Cava, R M Metzger *Synth. Met.* **70** 1169 (1995)
111. G Brocks *Phys. Rev. B: Condens. Matter* **55** 6816 (1997)
112. F Jäckel, U G E Perera, V Iancu, K-F Braun, N Koch, J P Rabe, S-W Hla *Phys. Rev. Lett.* **100** 126102 (2008)

113. K Kudo, M Nagaoka, S Kuniyoshi, K Tanaka *Synth. Met.* **71** 2059 (1995)
114. H Isotalo, G Yunome, R Azumi, M Matsumoto, T Nakamura, S Horiuchi, H Yamochi, G Saito *Synth. Met.* **70** 1229 (1995)
115. T Akutagawa, K Kakiuchi, T Hasegawa, T Nakamura, Ch A Christensen, J Becher *Langmuir* **20** 4187 (2004)
116. M J Allen, V C Tung, R B Kaner *Chem. Rev.* **110** 132 (2010)
117. K I Bolotin, K J Sikes, Z Jiang, M Klima, G Fudenberg, J Hone, P Kim, H L Stormer *Solid State Commun.* **146** 351 (2008)
118. A Ambrosi, S Y Chee, B Khezri, R D Webster, Z Sofer, M Pumera *Angew. Chem., Int. Ed.* **51** 500 (2012)
119. X Li, X Wang, L Zhang, S Lee, H Dai *Science* **319** 1229 (2008)
120. R Hao, W Qian, L Zhang, Y Hou *Chem. Commun.* 6576 (2008)
121. J T Sun, Y H Lu, W Chen, Y P Feng, A T S Wee *Phys. Rev. B: Condens. Matter* **81** 155403 (2010)
122. S Barja, M Garnica, J J Hinarejos, A L Vázquez de Parga, N Marttn, R Miranda *Chem. Commun.* **46** 8198 (2010)
123. C Wäckerlin, C Iakovita, D Chylarecka, P Fesser, T A Jung, N Ballav *Chem. Commun.* **47** 9146 (2011)
124. A Jain, K V Rao, U Mogera, A A Sagade, S J George *Chem. – Eur. J.* **17** 12355 (2011)
125. J M Fabre *J. Solid State Chem.* **168** 367 (2002)
126. T Mori *Chem. Rev.* **104** 4947 (2004)
127. H Kobayashi, H B Cui, A Kobayashi *Chem. Rev.* **104** 5265 (2004)
128. C Rovira *Chem. Rev.* **104** 5289 (2004)
129. G Saito, Y Yoshida *Bull. Chem. Soc. Jpn.* **80** 1 (2007)
130. A Ardavan, S Brown, S Kagoshima, K Kanoda, K Kuroki, H Mori, M Ogata, Sh Uji, J Wosnitza *J. Phys. Soc. Jpn.* **81** 011004 (2012)
131. T Mori, Y Misaki, K Kawakami, T Yamabe, H Mori, S Tanaka *Synth. Met.* **70** 875 (1995)
132. Y Misaki, T Miura, H Fujiwara, K Kawakami, T Yamabe, T Mori, H Mori, S Tanaka *Synth. Met.* **86** 1821 (1997)
133. T Sekikawa, T Kobayashi, H Okamoto, T Mitani, T Inabe, Y Maruyama *Synth. Met.* **70** 1213 (1995)
134. Y Morita, Y Yakiyama, T Murata, K Nakasuji *Solid State Sci.* **10** 1720 (2008)
135. T Murata, Y Morita, K Fukui, K Sato, D Shiomi, T Takui, M Maesato, H Yamochi, G Saito, K Nakasuji *Angew. Chem., Int. Ed.* **43** 6343 (2004)
136. T Murata, Y Morita, Y Yakiyama, K Fukui, H Yamochi, G Saito, K Nakasuji *J. Am. Chem. Soc.* **129** 10837 (2007)
137. K Heuzé, C Mézière, M Fourmigué, P Batail, C Coulon, E Canadell, P Auban-Senzier, D Jérome *Chem. Mater.* **12** 1898 (2000)
138. A J Moore, M R Bryce, A S Batsanov, J N Heaton, Ch W Lehmann, J A K Howard, N Robertson, A E Underhill, I F Perepichka *J. Mater. Chem.* **8** 1541 (1998)
139. S A Baudron, C Mézière, K Heuzé, M Fourmigué, P Batail, Ph Molinié, P Auban-Senzier *J. Solid State Chem.* **168** 668 (2002)
140. G Ono, H Terao, S Higuchi, T Sugawara, A Izuoka, T Mochida *J. Mater. Chem.* **10** 2277 (2000)
141. S Perruchas, K Boubekeur, Ph Molinié *Polyhedron* **24** 1555 (2005)
142. J-P Legros, F Dahan, L Binet, J-M Fabre *Synth. Met.* **102** 1632 (1999)
143. J-P Legros, F Dahan, L Binet, C Carcel, J-M Fabre *J. Mater. Chem.* **10** 2685 (2000)
144. T Murata, K Nakamura, H Yamochi, G Saito *Synth. Met.* **159** 2375 (2009)
145. T Murata, Y Enomoto, G Saito *Solid State Sci.* **10** 1364 (2008)
146. T Murata, G Saito, K Nishimura, Y Enomoto, G Honda, Y Shimizu, S Matsui, M Sakata, O O Drozdova, K Yakushi *Bull. Chem. Soc. Jpn.* **81** 331 (2008)
147. Y Morita, E Miyazaki, Y Umemoto, K Fukui, K Nakasuji *J. Org. Chem.* **71** 5631 (2006)
148. T Akutagawa, T Hasegawa, T Nakamura, G Sato *Cryst. Eng. Commun.* **5** 54 (2003)
149. T Akutagawa, T Hasegawa, T Nakamura, T Inabe, G Sato *Chem. – Eur. J.* **8** 4402 (2002)
150. T Akutagawa, S Takeda, T Hasegawa, T Nakamura *J. Am. Chem. Soc.* **126** 291 (2004)
151. M A M Alibadi, A S Batsanov, G Bramham, J P H Charmant, M F Haddow, L MacCay, S M Mansell, J E McGrady, N C Norman, A Roffey, C A Russell *Dalton Trans.* 5348 (2009)
152. N S Mani, L S Beatl, T Miller, O P Anderson, H Hope, S R Parkin, D J Williams, A G M Barrett, B M Hoffman *J. Chem. Soc., Chem. Commun.* 2095 (1994)
153. D M Eichhorn, S Yang, W Jarrell, Th F Baumann, L Scott Beall, A J P White, D J Williams, A G M Barrett, B M Hoffman *J. Chem. Soc., Chem. Commun.* 1703 (1995)
154. V Krstić, S Roth, M Burghard, K Kern, G L J A Rikken *J. Chem. Phys.* **117** 11315 (2002)
155. A Saad, O Jeannin, M Fourmigue *New J. Chem.* **35** 1004 (2011)
156. E Ribera, J Veciana, E Molins, I Mata, K Wurst, C Rovira *Eur. J. Org. Chem.* 2867 (2000)
157. S Yang, A C Brooks, L Martin, P Day, M Pilkington, W Clegg, R W Harrington, L Russo, J D Wallis *Tetrahedron* **66** 6977 (2010)
158. A Saad, O Jeannin, M Fourmigue *Tetrahedron* **67** 3820 (2011)
159. M A Rawashdech-Omary, M A Omary, J P Fackler Jr, R Galassi, B R Pietroni, A Burini *J. Am. Chem. Soc.* **123** 9689 (2001)
160. M R Haneline, F P Gabbaï *C. R. Chimie* **7** 871 (2004)
161. M J Matos, I C Santos, R T Henriques, M T Duarte *Synth. Met.* **42** 2155 (1991)
162. M Micuno, A F Garito, M P Cava *J. Chem. Soc., Chem. Commun.* 18 (1978)
163. T Mori, H Inokuchi *Solid State Commun.* **59** 355 (1986)
164. Y Iwasa, K Mizuhashi, T Koda, Y Tokura, G Saito *Phys. Rev. B: Condens. Matter* **49** 3580 (1994)
165. K Ishida, Y Niino, K Asayama, Y Iwasa, Y Tokura *Synth. Met.* **70** 881 (1995)
166. A Kawamoto, K Miyagawa, A Shimizu, K Kanoda *Synth. Met.* **85** 1601 (1997)
167. S Kagoshima, R Kondo, N Matsushita, M Higa, S V Ovsyannikov, N A Shaydarova, V V Shchennikov, A Y Manakov, A Y Likhacheva *Phys. Status Solidi B* **244** 418 (2007)
168. Y M Yamamoto, M Hagiwara, R Kato *Synth. Met.* **133 – 134** 449 (2003)
169. M Kimata, Y Oshima, K Koyama, H Ohta, M Motokawa, H M Yamamoto, R Kato *Synth. Met.* **153** 369 (2005)
170. M Aragaki, H Hoshino, T Mori, Y Misaki, K Tanaka, H Mori, Sh Tanaka *Adv. Mater.* **12** 983 (2000)
171. H Seo, C Hotta, H Fukuyama *Chem. Rev.* **104** 5005 (2004)
172. T Mori, K Murata, Y Misaki, K Tanaka *Chem. Lett.* 435 (1998)
173. N Sakurai, H Mori, Sh Tanaka, H Moriyama *Chem. Lett.* 1191 (1999)
174. J-i Yamada, R Oka, T Mangetsu, H Akutsu, Sh Nakatsui, H Nishikawa, I Ikemoto, K Kikuchi *Chem. Mater.* **13** 1770 (2001)
175. N Bellec, D Lorcy, K Boubekeur, R Carlier, A Tallec, S Los, W Pukacki, M Trybula, L Piekara-Sady, A Robert *Chem. Mater.* **11** 3147 (1999)

176. Z Časar, I Leban, A M Marechal, L Piekara-Sady, D Lorcy *C. R. Chimie* **12** 1057 (2009)
177. D Guerin, D Lorcy, R Carlier, S Los, L Piekara-Sady *J. Solid State Chem.* **168** 590 (2002)
178. G Saito, H Sasaki, T Aoki, Y Yoshida, A Otsuka, H Yamochi, O O Drozdova, K Yakushi, H Kitagawa, T Mitani *J. Mater. Chem.* **12** 1640 (2002)
179. S Horiuchi, H Yamochi, G Saito, K-i Sakaguchi, M Kusunoki *J. Am. Chem. Soc.* **118** 8604 (1996)
180. G Saito, H Ikegami, Y Yoshida, O O Drozdova, K Nishimura, S Horiuchi, H Yamochi, A Otsuka, T Hiramatsu, M Maesato, T Nakamura, T Akutagawa, T Yumoto *Bull. Chem. Soc. Jpn.* **83** 1462 (2010)
181. A Morikami, K Takimiya, Y Aso, T Otsubo *J. Mater. Chem.* **11** 2431 (2001)
182. S-S Pac, G Saito *Synth. Met.* **102** 1705 (1999)
183. G Saito, S-S Pac, O O Drozdova *Synth. Met.* **120** 667 (2001)
184. F Biaso, M Geoffroy, E Canadell, P Auban-Senzier, E Levillain, M Fourmigué, N Avarvari *Chem. – Eur. J.* **13** 5394 (2007)
185. M Ashizawa, A Nakao, H M Yamamoto, R Kato *J. Low Temp. Phys.* **142** 215 (2006)
186. S S Batsanov *Inorg. Mater.* **37** 871 (2001)
187. T Jigami, K Takimiya, T Otsubo *J. Org. Chem.* **63** 8865 (1998)
188. M Iyoda, Y Kuwatani, E Ogura, K Hara, H Suzuki, T Takano, K Takeda, J-i Takano, K Ugawa, M Yoshida, H Matsuyama, H Nishikawa, I Ikemoto, T Kato, N Yoneyama, J-i Nishijo, T Enoki *Heterocycles* **54** 833 (2000)
189. M Iyoda, H Suzuki, Sh Sasaki, H Yoshino, K Kikuchi, K Saito, I Ikemoto, H Matsuyama, T Mori *J. Mater. Chem.* **6** 501 (1996)
190. A S Batsanov, M R Bryce, A Chesney, J A K Howard, D E John, A J Moore, C L Wood, H Gerstenman, J Y Becker, V Y Khodorkovsky, A Ellern, J Bernstein, I F Perepichka, V Rotello, M Gray, A O Cuello *J. Mater. Chem.* **11** 2181 (2001)
191. O J Dautel, M Fourmigué *New J. Chem.* **25** 834 (2001)
192. T Hasegawa, K Inukai, S Kagoshima, T Sugawara, T Mochida, S Sugiura, Y Iwasa *Chem. Commun.* 1377 (1997)
193. K Yonemitsu *J. Phys. Chem. Solids* **63** 1495 (2002)
194. T Hasegawa, T Mochida, R Kondo, S Kagoshima, Y Iwasa, T Akutagawa, T Nakamura, G Saito *Phys. Rev. B: Condens. Matter* **62** 10059 (2000)
195. T Hasegawa, T Akutagawa, T Nakamura *Synth. Met.* **133 – 134** 623 (2003)
196. R Kondo, T Hasegawa, T Mochida, S Kagoshima, Y Iwasa *Chem. Lett.* 333 (1999)
197. K Hiraki, T Takahashi, R Kondo, S Kagoshima, T Hasegawa, T Mochida, Y Iwasa *J. Phys. Chem. Solids* **62** 401 (2001)
198. R Kondo, T Hasegawa, T,Mochida, S Kagoshima, Y Iwasa, K-i Hiraki, T Takahashi *J. Phys. Soc. Jpn.* **70** 3023 (2001)
199. I Shirotani, J Hayashi, K Yakushi, K Takeda, T Yokota, K Shimizu, K Amaya, A Nakayama, K Aoki *Physica B* **304** 6 (2001)
200. H Kurebayashi, M Sakaguchi, T Okajima, T Haino, Sh Usui, Y Fukazawa *Tetrahedron Lett.* **40** 5545 (1999)
201. H Kurebayashi, T Haino, Sh Usui, Y Fukazawa *Tetrahedron* **57** 8667 (2001)
202. H Kurebayashi, T Haino, Y Fukazawa *Tetrahedron Lett.* **41** 477 (2000)
203. F G Klärner, U Burkert, M Kamieth, R Boese, J Benet-Buchholz *Chem. – Eur. J.* **5** 1700 (1999)
204. F G Klärner, J Polkowska, J Panitzky, U P Seelbach, U Burkert, M Kamieth, M Baumann, A E Wigger, R Boese, D Bläser *Eur. J. Org. Chem.* 1405 (2004)
205. E W Reinheimer, H Zhao, K R Dunbar *J. Chem. Crystallogr.* **40** 514 (2010)
206. E W Reinheimer, M F B Rivas, H Zhao, K R Dunbar *J. Chem. Crystallogr.* **41** 936 (2011)
207. J D Bagnato, W W Shum, M Strohmeier, D M Grant, A M Arif, J S Miller *Angew. Chem., Int. Ed.* **45** 5322 (2006)
208. R E Del Sesto, M Botoshansky, M Kaftory, A M Arif, J S Miller *Cryst. Eng. Commun.* **4** 117 (2002)
209. S V Rosokha, J Lu, B Han, J K Kochi *New J. Chem.* **33** 545 (2009)
210. K Takahashi, Sh Tarutani *Chem. Commun.* 1233 (1998)
211. T Fukushima, N Okazeri, T Miyashi, K Suzuki, Y Yamashita, T Suzuki *Tetrahedron Lett.* **40** 1175 (1999)
212. K Yui, Y Aso, T Otsubo, F Ogura *Bull. Chem. Soc. Jpn.* **62** 1539 (1989)
213. K Suzuki, M Tomura, S Tanaka, Y Yamashita *Tetrahedron Lett.* **41** 8359 (2000)
214. K Takahashi, Sh Tarutani *Synth. Met.* **70** 1165 (1995)
215. E Günther, S Hünig, J-U von Schütz, U Langohr, H Rieder, S Söderholm, H-P Werner, K Peters, H G von Schnering, H J Lindner *Chem. Ber.* **125** 1919 (1992)
216. S Hünig, E Herberth *Chem. Rev.* **104** 5535 (2004)
217. S A Bewick, R A Pascal Jr, D M Ho, Z G Soos *J. Chem. Phys.* **122** 024710 (2005)
218. R Gómez, C Seoane, J L Segura *Chem. Soc. Rev.* **36** 1305 (2007)
219. K Nishimura, T Kondo, O O Drozdova, H Yamochi, G Saito *J. Mater. Chem.* **10** 911 (2000)
220. T Murata, Y Yakiyama, K Nakasuji, Y Morita *Cryst. Eng. Commun.* **13** 3689 (2011)
221. S Horiuchi, R Kumai, Y Tokura *J. Am. Chem. Soc.* **127** 5010 (2005)
222. S Horiuchi, R Kumai, Y Tokura *Angew. Chem., Int. Ed.* **46** 3497 (2007)
223. Md B Zaman, J Toyoda, Y Morita, S Nakamura, H Yamochi, G Saito, K Nishimura, N Yoneyama, T Enoki, K Nakasuji *J. Mater. Chem.* **11** 2211 (2001)
224. Y Morita, S Maki, M Ohmoto, H Kitagawa, T Okubo, T Mitani, K Nakasuji *Org. Lett.* **4** 2185 (2002)
225. D A Clemente, A Marzotto *J. Mater. Chem.* **6** 941 (1996)
226. M Capdevila-Cortada, J J Novoa, J D Bell, C E Moore, A L Rheingold, J S Miller *Chem. – Eur. J.* 9326 (2011)
227. J J Novoa, P Lafuente, R E Del Sesto, J S Miller *Angew. Chem., Int. Ed.* **40** 2540 (2001)
228. R E Del Sesto, J S Miller, P Lafuente, J J Novoa *Chem. – Eur. J.* **8** 4894 (2002)
229. J J Novoa, P Lafuente, R E Del Sesto, J S Miller *Cryst. Eng. Commun.* **4** 373 (2002)
230. J-M Lü, S V Rosokha, J K Kochi *J. Am. Chem. Soc.* **125** 12161 (2003)
231. J Jakowski, J Simons *J. Am. Chem. Soc.* **125** 16089 (2003)
232. Y Jung, M Head-Gordon *Phys. Chem. Chem. Phys.* **6** 2008 (2004)
233. I Garcia-Yoldi, J S Miller, J J Novoa *J. Phys. Chem. A* **111** 8020 (2007)
234. J S Miller, J J Novoa *Acc. Chem. Res.* **40** 189 (2007)
235. M Capdevila-Cortada, J J Novoa *Chem. – Eur. J.* **18** 5335 (2012)
236. F Li, Y Li, B Zhang, Z Shi, D Zhu *Synth. Met.* **102** 1494 (1999)
237. T Mochida, S Yamazaki *J. Chem. Soc., Dalton Trans.* 3559 (2002)
238. T Michinobu, C Boudon, J-P Gisselbrecht, P Seiler, B Frank, N N P Moonen, M Gross, F Diederich *Chem. – Eur. J.* **12** 1889 (2006)
239. T Michinobu, J C May, J H Lim, C Boudon, J P Gisselbrecht, P Seiler, M Gross, I Biaggio, F Diederich *Chem. Commun.* 737 (2005)

240. B Breiten, Y-L Wu, P D Jarowski, J-P Gisselbrecht, C Boudon, M Griesser, C Onitsch, G Gescheidt, W B Schweizer, N Langer, C Lennartz, F Diederich *Chem. Sci.* **2** 88 (2011)
241. M Kivala, C Boudon, J P Gisselbrecht, P Seiler, M Gross, F Diederich *Chem. Commun.* 4731 (2007)
242. P Reutenauer, M Kivala, P D Jarowski, C Boudon, J P Gisselbrecht, M Gross, F Diederich *Chem. Commun.* 4898 (2007)
243. S-I Kato, F Diederich *Chem. Commun.* **46** 1994 (2010)
244. N Gautier, F Dumur, V Lloveras, J Vidal-Gancedo, J Veciana, C Rovira, P Hudhomme *Angew. Chem., Int. Ed.* **42** 2765 (2003)
245. F Dumur, X Guégano, N Gautier, S-X Liu, A Neels, S Decurtins, P Hudhomme *Eur. J. Org. Chem.* 6341 (2009)
246. F Otun, V Lloveras, M Mas-Torrent, J Vidal-Gancedo, J Veciana, C Rovira *Angew. Chem., Int. Ed.* **50** 10902 (2011)
247. D F Perepichka, M R Bryce, Ch Pearson, M C Petty, E J L McInnes, J P Zhao *Angew. Chem., Int. Ed.* **42** 4636 (2003)
248. S Y AlQaradawi, E M Nour *J. Mol. Struct.* **794** 251 (2006)
249. C Katayama, M Honda, H Kumagai, J Tanaka, G Saito, H Inokuchi *Bull. Chem. Soc. Jpn.* **58** 2272 (1985)
250. G Saito, S Sekizaki, A Konsha, H Yamochi, K Matsumoto, M Kusunoki, K-i Sakaguchi *J. Mater. Chem.* **11** 364 (2001)
251. SSSR P. 1389226 (1986)
252. SSSR P. 1696428 (1989); *Byull. Izobret.* (45) 92 (1991)
253. V A Starodub, E M Gluzman, K I Pokhodnya, M Ya Valakh *Teor. Eksp. Khim.* **29** 361 (1993) [c]
254. J Ziman *Models of Disorder* (Cambridge: Cambridge University Press, 1979)
255. W Bunzel, F Vögtle, S Franken, H Puff *J. Chem. Soc., Chem. Commun.* 1035 (1984)
256. V A Starodub, E M Gluzman, Yu A Kaftanova, I Oleinichak *Teor. Eksp. Khim.* **33** 111 (1997) [c]
257. U Fano *Phys. Rev.* **24** 1866 (1961)
258. T Kondow, T Sakata *Phys Status Solidi A* **6** 551 (1971)
259. M J Rice *Phys. Rev. Lett.* **37** 36 (1976)
260. L P Gor kov, E I Rashba *Solid State Commun.* **27** 1211 (1978)
261. K Bocer, V A Starodub, R Świetlik *Adv. Mater. Opt. Electron.* **8** 97 (1998)
262. K Nishimura, G Saito *Synth. Met.* **153** 385 (2005)
263. V A Starodub, A V Kravchenko, A R Kazachkov, V V Khotkevich, A V Khotkevich, O S Pyshkin, G V Kamarchuk *Funct. Mater.* **10** 739 (2003)
264. D V Ziolkovskiy, A V Kravchenko, V A Starodub, A R Kazachkov, V V Khotkevich, G V Kamarchuk, A V Khotkevich, O S Pyshkin *Funct. Mater.* **11** 316 (2004)
265. D V Ziolkovskiy, A V Kravchenko, V A Starodub, O N Kazheva, A V Khotkevich *Funct. Mater.* **12** 577 (2005)
266. R H Harms, H J Keller, D Nöthe, M Werner, D Gundel, H Sixl, Z G Soos, M Robert *Mol. Cryst. Liq. Cryst.* **65** 179 (1981)
267. A Lapisski, M Golub, V A Starodub, in *Proceedings of the 10th International Conference ERPOS (Electrical and Related Properties of Organic Solids and Polymers), Cargese, 2005* p. A 094
268. D V Ziolkovskiy, O N Kazheva, G V Shilov, O A Dyachenko, A V Kravchenko, A V Khotkevich, V A Starodub *Funct. Mater.* **13** 119 (2006)
269. O N Kazheva, D V Ziolkovskiy, G G Alexandrov, A N Chekhlov, O A Dyachenko, V A Starodub, A V Khotkevich *Synth. Met.* **156** 1010 (2006)
270. Y-C Chen, F- F Wang, R-Y Hung, Y Wang, K-B Wang, X-J Kong *Chin. J. Struct. Chem.* **30** 79 (2011)
271. T Murata, Y Morita, Y Yakiyama, Y Yamamoto, S Yamada, Y Nishimura, K Nakasuji *Cryst. Growth Des.* **8** 3058 (2008)
272. H Peng, C Ran, Z Liu, Y Long, Z Wang, Z Yu, H Sun, Y Wei, S Gao, Z Chen, E-Q Chen *J. Phys. Chem. C* **112** 11001 (2008)
273. T Murata, Y Morita, K Tamaki, K Nakasuji *J. Low Temp. Phys.* **142** 425 (2006)
274. T Murata, E Miyazaki, T Yokoyama, K Nakasuji, Y Morita *Cryst. Growth Des.* **12** 804 (2012)
275. B H Ward, G E Granroth, J B Walden, K A Abboud, M W Meisel, P G Rasmussen, D R Talham *J. Mater. Chem.* **8** 1373 (1998)
276. R E Del Sesto, A M Arif, J J Novoa, I Anusiewicz, P Skurski, J Simons, B C Dunn, E M Eyring, J S Miller *J. Org. Chem.* **68** 3367 (2003)
277. H Akutsu, T Sasai, J Yamada, S Nakatsuji, S S Turner *Physica B: Condens. Matter* **405** S52 (2010)
278. W Heisenberg *Z. Phys.* **49** 619 (1928)
279. A A Ovchinnikov *Dokl. Akad. Nauk SSSR* **236** 928 (1977) [e]
280. A A Ovchinnikov *Theor. Chim. Acta* **47** 293 (1978)
281. Yu V Korshak, T V Medvedeva, A A Ovchinnikov, V N Spector *Nature (London)* **326** 370 (1987)
282. P-M Allemand, K C Khemani, A Koch, F Wudl, K Holczer, S Donovan, G Grüner, J D Thompson *Science* **253** 301 (1991)
283. T Sugimoto, K Ueda, M Tsujii, H Fujita, N Hosoito, N Kanehisa, Y Shibamoto, Y Kai *Chem. Phys. Lett.* **249** 304 (1996)
284. T Sugimoto, K Shiwaku, M Kohama, K Ueda, S Endo, N Toyota, H Fujita *Synth. Met.* **103** 2300 (1999)
285. T Sugimoto, K Shiwaku, M Kohama, K Ueda, H Fujita *Synth. Met.* **103** 2312 (1999)
286. G A Candela, L J Swartzendruber, J S Miller, M J Rice *J. Am. Chem. Soc.* **101** 2755 (1979)
287. J S Miller, J C Calabrese, A J Epstein, R W Bigelow, J H Zhang, W M Reiff *J. Chem. Soc., Chem. Commun.* 1026 (1986)
288. J S Miller, J C Calabrese, H Rommelmann, S R Chittipeddi, J H Zhang, W M Reiff, A J Epstein *J. Am. Chem. Soc.* **109** 769 (1987)
289. K-M Chi, J C Calabrese, W M Reiff, J S Miller *Organometallics* **10** 688 (1991)
290. L Ballester, A M Gil, A Gutiérrez, M F Perpiñán, A E Sánchez, M Fonari, K Suwinska, V Belsky *Eur. J. Inorg. Chem.* 3034 (2003)
291. J S Miller, A J Epstein *Chem. Commun.* 1319 (1998)
292. J S Miller, A J Epstein *Coord. Chem. Rev.* **206 – 207** 651 (2000)
293. K I Pokhodnya, D Pejakovic, A J Epstein, J S Miller *Phys. Rev. B: Condens. Matter* **63** 174408 (2001)
294. M S Thorum, K I Pokhodnya, J S Miller *Polyhedron* **25** 1927 (2006)
295. K I Pokhodnya, A J Epstein, J S Miller *Adv. Mater.* **12** 410 (2000)
296. E B Vickers, A Senesi, J S Miller *Inorg. Chim. Acta* **357** 3889 (2004)
297. J-H Her, P W Stephens, K I Pokhodnya, M Bonner, J S Miller *Angew. Chem., Int. Ed.* **46** 1521 (2007)
298. J W Raebiger, J S Miller *Inorg. Chem.* **41** 3308 (2002)
299. K H Stone, P W Stephens, A C McConnell, E Shurdha, K I Pokhodnya, J S Miller *Adv. Mater.* **22** 2514 (2010)
300. S H Lapidus, A C McConnell, P W Stephens, J S Miller *Chem. Commun.* **47** 7602 (2011)
301. E B Vickers, T D Selby, M S Thorum, M L Taliaferro, J S Miller *Inorg. Chem.* **43** 6414 (2004)
302. H Zhao, R A Heintz, X Ouyang, K R Dunbar *Chem. Mater.* **11** 736 (1999)
303. R Clérac, Sh O'Kane, J Cowen, X Ouyang, R A Heintz, H Zhao, M J Bazile Jr, K R Dunbar *Chem. Mater.* **15** 1840 (2003)

304. A M Madalan, H W Roesky, M Andruh, M Noltemeyer, N Stanica *Chem. Commun.* 1638 (2002)
305. H Zhao, M J Bazile Jr, J R Calán-Mascarós, K R Dunbar *Angew. Chem., Int. Ed.* **42** 1015 (2003)
306. J Zhang, P Yan, G Li, G Hou, M Suda, Y Einaga *Dalton Trans.* 10466 (2009)
307. N Lopez, H Zhao, A V Prosvirin, W Wernsdorfer, K R Dunbar *Dalton Trans.* **39** 4341 (2010)
308. M Ballesteros-Rivas, H Zhao, A Prosvirin, E W Reinheimer, R A Toscano, J Valdés-Martínez, K R Dunbar *Angew. Chem., Int. Ed.* **51** 5124 (2012)
309. E B Vickers, T D Selby, J S Miller *J. Am. Chem. Soc.* **126** 3716 (2004)
310. M L Taliaferro, M S Thorum, J S Miller *Angew. Chem., Int. Ed.* **45** 5326 (2006)
311. G Long, R D Willett *Inorg. Chim. Acta* **313** 1 (2001)
312. H Suzuki, H Akutsu, J-i Yamada, S Nakatsuji *Crystals* **2** 662 (2012)
313. L Ballester, A M Gil, A Gutiérrez, M F Perpiñan, M T Azcondo, A E Sánchez, C Marzin, G Tarrago, C Bellitto *Chem. – Eur. J.* **8** 2539 (2002)
314. L Ballester, A Gutiérrez, M F Perpiñan, A E Sánchez, M T Azcondo, M J Gonzáles *Inorg. Chim. Acta* **357** 1054 (2004)
315. Y-C Chen, P-F Wang, G-X Liu, H Xu, X-M Ren, Y Song, Z-P Ni *J. Phys. Chem. Solids* **69** 2445 (2008)
316. G-X Liu, R-Y Huang, X-M Ren *J. Mol. Struct.* **891** 11 (2008)
317. G X Liu, X M Ren, R K Kremer, Q J Meng *J. Mol. Struct.* **743** 125 (2005)
318. G X Liu, W Guo, H Yang, S Nishihara, X M Ren *J. Chem. Crystallogr.* **41** 1262 (2011)
319. G X Liu, H Xu, X M Ren, W-Y Sun *Cryst. Eng. Commun.* **10** 1574 (2008)
320. Y C Chen, G X Liu, P F Wang, H Xu, X M Ren, Y Song, Y X Sui *Polyhedron* **26** 1781 (2007)
321. G X Liu, J Yan, K Zhu, H Chen, X M Ren *Chin. J. Struct. Chem.* **28** 181 (2009)
322. Y Liu, Y Y Xu, G X Liu, S Nishihara, X M Ren *J. Inorg. Organomet. Polym.* **20** 177 (2010)
323. L Ballester, A Gutiérrez, M F Perpiñan, M T Azcondo *Coord. Chem. Rev.* **190 – 192** 447 (1999)
324. E Pytte *Phys. Rev. B: Solid State* **10** 4637 (1974)
325. J W Bray, H R Hart, I V Interrante, I S Jacobs, J S Kasper, G D Watkins, S H Wee, J C Bonner *Phys. Rev. Lett.* **35** 744 (1975)
326. S Huisinga, J Kommandeur, G A Sawatzky, B T Thole, K Kopinga, W J M de Jonge, J Roos *Phys. Rev. B: Condens. Matter* **19** 4723 (1979)
327. H Noiri, T Hamamoto, O Fujita, J Akimitsu, S Takagi, M Motokawa *J. Magn. Magn. Mater.* **177 – 181** 687 (1998)
328. S Takagi, K Irie, T Suematsu, M Yoshihiro, M Mito, H Deguchi *Polyhedron* **24** 2716 (2005)
329. C F Schwerdtfeger, S Oostra, G A Sawatzky *Phys. Rev. B: Condens. Matter.* **25** 1786 (1982)
330. Y Lepine, A Caille, V Larochelle *Phys. Rev. B: Solid State* **18** 3585 (1978)
331. J L Goudard, A A Lakhani, N K Hota *Solid State Commun.* **41** 423 (1982)
332. J C Vegter, J Kommandeur *Mol. Cryst. Liq. Cryst.* **30** 11 (1975)
333. J J Andre, A Bieber, F Gautier *Ann. Phys. (Paris)* **1** 145 (1976)
334. M Yoshikawa, S Nakashima, A Wada, A Mitsuishi *J. Phys. Soc. Jpn.* **55** 1177 (1986)
335. T Kotani, M Sorai, H Suga *J. Phys. Chem. Solids* **70** 1066 (2009)
336. B Barszcz, A Graja, D V Ziolkovskiy,V A Starodub *Synth. Met.* **158** 246 (2008)
337. A Radvvkovv, D V Ziolkovskiy, V O Cheranovskii, A Feher, M Kajñakova, O N Kazheva, G G Alexandrov, O A Dyachenko, V A Starodub *J. Phys. Chem. Solids* **70** 1471 (2009)
338. O N Kazheva, D V Ziolkovskiy, G G Alexandrov, O A Dyachenko, V A Starodub, A V Khotkevich, G Y Vasilets *Funct. Mater.* **13** 692 (2006)
339. T Barnes, J Rivera *Phys. Rev. B: Condens. Matter* **50** 6817 (1994)
340. V O Cheranovskii, A A Chovpan, E V Ezerskaya, I Özkan *Int. J. Quant. Chem.* **106** 2254 (2006)
341. A Radváková, O Kazheva, A Chekhlov, O Dyachenko, M Kucmin, M Kajñakova, A Feher, V Starodub *J. Phys. Chem. Solids* **71** 752 (2010)
342. T Yamaguchi, Y Narumi, J Kikuchi, Y Ueda, K Tatani, T C Kobayashi, K Kindo, K Motoya *Phys. Rev. Lett.* **83** 3729 (1999)
343. US P. 20090290291 (2009)
344. T Nakamura, G Yunome, M Matsumoto, Y F Miura, S Horiuchi, H Yamochi, G Saito, H Isotalo, H Stubb *Synth. Met.* **71** 1993 (1995)
345. T W Kim, S-K Lee, M-J Song, D-M Shin, Y-S Kwon, D-Y Kang *Synth. Met.* **71** 2029 (1995)
346. J K Jeszka, A Tracz, G Boiteux, G Seytre, M Kryszewski *Synth. Met.* **71** 2205 (1995)
347. T Mathis, K Mattenberger, P Moll, B Batlogg *Appl. Phys. Lett.* **101** 023302 (2012)
348. H J Yan, S S Li, C J Yan, Q Chen, L J Wan *Sci. China, Ser. B: Chem.* **52** 559 (2009)
349. T R Umbach, I Fernandez-Torrente, J N Ladenthin, J I Pascual, K J Franke *J. Phys.: Condens. Matter* **24** 354003 (2012)
350. H Salem J Pharm *Biomed. Anal.* **29** 527 (2002)
351. L M Du, Y Q Yang, Q M Wang *Anal. Chim. Acta* **516** 237 (2004)
352. N Rahman, N Anwar, M Kashif *Pharmaco* **60** 605 (2005)
353. H Salem *African J. Pharm. Pharmacol.* **2** 136 (2008)
354. N N Salama, S A Abdel-Razeq, Sh Abdel-Atty, N El-Kosy *Bull. Fac. Pharm. Cairo Univ.* **49** 13 (2011)
355. H Salem *e-J. Chem.* **6** 332 (2009)
356. E Y Frag, G G Mohamed, A B Farag, E B Yussof *Insight Pharm. Sci.* **1** 47 (2011)
357. M S Refat, O B Ibrahim, H Al-Didamony, Kh M Abou El-Nour, L El-Zayat *J. Saudi Chem. Soc.* **16** 227 (2012)
358. A L Saber, A S Amin *J. Anal. Bioanal.Techn.* **1** 1 (2011)
359. A Raza, M Zia-ul-Haq *Int. J. Anal. Chem.* 1 (2011)
360. R I El-Bagary, E F Elkady, B M Ayoub *Int. J. Biomed. Sci.* **7** 55 (2011)
361. S Y Li, Q L Guo, W Yuan, Y C Hou, L M Du *Bull. Chem. Soc. Ethiop.* **24** 21 (2010)
362. A A Gouda, R El Sheikh, Rh M El-Azzazy *J. Anal. Bioanal. Tech.* **3** 1000149 (2012)
363. H Demirhan, M Arslan, M Zengin, M Kucukislamoglu *J. Spectrosc.* ID 875953 (2013)
364. P C Pandey, S Upadhyay, S Sharma *Electroanalysis* **15** 1115 (2003)
365. M Cano, B Palenzuela, R Rodrígues-Amaro *Electroanalysis* **18** 1068 (2006)
366. M Cano, B Palenzuela, R Rodrígues-Amaro *Electroanalysis* **18** 1727 (2006)
367. M Cano, B Palenzuela, R R Rodrígues-Amaro *Portug. Elecrochim. Acta* **25** 67 (2007)
368. R Pauliukaite, A Malinauskas, G Zhylyak, U E Spichiger-Keller *Electroanalysis* **19** 2491 (2007)
369. M Cano, B Palenzuela, J L Ávila, R Rodrígues-Amaro *Electroanalysis* **19** 973 (2007)
370. X Jiang, Z Li, C Sun, X Zhang *Int. J. Phys. Sci.* **7** 901 (2012)

371. R M Metzger *J. Mater. Chem.* **18** 4364 (2008)
372. J Caro, S Garelik, A Figueras *Chem. Vap. Deposition* **2** 251 (1996)
373. J Caro, J Fraxedas, A Figueras *Chem. Vap. Deposition* **3** 263 (1997)
374. M Hiraoka, T Hasegawa, T Yamada, Y Takahashi, S Horiuchi, Y Tokura *Adv. Mater.* **19** 3248 (2007)
375. C D Dimitrakopoulos, P R L Malenfant *Adv. Mater.* **14** 99 (2002)
376. E Menard, V Podzorov, S-H Hur, A Gaur, M E Gershenson, J A Rogers *Adv. Mater.* **16** 2097 (2004)
377. T Sumimoto, Y Shiratori, M Iizuka, S Kuniyoshi, K Kudo, K Tanaka *Synth. Met.* **86** 2259 (1997)
378. K Kudo, M Iizuka, S Kuniyoshi, K Tanaka *Electr. Eng. Jpn.* **134** 1440 (2001)
379. B Mukherjee, M Mukherjee *Langmuir* **27** 11246 (2011)
380. M Iizuka, Y Shiratori, S Kuniyoshi, K Kudo, K Tanaka *Appl. Surf. Sci.* **130 – 132** 914 (1998)
381. N A Kato, M Fujimura, S Kuniyoshi, K Kudo, M Hara, K Tanaka *Appl. Surf. Sci.* **130 – 132** 658 (1998)
382. Y Takahashi, T Hasegawa, Y Abe, Y Tokura, K Nishimura, G Saito *Appl. Phys. Lett.* **86** 063504 (2005)
383. Y Abe, T Hasegawa, Y Takahashi, T Yamada, Y Tokura *Appl. Phys. Lett.* **87** 153506 (2005)
384. Y Takahashi, T Hasegawa, Y Abe, Y Tokura, G Saito *Appl. Phys. Lett.* **88** 073504 (2006)
385. K Shibata, H Wada, K Ishikawa, H Takezoe *Appl. Phys. Lett.* **90** 193509 (2007)
386. M Sakai, M Iizuka, M Nakamura, K Kudo *Synth. Met.* **153** 293 (2005)
387. T Minari, T Miyadera, K Tsukagoshi, Y Aoyagi *Appl. Phys. Lett.* **91** 053505 (2007)
388. T Kever, U Böttger, C Schindler, R Waser *Appl. Phys. Lett.* **91** 083506 (2007)
389. M Sakai, H Sakuma, Y Ito, A Saito, M Nakamura, K Kudo *Phys. Rev. B: Condens. Matter* **76** 045111 (2007)
390. T Mori *J. Phys.: Condens. Matter* **20** 184010 (2008)
391. T Mori *Chem. Lett.* **40** 428 (2011)
392. Y Guo, G Yu, Y Liu *Adv. Mater.* **22** 4427 (2010)
393. R Otero, J M Gallego, A L Vásguez de Parga, N Martín, R Miranda *Adv. Mater.* **23** 5148 (2011)
394. A Fedorov *Physics* **3** 46 (2010)
395. L Rodríguez-Pérez, M Ángeles Herranz, N Martin *Chem. Commun.* **49** 26 (2014)
396. C Coletti, C Riedl, D S Lee, B Krauss, L Patthey, K von Klitzing, J H Smet, U Starke *Phys. Rev. B: Condens. Matter* **81** 235401 (2010)
397. O Rana, R Srivastava, G Ghauhan, M Zulfequar, M Husain, P C Srivastava, M N Kamalasanan *Phys. Statue Solidi A* **209** 2539 (2012)
398. M Iizuka, K Kudo, S Kuniyoshi, K Tanaka *Electr. Eng. Jpn.* **140** 628 (2002)
399. M Sakai, M Iizuka, M Nakamura, K Kudo *J. Appl. Phys.* **97** 053509 (2005)
400. M Sakai, H Yamauchi, M Nakamura, K Kudo *J. Phys.: Conf. Ser.* **358** 012011 (2012)
401. H Liu, J Li, C Lao, C Huang, Y Li, Z L Wang, D Zhu *Nanotechnology* **18** 495704 (2007)
402. T Phanindra Sai, A K Rauchaudhuri *Nanotechnology* **21** 945703 (2010)
403. T Akutagawa, T Ohta, T Hasegawa, T Nakamura, C A Christensen, J Becher *Proc. Natl. Acad. Sci. USA* **99** 5028 (2002)
404. L Ren, X Xian, K Yan, L Fu, Y Liu, Sh Chen, Z Liu *Adv. Funct. Mater.* **20** 1209 (2010)
405. S A Odom, M M Caruso, A D Finke, A M Prokup, J A Ritchey, J H Leonard, S R White, N R Sottos, J S Moore *Adv. Funct. Mater.* **20** 1721 (2010)
406. E F Aziz, A Vollmer, S Eisebitt, W Eberhardt, P Pingel, D Neher, N Koch *Adv. Mater.* **19** 3257 (2007)
407. X Mei, J Ouyang *Langmuir* **27** 10953 (2011)
408. M Szablewski, Ph R Thomas, A Thornton, D Bloor, G H Cross, J M Cole, J A K Howard, M Malagoli, F Meyers, J L Bridas, W Wenseleers, E Goovaerts *J. Am. Chem. Soc.* **119** 3144 (1997)
409. A Funabiki, T Mochida, K Takahashi, H Mori, T Sakurai, H Ohta, M Uruichi *J. Mater. Chem.* **22** 8361 (2012)
410. D J Press, Th G Back, T C Sutherland *Tetrahedron Lett.* **53** 1603 (2012)
411. M Hiraoka, T Hasegawa, Y Abe, T Yamada, Y Tokura, H Yamochi, G Saito, T Akutagawa, T Nakamura *Apll. Phys. Lett.* **89** 173504 (2006)
412. S Chae, S W Kang, J Y Park, Y-G Lee, J H Lee, J Won, Y S Kang *Angew. Chem., Int. Ed.* **50** 2982 (2011)
413. H Peng, C Ran, X Yu, R Zhang, Z Liu *Adv. Mater.* **17** 459 (2005)
414. H Peng, Z Chen, L Tong, X Yu, C Ran, Z Liu *J. Phys. Chem. B* **109** 3526 (2005)
415. H Peng, Z Liu *Coord. Chem. Rev.* **254** 1151 (2010)
416. R Ishikawa, M Bando, Y Morimoto, A Sandhu *Nanoscale Res. Lett.* **6** 1 (2011)
417. A Suzuki, T Ohtsuki, T Oku, T Akiyama *Mater. Sci. Eng., B* **177** 877 (2012)
418. M Shiraishi, T Ikoma *Physica E* **43** 1295 (2011)
419. S Shimomura, S Kitagawa *J. Mater. Chem.* **21** 5537 (2011)
420. B F Abrahams, R W Elliott, T A Hudson, R Robson *Cryst. Eng. Commun.* **14** 351 (2012)
421. Z Zhang, H Zhao, H Kojima, T Mori, K R Dunbar *Chem. – Eur. J.* **19** 3348 (2013)

[a] — *J. Exp. Theor. Phys. Lett. (Engl. Transl.)*
[b] — *Russ. Chem. Bull., Int. Ed. (Engl. Transl.)*
[c] — *Theor. Exp. Chem. (Engl. Transl.)*
[d] — *J. Struct. Chem. (Engl. Transl.)*
[e] — *Dokl. Phys. Chem. (Engl. Transl.)*